TECHNISCHE UNIVERSITÄT DRESDEN

FACULTY OF ENVIRONMENTAL SCIENCES

ANALYSIS AND MODEL-BASED ASSESSMENT OF WATER QUALITY UNDER DATA SCARCITY CONDITIONS IN TWO RURAL WATERSHEDS

DISSERTATION

to achieve the academic degree

Doctor rerum naturalium (Dr. rer. nat.)

by:

Filipa Isabel Lopes Tavares Wahren

Environmental Eng. (Universidade Nova de Lisboa, Portugal)

M.Sc. Environmental Management (Christian-Albrechts-Universität zu Kiel)

born on November 17, 1980 in Lissabon, Portugal

SUPERVISORS:

Prof. Dr. Karl-Heinz Feger (TU Dresden)

Dr. Joao Pedro Nunes (University of Aveiro, Portugal)

REFEREES:

Prof. Dr. Karl-Heinz Feger (TU Dresden)

Prof. Dr. Nicola Fohrer (Christian-Albrechts-Universität zu Kiel)

Prof. Dr. Martin Volk (UFZ Leipzig / Martin-Luther-Universität Halle)

TO MY FATHER

IN PIAM MEMORIAM

Acknowledgments

Many are the people that in a direct or indirect way have made this dissertation possible and it is my greatest pleasure to express my most sincere gratitude.

Firstly, I would like to thank my supervisor Karl-Heinz Feger, without his guidance and support this work would not have been possible. Thank you for all the confidence in my work and for being patient with me, when life turns out to be a tough project to manage.

I would like to thank all the present and past colleagues in the Institute of Soil Science and Site Ecology (TUD) who have been involved in so many activities contributing to this dissertation. Thank you: Daniel Hawtree, Raphael Bening, Stefan Julich, Georg Richter, Gabriela Fontenla, Rainer Petzold, Kai Schwärzel for embarking in field trips together. Thank you: Manuela Unger, Thomas Klinger, Gisela Ciesielski for all the help in the laboratories. Thank you Birgit Ziegelmayer for the essential help with all formalities.

Thank you for all the amazing conversations after lunch, all the incentives, all the laughter and for the sense of belonging. Thank you at all the Master Students I have had the pleasure working with (among others: Gabriela Fontenla, Frederike Schumacher, Lennart Gosch, Louise Maryonoputri).

Special thanks goes to Stefan Julich for the SWAT related help, guidance, problem solving, writing support and I could go on and on. Your assistance was fundamental for the completion of my thesis. Equally, I would like to thank João Pedro Nunes for the valuable advices and all the help at applying for funds. I fondly remember the time spent at the sea shore. The most fruitful discussions have indeed sometimes the most amazing landscape view. On the same level of gratitude I would like to thank Kai Schwärzel. Your initial guidance has outlined my research path. Thank you for good advice and for the many discussions.

I'm also truly grateful to Jan Jacob Keizer and his working team at the Coastal Zone Planning & Management Research Group (University of Aveiro). Thank you Oscar Gonzalez Pelayo, María Ermitas Rial, Juliana dos Santos, Sérgio Prats, Maruxa Malvar, Martinho Martins, Dalila Serpa, Léonard Bernard-Jannin and Diana Vieira. Without your help, data collection in the Águeda watershed would not have been possible.

I would also like to thank to the colleagues involved in the IWAS Project, for the good cooperation and particularly for the colleagues in the Lviv Ivan Franko National University, especially to Maria Tarasiuk, Myron Kit and Andriy Mykhnovych.

Special thanks goes to the SWAT model community, particularly all of those that joined in the past years the SWAT-DE community and contributed to problem solving of so many modellers, me included.

I would like to acknowledge Nicola Fohrer and Martin Volk for agreeing to serve as referees and for all the encouraging words throughout the years.

Last but not least to my family. Thank you Mother for the empowerment you give me in life, for taking over the children during intensive writing time periods. Thank you Irmhild Wahren without your help I could not have embarked in so many field trips over the years. To my three children, thank you for being the most wonderful distraction.

And above all thank you to my husband Andreas, your support both on private as on professional level is essential. Thank you for always taking the time to wholehearted listen to my doubts and objectively solve them. Your motivating nature gets me back on track and inspires me to pursue the goals I've outlined.

Summary

Pollution of surface and groundwater, due to improper land management, has become a major problem worldwide. Integrated watershed modelling provides a tool for the understanding of the processes governing water and matter transport at different scales within the watershed. The Soil Water Assessment Tool (SWAT) has been successfully utilized for the combined modelling of water fluxes and quality within a large range of scales and environmental conditions across the world. For suitable assessments integrated watershed models require large data sets of measured information for both model parameterization as for model calibration and validation.

Data scarcity represents a serious limitation to the use of hydrologic models for supporting decision making processes, and may lead unsupported statements, poor statistics, misrepresentations, and, ultimately, to inappropriate measures for integrated water resources management efforts. In particular, the importance of spatially distributed soil information is often overlooked.

In this thesis the eco-hydrological SWAT model was been applied to assess the water balance and diffuse pollution loadings of two rivers within a rural context at the mesoscale watershed level: 1) the Western Bug River, Ukraine, 2) the Água River, Portugal. Both watersheds in focus serve as examples for areas where the amount and quality of the measured data hinders a strait forward hydrologic modelling assessment. The Dobrotvir watershed (Western Bug River, Ukriane) is an example of such a region. In the former Soviet Union, soil classification primarily focused on soils of agricultural importance, whereas, forested, urban, industrial, and shallow soil territories were left underrepresented in the classification systems and resulting soil maps. Similarly the forest-dominated Água watershed in North-Central Portugal is a second example of a region with serious soil data availability limitations.

Through the use of pedotransfer functions (PTFs) and the construction of soil-landscape models the data gaps could be successfully diminished, allowing a subsequent integrated watershed modelling approach. A valuable tool for the data gap closure was the fuzzy logic Soil Land Inference Model (SoLIM) which, combined with information from several soil surveys, was used to create improved maps. In the Dobrotvir watershed the fuzzy approach was used to close the gaps of the existing soil map, while in the Água watershed a new soil properties map, based upon the effective soil depths of the landscape, was constructed.

While the water balance simulation in both study areas was successful, a calibration parameter ensemble approach was tested for the Água watershed. In the common modelling practice the individual best simulation and best parameter set is considered, the tested approach involved merging individual model outputs from numerous acceptable parameter sets, tackling the problematic of parameter equifinality. This procedure was tested for both original soil map and the newly derived soil map with differentiation of soil properties. It was noticeable that a better model set-up, with a better representation of the soil spatial distribution, was reflected in tighter model output spreads and narrower parameter distances.

A further challenge was the calibration of water quality parameters, namely nitrate-N in the Dobrotvir watershed and sediment loads in the Água watershed. The limited amount of water quality observations were handled by assessing and by process verification at the smallest modelling unit, the hydrological response unit (HRU). The ruling hydrological processes could be depicted by combining own measured data and modelling outputs. The management scenario simulations showed the anticipated response to changes in management and reflected the rational spatial variation within the watershed reasonably well. The impacts of the different intervention options were evaluated on water balance, nitrate-N export and sediment yield at the watershed, sub-watershed and, when feasible, HRU level.

This thesis covers two regional case studies with particular data limitations and specific processes of water and matter fluxes. Still, data reliability is a problem across the globe. This

thesis demonstrates how relevant it is to tackle shortages of spatially differentiated soil information. The considered approaches contribute toward more reliable model predictions. Furthermore, the tested methods are transferable to other regions with differing landscape and climate conditions with similar problems of data scarcity, particularly soil spatially differentiated information.

Zusammenfassung

Weltweit entstehen Verunreinigungen von Oberflächen- und Grundwasser durch Nähr- und Schadstoffeinträge, die aus der teilweise unsachgemäßen Flächenbewirtschaftung (Land- und Forstwirtschaft) resultieren.

Mit der integrierten Modellierung auf der Ebene von Wassereinzugsgebieten steht ein Werkzeug zur Verfügung, um die Prozesse, die den Wasser- und Stofftransport auf verschiedenen Ebenen innerhalb der Wassereinzugsgebiete steuern, zu verstehen und zu analysieren.

Das Soil Water Assessment Tool (SWAT) wurde weltweit erfolgreich eingesetzt, um Wasserhaushalt und -qualität in unterschiedlichen Zeit- und Raumskalen und unter unterschiedlichen Umweltbedingungen zu modellieren.

Um aus der integrierten Einzugsgebietsmodellierung belastbare Ergebnisse abzuleiten, die als Grundlage für Managemententscheidungen herangezogen werden können, sind sowohl für die Modellparametrisierung als auch für Modellkalibrierung und -validierung große Datensätze (Messdaten, Parameter) erforderlich.

Datenknappheit schränkt den Einsatz integrierter hydrologischer Modelle erheblich ein und kann zu nicht belastbaren Aussagen, unzureichenden Statistiken, Fehlinterpretationen und letztendlich zu unangemessenen Maßnahmen im Rahmen des Wasserressourcen-management führen. Insbesondere die Bedeutung räumlich verteilter Bodeninformationen wird häufig vernachlässigt.

In dieser Arbeit wurde das ökohydrologische SWAT-Modell angewendet, um den Wasserhaushalt und die diffusen Belastungen zweier Flüsse im ländlichen Kontext auf der Ebene von Einzugsgebieten zu bewerten: 1) der Westlicher Bug, Ukraine, 2) der Águeda, Portugal. Beide im Fokus stehenden Einzugsgebiete dienen als Beispiele für Bereiche, in

denen die unzureichende Menge und Qualität der gemessenen Daten eine direkte hydrologische Modellierung erheblich erschwert.

Das Dobrotvir Einzugsgebiet (Westlicher Bug, Ukriane) liegt in der ehemaligen Sowjetunion. Dort konzentrierte sich die Bodenklassifizierung in erster Linie auf Böden von landwirtschaftlicher Bedeutung, während bewaldete, städtische, industrielle und flachgründige Gebiete in den Klassifizierungssystemen und bestehende Bodenkarten unterrepräsentiert blieben. Ähnliches gilt für das walddominierte Águeda Einzugsgebiet in mittleren-Nordportugal. Auch in dieser Region ist die Verfügbarkeit von Bodendaten sehr eingeschränkt.

Durch den Einsatz von Pedotransfer-Funktionen (PTFs) und die Erstellung von Boden-Landschaftsmodellen konnten die Datenlücken geschlossen und ein integrierter Ansatz zur Modellierung der Wassereinzugsgebiete ermöglicht werden.

Ein wertvolles Werkzeug zur Schließung von Datenlücken war das Fuzzy-Logik Soil-Land-Inference-Modell (SoLIM), mit dem, in Verbindung mit Informationen aus mehreren Bodenuntersuchungen, verbesserte Karten erstellt wurden.

Im Dobrotvir Einzugsgebiet wurde der Fuzzy-Ansatz verwendet, um die Lücken der ursprünglichen Bodenkarte zu schließen, während im Águeda Einzugsgebiet eine neue Karte physikalischen Bodeneigenschaften erstellt wurde, die auf den effektiven Bodentiefen der Landschaft basiert.

Die Wasserhaushaltssimulationen in beiden Untersuchungsgebieten waren erfolgreich. Zusätzlich wurde im Einzugsgebiet von Águeda ein Kalibrierungsparameter-Ensemble-Ansatz getestet. Während in der gängigen Modellierungspraxis die jeweils beste Simulation und der jeweils beste Parametersatz berücksichtigt werden, bestand dieser getestete Ansatz darin, die einzelnen Modellergebnisse aus mehreren akzeptablen Parametersätzen zur Lösung des, Äquifinalitätsproblems zusammenzuführen. Dieses Verfahren wurde sowohl für die

ursprüngliche Bodenkarte als auch für die neu abgeleitete Bodenkarte mit Differenzierung der Bodeneigenschaften getestet. Es fiel auf, dass sich ein detaillierter Modellaufbau, der die räumliche Verteilung des Bodens besser wiedergibt, in besseren Modellergebnissen und engeren Parameterabständen resultierte.

Eine weitere Herausforderung war die Kalibrierung der Wasserqualitätsparameter Nitrat-N im Dobrotvir EZG und Sediment im Água Einzugsgebiet. Die begrenzte Menge an Wasserqualitätsbeobachtungen erfordert die Bewertung und Prozessverifizierung in der kleinsten Modellierungseinheit, der Hydrotope (Hydrological Response Unit - HRU). Die vorherrschenden hydrologischen Prozesse konnten durch Kombination von eigenen Messdaten und Modellierungsergebnissen abgebildet werden. Die Simulation verschiedener Managementszenarien errechneten plausible Reaktionen der Einzugsgebiete auf Änderungen im Management und spiegelten die räumliche Variation innerhalb des EZG gut wider. Die Auswirkungen der verschiedenen Interventionsoptionen wurden auf den Wasserhaushalt, den Nitrat-N-Export und Sedimentaustrag auf der Einzugsgebietsebene, der Sub-Einzugsgebietsebene und, sofern möglichr, auf der HRU-Ebene bewertet.

Diese vorliegende Arbeit umfasst zwei regionale Studien mit besonderen Dateneinschränkungen und einem jeweils spezifischen Fokus auf besondere Prozesse des Wasser- und Stofftransportes. Die Zuverlässigkeit von Daten für die hydrologische Modellierung bleibt weltweit ein Problem. Diese vorliegende Arbeit zeigt, wie wichtig es ist, den Mangel an räumlich differenzierten Bodeninformationen zu überbrücken. Die betrachteten Ansätze tragen zu zuverlässigeren Modellvorhersagen bei. Außerdem sind die getesteten Methoden auf andere Regionen und unterschiedliche Landschafts- und Klimabedingungen, insbesondere bei vergleichbarer Datenknappheit, übertragbar.

Erklärung des Promovenden

Die Übereinstimmung dieses Exemplars mit dem Original der Dissertation zum Thema: "Analysis and Model-Based Assessment of Water Quality under Data Scarcity Conditions in two rural Watersheds" wird hiermit bestätigt.

…………………………………………….
Ort, Datum

…………………………………………….
Filipa Isabel Lopes Tavares Wahren

Author Declaration

I hereby declare that the dissertation titled "Analysis and Model-Based Assessment of Water Quality under Data Scarcity Conditions in two rural Watersheds" is my own work. All direct or indirect sources that are used in this dissertation are acknowledged as references. There were no other references and resources used in this work.

………………………………………………

Ort, Datum

………………………………………………

Filipa Isabel Lopes Tavares Wahren

Table of Contents

List of Tables

List of Figures

1.   INTRODUCTION

1.1   Motivation

In many parts of the world the rapid population growth and economic development have led to a growing scarcity of freshwater relative to human demand. According to the *World Health Organization* (2011), water scarcity affects one in three people on every continent of the globe and the predicted change in climate will further exacerbate this situation (European Commission *Environment*, 2011). Chronic water shortages threaten food production and hinder economic development (*Johnson et al.,* 2001). However, water is not only becoming scarce due to an increased demand, but also because of higher pollution levels and habitat degradation (*Johnson et al.,* 2001). Pollution of surface and underground water, due to improper land management, has become a major problem worldwide (*e.g. FAO*, 1996; *Carpenter et al*., 1998). It has been predicted that, as pollution can no longer be remedied by dilution in many countries, freshwater quality will become the principal limitation for sustainable development in these countries early in the 21st century (*FAO*, 1996). Probably one of the most important pressures to water quality is diffuse pollution. As the term "diffuse" suggests it is difficult to locate the specific source of such pollution, notably when it may originate both in urban as in rural areas. In rural areas with predominately agricultural, agro-forestry or agro-pastoral management, the joining of these activities may lead to contamination of waterbodies with pesticides, fertilizers (*e.g.* nitrates), sediment etc.

The Water Framework Directive (*EC*, 2000) has as goal to achieve a good quality of water across the European Union. Under this directive, water management is based on river basins (rather than administrative boundaries), and as a result some watersheds covered by the Directive are partially contained within non-EU countries. As a result there is a need to adapt land management, not only on EU watersheds, but also in cross-boundary watersheds in order to minimize export of nutrients and other chemicals into water bodies. This requires the

development and successful implementation of new concepts of land management and that the knowledge generated about possible solutions, for the improvement of water quality, is well rooted within the originating region (*Leidel et al*., 2012).

1.2   The need of spatially distributed soil data in model based assessments

Soils are a key driver regulating and modifying material and energy fluxes at the earth's surface (*e.g.*, *Gessler et al*., 1995; *Milly and Eagleson*,1987), and therefore obtaining sufficient information on their properties is a pre-requisite for many types of environmental and land management assessments (*Beven and Kirkby*, 1979; *Romanowicz et al*., 2005; *Zhu et al*., 2001). With respect to hydrologic assessments, soil properties are a critical factor controlling streamflow generation processes and the overall water balance (*Merz and Mosley*, 1998). *Milly* (1994) states that the annual water balance is determined by the distributions of water (from precipitation) and energy (potential evaporation) over the land surface, and by the plant-available water holding capacity of the soil.

When considering integrated modelling and simulation of eco-hydrological processes, the availability of spatially distributed soil information is a (*e.g. Mueller et al*. 2008). Analysis of the spatial variability of soil properties is important to explain the site-specific dynamics of ecosystems (*Some'e et al*. 2011). Soil hydraulic characteristics, in particular, are known to be highly variable in space (*e.g. Mallants* et al. 1996; *Hendrayanto* et al. 1999; *Schwärzel et al*. *2009a*). In many regions of the world, the limited availability of soil information may lead to unsupported statements, poor statistics, misrepresentations, and bad resource management.

Soil maps are essential for the spatial modelling of hydrological and biogeochemical fluxes, although, these are often not available area wide. This type of data limitation is a common issue in many areas of the globe, where spatially distributed soil information is scarce and/or incomplete. One reason for this limitation is that conventional soil survey methods are time consuming, labour intensive, and expensive *(Moore et al*., 1993). Scarce soil information is

problematic for making hydrological assessments, as numerous studies have shown the importance of soil input data on modelling rainfall runoff processes (*Becker and Braun*, 1999; *Romanowicz et al*., 2005*; Diek et al*., 2014). For hydrological modelling purposes, a number of soil characteristics are needed (*i.e.*, texture, hydraulic properties, and profile depth) which have a major impact on the hydrological cycle, as they are typically directly correlated with soil moisture variability (*Geroy et al*., 2011; *Vachaud et al*., 1985; *Takagi and Lin,* 2012). *Diek et al.* (2014) show that spatial variations in effective soil depth and hydraulic properties play an important role in the variability of both net bottom out flux and transpiration rates.

Soil maps derived from conventional soil surveys are not designed to provide the same level of spatial detail as information derived from digital terrain analysis and remote sensing techniques (*Quinn et al*. 2005).A digital elevation model (DEM) is convenient for representing the continuously varying topographic surface of the earth and is a globally available data source for terrain analysis, as well as other spatial applications (*Thompson et al.* 2001; *McBratney et al.* 2003; *Behrens et al.* 2010). Common terrain attributes that are readily computed from DEM include slope gradient, slope aspect, and slope curvature, among others. The construction of soil landscape models can be useful, not only to model the spatial distribution of soils, but also to model specific soil properties, including top soil thickness, organic matter content, extractable P, pH, and soil hydraulic properties (*Moore et al.* 1993; *Elsenbeer et al.* 2002).

Soil hydraulic properties play an important role in hydrological modelling. In order to derive this, soil texture data is required. This can be achieved using pedotransfer functions (PTF), which represent relationships between soil hydraulic parameters and easily measurable properties usually available from a soil survey (*Bouma, 1989*). Although, PTFs developed in a region, or from a database, have a limited applicability in other conditions *(Williams et al*., 1992; *Wösten et al.* 2001), by articulating and integrating field surveys, laboratory analyses, PTFs, and modelling techniques it may be possible to expand their practical application potential.

1.3   Framing research projects

The present work was carried out within the framework of the two following research projects:
(I) IWAS, the "International Water Research Alliance of Saxony - Water Research in the Ukraine". Within this project a wide range of fields were investigated *e.g.* focusing on the impacts of climate change (*Pavlik et al*. 2012) to studies addressing the modelling of urban drainage systems (*Blumensaat et al.* 2012) or even capacity building within an IWRM frame (*Leidel et al.* 2012).The overall IWAS project aimed to contribute to an Integrated Water Resources Management approach in hydrologically sensitive regions by developing specific system solutions as a response to some of the most pressing water-related problems of our time. The aspects of this project here presented were included in a work package aiming to assess how severe the diffused pollution has impacted the Western Bug watershed by means of spatially distributed water and matter modelling. The models resultant from the IWAS project research were combined into a toolbox in order to address coupled complex processes in the hydrosphere, especially for the analysis of hydrological systems in sensitive regions (*Kalbacher et al.* 2012).

(II) Água watershed project in Portugal within the frame of two consecutive DAAD-PPP exchange programs together with the University of Aveiro (UA, Portugal). Titles: "Impact of Mediterranean forestry practices on soil hydrological properties: measurement and modelling" (from 2011 until 2012 – Grant Agreement 50750909) and "Impacts of afforestation and climate variability on water related ecosystem services in Mediterranean river basins" (from 2013 until 2015 – Grant Agreement 50736347 and 57156793). The two sub-projects had as main goals quantifying the impact of vegetation cover changes, related with different management practices (notably in eucalypt and maritime pine plantations), on soil structure and hydraulic characteristics; and study how recent afforestation in northern and central Portugal has impacted eco-hydrological processes, and to evaluate the how these impacts have affected the provision of water-related ecosystem services.

The two study sites in Ukraine and Portugal were rural watersheds where water quantity was not the main point of concern. The data scarcity, both for model parameterization (mostly soil related) as for model calibration was a common point in both regions. The two watersheds were taken as case studies despite the differences in landscape and climatic conditions, since these differences may give hints on the methods transferability to other regions. The tackled water quality issues were chosen according to their relevance to the respective watershed.

1.4   Model choice for the representation of rural watersheds

Several authors (e.g. *Young et al*., 1996; *Lal,* 2015; *Liu et al*., 2015) have described the environment as a complex assembly of non-linear dynamic and interacting physical, chemical and biological systems, where still considerable uncertainty about both their nature and their interconnections remains. According to *Young et al.* (1996) this leads inevitably to large, non-linear models which reflect the scientist's perception of the complexity and dynamics of the environment system. Complex distributed hydrological models are valuable tools for land use planning and decision making, in the context of dealing with emerging environmental stressors, such as climate change and water resource competition. In the last decades numerous watershed models have been developed to describe hydrological processes at different temporal and spatial scales (*e.g. Julich, 2009*; *Daniel et al*., 2011; *Jajarmizadeh et al*., 2012). Model approaches allow for the examination of landscape dynamics and ecological processes aiming to get a better understanding of the ruling processes of water flows and matter fluxes. At present, the SWAT model, within the large number of existing watershed models, holds an outstanding usage rate. This model has been widely applied across many climate zones and for a large number of meso-scale rural watersheds tackling problematics from water scarcity to water quality (e.g. nitrate pollution, sediment transport) (e.g. Gassman et al., 2007, *Julich*, 2009, Krysanova and Arnold, 2008; *Bieger et al., 2015*; *Pott and Fohrer*, 2017; *Malagó et al*., 2017). Furthermore, in the review by *Daniel et al*. (2011) the suitability of SWAT to simulate a wide variety of conservation practices and best management practices

(BMP) is illustrated. The popularity of this model may also be brought by the large spectrum of easily accessible resources e.g. free model download (both source code as companion tools), linkage to databases with default parameterization or even community inter-support to overcome model errors.

1.5   Aims of the thesis and research questions

The work here presented focused on testing an approach to analyze the effect of different management practices on water quality parameters through model-based assessment with limited amount of available data for model parameterization and calibration. In detail, this thesis considers model uncertainties brought by data scarcity by examining hydrological processes in two case studies with different water quality focus: at the western Bug River (N pollution), Ukraine; and at the Águeda watershed, Portugal (sediment export to rivers). Under the light of this overall aim the following research questions will be addressed:

1) *Can Soil-landscape models close gaps in spatially distributed soil data for hydrological modelling?*

2) *How adequately could SWAT be parameterized in order to simulate water balance and water quality under data scarcity conditions?*

3) *To which extent does a HRU-based assessment allow model verification under data scarcity conditions?*

4) *Do analysis of observed data and model outputs help to acquire information about ruling hydrological processes?*

5) *Under data scarcity condition, to what extent can the model be used to simulate management scenarios of rural systems?*

1.6 Structure of the thesis

The dissertation is organized in four Chapters. The grand majority of the work presented in Chapters 2 and 3 has been published in three peer-reviewed publications listed as follows:

- Tavares Wahren, F., Julich, S., Nunes, J.P., Gonzalez-Pelayo, O., Hawtree, D., Feger. K.H., Keizer, J.J. (2016): Combining digital soil mapping and hydrological modelling in a data scarce watershed in north-central Portugal, Geoderma, 264, 350-362.

- Tavares Wahren, F., Helm, B., Schumacher, F., Pluntke, T., Feger, K.H., Schwärzel, K. (2012): A modelling framework to assess water and nitrate balances in the Western Bug river basin, Ukraine. - Adv. Geosci. 32, 85–92.

- Tavares Wahren, F., Tarasiuk, M., Mykhnovych, A., Kit, M., Feger, K.H., Schwärzel, K. (2012): Estimation of spatially distributed soil information: dealing with data shortages in the Western Bug Basin, Ukraine. Environ Earth Sci. 65, 1501-1510.

In this dissertation selected Figures, Tables as well as integral text passages of the above mentioned publications have been used. For comprehension purposes, and to avoid methodologic description repetition, the "Materials and methods" Chapter 2 and further "Results and discussion" Chapter 3 were organized by methodology, being then presented the application for each of the research locations. Chapter 2 opens with a detailed study site characterization and data scarcity problematic exposition. Further in this chapter the methodology to handle soil data shortages for hydrological modelling are portrayed and the developed soil-landscape model for each watershed is presented. At the end of Chapter 2 the SWAT model theoretical frame and implementation in both watershed is given. The respective results and discussion follows in Chapter 3. Similarly, this chapter starts by presenting the results, for both watersheds, to bridge the gap of soil information, where soil texture transformations, pedotransfer functions, digital mapping and infiltration experiments are presented. The second large block of Chapter 3 presents and discusses

the results of the SWAT model simulations and scenario implementation. The answers to

the research questions are given in Chapter 4 together with a conclusion and an outlook.

2.   MATERIALS AND METHODS

2.1   Research Location: Western Bug River, Ukraine

The total area of the Western Bug River basin covers 39,400 km^2, which is 19.3% of the Vistula basin. The total length of the river is 755 km, of which 184 km are located on Ukrainian territory and further 185 km mark the border between Ukraine and Poland (*TACIS*, 2001). This work focuses on the Ukrainian portion of the Western Bug River basin until the Dobrotvir Reservoir. Therefore, the watershed in focus was denominated as *Dobrotvir watershed*. The study area (Fig. 2.1), covering about 2,616 km^2, is predominantly a rolling plain with elevations between 200 and 250 m above sea level. It is characterized by a hilly topography and elevations ranging between 300 m and 400 m above sea level at its western and southern periphery (*Schanze et al.*, 2012), a temperate continental climate with an average annual precipitation of 800 mm and an average temperature of 7.1 °C. Loess covers underlain by a highly cracked and karsted limestone and marls from the Upper Cretaceous form the hydrogeological structure of the Dobrotvir watershed (*Terekhanova*, 2009). There is one important tributary in the eastern part of the watershed, Poltva River, which flows through L'viv, the largest city in the Bug watershed with a population of approximately 750,000. Within the study area, nutrients enter the river systems from agricultural land and from obsolete or overloaded wastewater treatment plants (WWTPs) impairing surface water quality. In contrast to the poor water quality status, the river's hydromorphology is primarily of good quality for large stretches (*Zingstra* et al., 2009; *Ertel et al*., 2012; *Scheifhacken et al*., 2012).
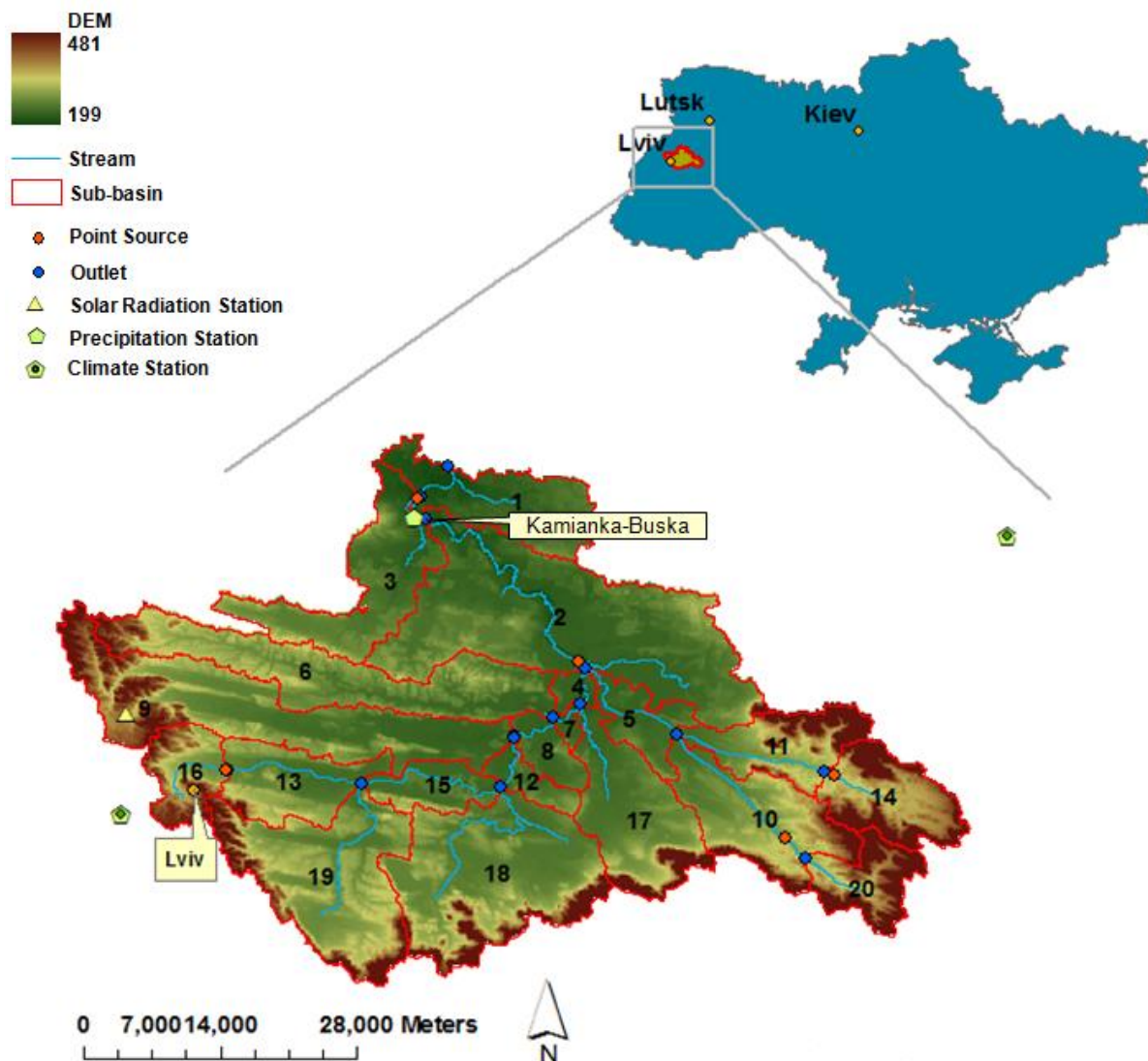
Fig. 2. 1: The Dobrotvir study area in western Ukraine, meteorological stations location and watershed delineation.

The geographical location and natural resources give the western Ukraine a high potential for agricultural activities. Due to the presence of highly fertile soils, the region underwent large scale deforestation and replacement of forests with agricultural activities currently occupying approximately half of the watershed's area (Fig. 2.2). The main agricultural crops growing are winter wheat and sugar beet. *Pospelova* (1997) and *Pospelova and Schinke* (1997) report for these crops yields of 3 ton.ha^{-1}yr^{-1} and 26 ton.ha^{-1}yr^{-1} respectively. The causes for such low yields are manifold. Following the independence in 1991 Ukraine's agricultural sector entered a decade of decline as a result to the severe financial crisis (*Stalnacke et al.,* 2003).
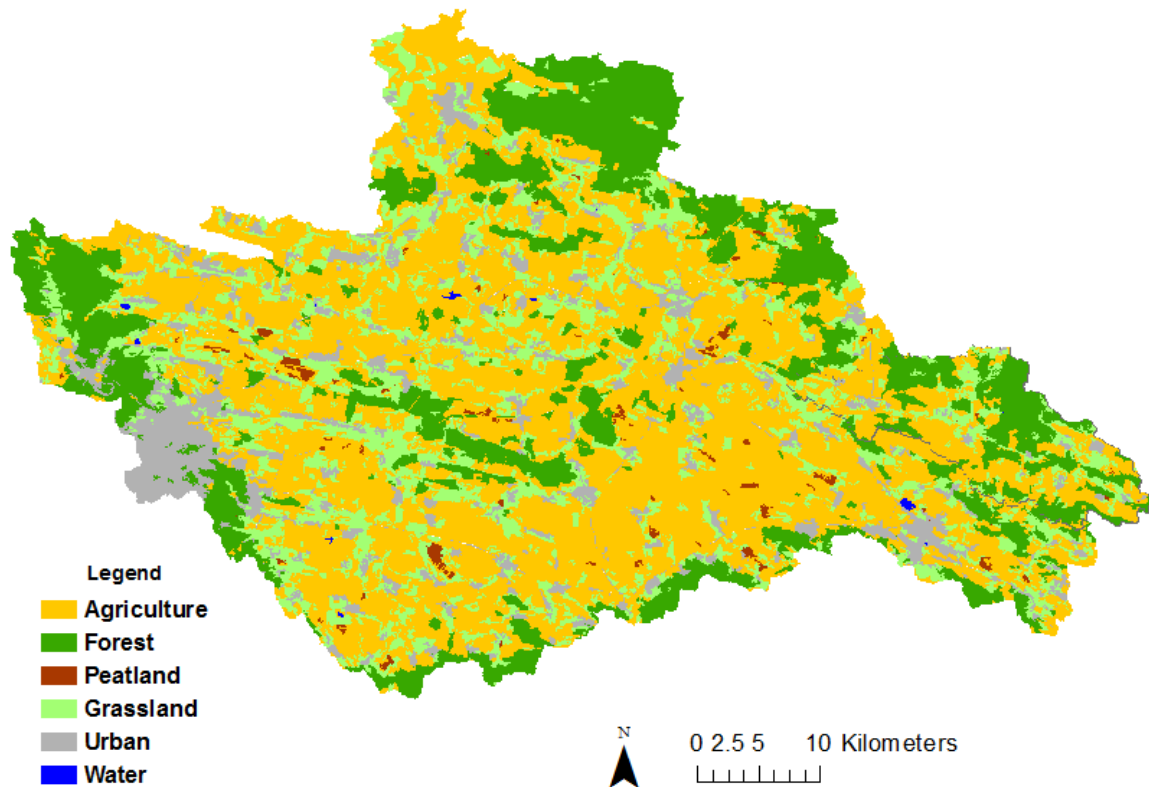
Fig. 2. 2: Land-use distribution in the Dobrotvir study area (*Schanze et al*. 2012).

During the 1990s there was a decline in consumer purchasing power and farm inputs including fuel and fertilizer (Fig. 2.3). Mineral fertilizer use decreased by 85 % over a 10-year period after the political change. Furthermore, with the sharp-fall of livestock production, the availability of cattle manure was greatly reduced (FAO, 2005; Stalnacke et al., 2003).
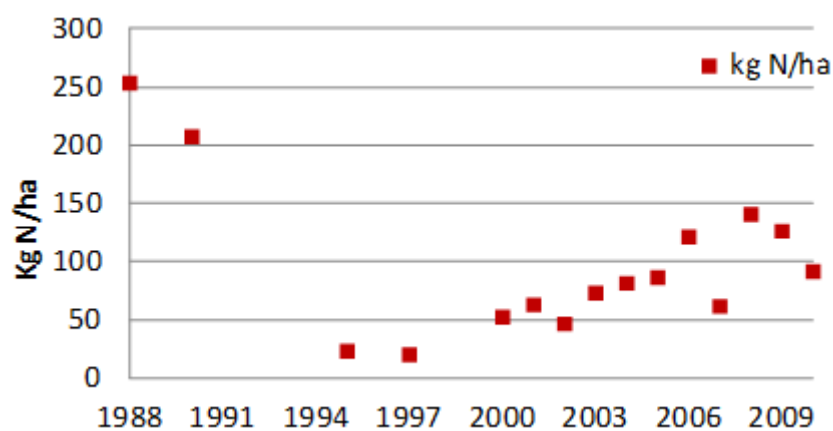
Fig. 2. 3: Mineral nitrogen fertilizer consumption on arable + permanent cropland for the time period 1988 – 2009. Source: Department of Statistics for the L'viv Region.

In the Dobrotvir watershed forest areas occupy only about 20 % of the watershed, other land-uses such as grassland and urban settlements occupy about 19 % and 9 %, respectively.

Given the large size of the Dobrotvir watershed, a sub-watershed of the Western Bug basin was chosen for testing purposes. The 204 km^2 headwater sub-watershed (Fig. 2.4) is located between the Western Bug headwaters, in the Voroniaky Hills (about 400 m above sea level), and the city of Sasiv, in the Male Polissia lowlands (about 250 m above sea level).
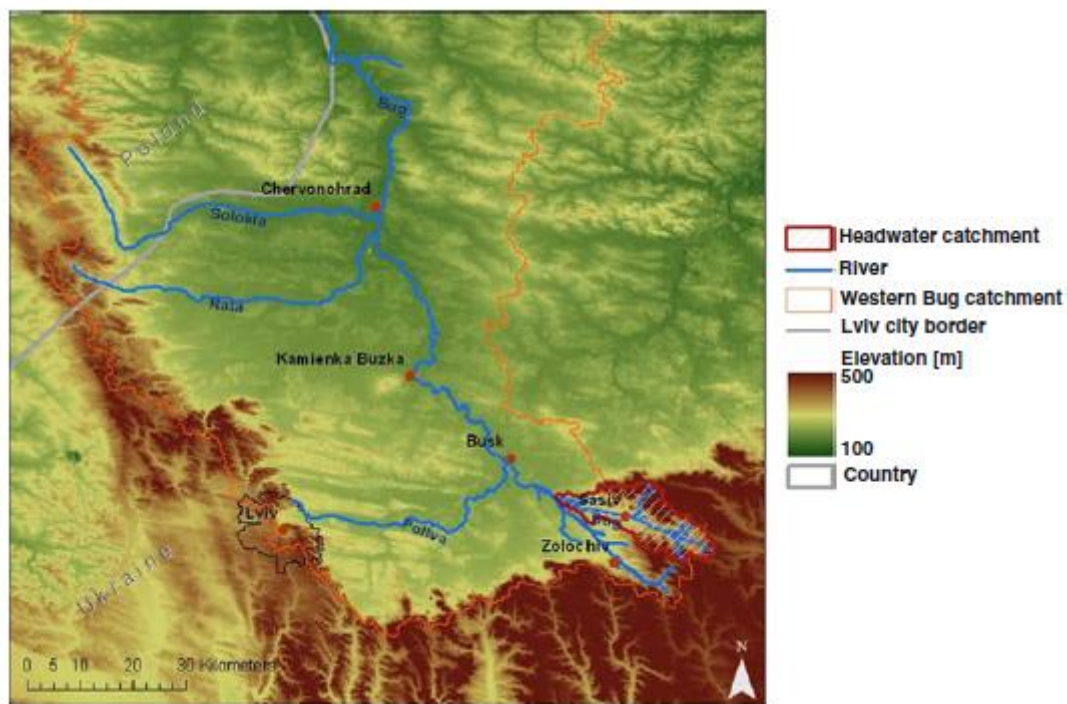
Fig. 2. 4: Location of the headwaters sub-watershed within the Western Bug watershed (ASTER GDEM 30, METI (2009), Landsat 7 2000).

In the past, the sub-watershed was dominated by forestland. However, due to the presence of fertile soils, vast areas were cleared from forests until the 1970s (*Nijnik,* 2017), a trend which could be observed throughout the whole country. This led to new land-use schemes where agricultural activities were predominant, with 39 % of the area being used for crop cultivation. At the present time, 20 % of the sub-watershed's area is occupied by grassland, which mainly results from the abandonment of agricultural practices due to lack of financial support. Nevertheless, forest still occupies 37 % of the watershed, where 29 % of this is made up of deciduous forests with oak, beech, hornbeam and linden trees, and 8 % consists of

conifer forests with mostly *P. Sylvestris* (Fig. 2.5). Within the headwater sub-watershed soils have formed on carbonate rocks, river alluvium, and loess.
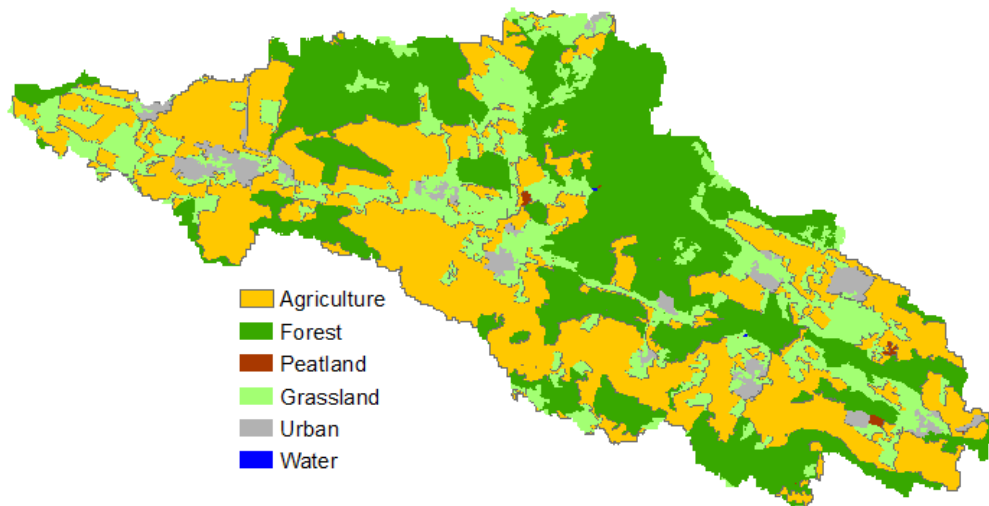
Fig. 2. 5: Land-use distribution in the Sasiv sub-watershed (*Schanze et al*. 2012).

2.1.1 Soil data availability concerns

The Ukrainian soil classification system is based upon the idea that soil types, which are formed under comparable conditions and temperature/moisture regimes, have the same major soil forming processes and similar profile structures (*Krasilnikov et al.*, 2009). However, this classification is often a subjective interpretation of soil genesis by the researcher and was designed to support the mapping of the soils used in agriculture (*Krasilnikov et al.,* 2009). The available soil maps, with a scale of 1:200,000 and 1:10,000, only covers around 21 % and 40% of the respective study areas. Most of the soil information gaps occur in forested areas. Still, the available soil map, produced from conventional soil surveys, contain a wealth of information that served as a starting point for predicting the soil distribution within the watershed.

The main existing soil types (transferred from Ukrainian into the FAO-WRB classification, Krupskyi M.K. L'viv Land Planning Institute) in the Dobrotvir basin are: Haplic Albeluvisols,

Gleyic Phaeozems, Rendzic Phaeozems, Greyic Arenosols, Gleyic Phaeozems, Histosols, Chernozems and Histic Gleysols. The level of detail on the 1:10,000 scale soil map was, as expected, greater than in the large-scale map. However, when examining both maps for the Sasiv region some discrepancies in classification were found. Generally, Gleyic Albeluvisols areas at the large-scale map were mapped as Gleyic Phaeozems or Haplic Albeluviols at the detailed soil map and Chernozems to be either Histosols or Rendzic Phaeozems. During the field campaigns (described below) the sampling points matched primarily the 1:10,000 soil map classification. Therefore, the gap filling approach was applied based on the detailed soil map and tested in the Sasiv region before extrapolation was done for the Dobrotvir basin.

Soil sampling

The predominant soil map units, including Rendzic Phaeozems, Greyic Arenosols, Haplic Albeluvisols, Gleyic Phaeozems and Histosols, were examined to gain a better understanding of the Ukrainian soil classification/soil maps. For this purpose, eight soil pits were opened incorporating a land-use gradient. These soil profiles were described according to the specific guidelines in Ukraine (*Publishing House of Ukrainian Academy of Agrological Sciences*, 1998) and Germany (KA5: *Boden AG*, 2005). Subsequently, disturbed and undisturbed samples cores, with volumes of 100 cm^3, taken from each horizon were analysed for organic carbon, texture, bulk density, and water retention characteristics. The carbon content of each sample was measured using aVario ELIII. The soil texture was determined according to Katschinski's particle size limits (1, 5, 10, 50, 250, and 1,000 µm) and to the particle size limits (2, 6.3, 20, 63, 200, 630, and 2,000 µm) used in Germany. To analyze particle size distribution, the sieve method was applied for soil particles ranging from 50 to 2,000 µm, while the pipette method was used for particles >50 µm. For the measurement of soil water retention, the dewatering process was performed using ceramic plates connected to a hanging water column down to a pressure of -100 cm, while a pressure cell (Soil Moisture Equipment Corp., Santa Barbara, CA, USA) was used for pressures <-100 cm. The following pressure heads were applied:

log10|h/cm| = 1.0, 1.5, 2.0, 2.5, 3.0, and 4.2. At log10|h/cm| = 4.2, repacked cores (6 cm^3 in volume) were measured using soil from the disturbed samples. To close the gaps in the existing soil map, 34 additional sites of the region were mapped using soil augers. Disturbed samples of the topsoil and subsoil horizons from all sites were taken for the measurement of soil texture, according to the particle size classes according to the standards in Germany, and organic carbon. Seventeen of the 34 sampling points are situated along a transect crossing a valley within the headwater watershed, on a north to south gradient, near Koltiv village. With this approach, factors as relief and parent material, which form the soils in the region, could be studied.

Soil texture transformations

For the use of commonly available PTFs, the soil texture data deducible from existing Ukrainian soil maps/soil databases had to be converted from the texture scheme by *Katschinski* (1956) to the texture schemes used by the appropriate PTFs. *Rousseva* (1997) developed a procedure to transfer data between soil texture schemes that use different size ranges of the particle fractions. In the first step of this procedure, the following exponential functions were used to fit the cumulative particle sizes:

$$F_1(D) = a + (100 - a)D^n\{1 + b\exp(mD)\}^{-1}$$

(eq. 1)

and

$$F_2(D) = a + (100 - a)D^n(1 + bD^m)^{-1}$$

(eq. 2)

where F1(D) and F2(D) are the cumulative percentages of the particle size distribution (PSD) curve, D is the log10 value of the particle size limits (1 μm to 2000 μm), and a, b, m, n are fitted parameters. *Rousseva* (1997) recommended the use of Eq. (1) for fine-textured soils, which are classified according to the USDA texture scheme of loam, silt, clay, silt loam, clay loam, silty clay, and silty clay loam. Eq. (2) can be used for coarse textured soils, classified

according to the USDA texture scheme of sand, loamy sand, sandy loam, sandy clay, and sandy clay loam. In the second step, the found parameters were used to transform the PSD from the texture scheme by *Katschinski* (1956) to texture schemes with alternative particle size limits by simple calculations using both equations. To evaluate the accuracy of the method, the PSDs measured were fitted to Eqs (1) and (2) and then converted to the texture scheme used in Germany.

Water retention and pedotransfer functions

Three different PTFs were applied according to the approaches by (1) *Wösten et al*. (1999) (2) *Walczak et al.* (2004), and (3) *Zacharias and Wessolek* (2007). *Wösten et al*. (1999) developed PTFs for Europe using soil data from 12 European countries (HYPRES database). These PTFs predict the parameter of the van-Genuchten equation to describe the water retention curve, using the percentage of sand, silt, and clay, the amount of organic matter, and the bulk density as predictors. The PTFs by *Walczak et al*. (2004) were developed using soil data from Poland, predicting soil water contents at defined pressure head values. The predictors include the specific surface area, weighted mean diameter of soil particles, and bulk density. Values from the specific surface area were not available for the soils of the region. Therefore, these values were replaced by the calculated values of the geometrical surface area as proposed by *Walczak et al.* (2006). *Zacharias and Wessolek* (2007) developed PTFs using soil data from around the world (UNSODA and IGB-DIS soil data bases), estimating the parameter of the van-Genuchten equation using only the amount of sand, silt, and clay, and the bulk density. The PTFs by *Wösten et al.* (1999) and *Zacharias and Wessolek* (2007) use the texture scheme according to the USDA, whereas the PTFs of *Walczak et al.* (2004) requires the texture scheme used in Poland. Therefore, the measured pore size distributions were converted from the texture scheme by *Katschinski* (1956) to the required texture scheme outlined above.

2.1.2 Stream flow and water quality data availability concerns

Runoff of the Western Bug River basin is characterized by spring and early summer floods and low water levels in summer (*TACIS*, 2001). Continuous runoff measurements are conducted at the gage of Kamianka-Buska (Fig. 2.1) at the daily time step from 1980-2008 and at the monthly time step from 1963-2003, and at the gage of Sasiv at the daily time step from 1980-1997 and the monthly time step from 1963-2000 (*Pluntke et al.,* 2014). During the field campaigns the gauging stations were visited, time at which several questions regarding the reliability of stream flow data arose due to the obvious degradation state of the gauging station (Fig. 2.6).

Fig. 2. 6: Water level at the deactivated Sasiv River gauge. Photo taken in 2009, while there were measurements at this gage until the year 2000.

Lack of data and poor data reliability are major issues confronting environmental research in the Ukraine (*Blumensaat et al.*, 2012). A common constraint to model development and

verification is that water quality and discharge data are often not simultaneously collected at a temporal/spatial resolution which, however, is useful for analysis. This situation was the case for this study with only the monitoring point Kamianka-Buzka having both daily discharge measurements and water quality measurements available. A further limitation is that the water quality measurements were conducted from only once per month to once per quarter year. Further, there were four different institutions responsible for the monitoring of water quality throughout the period from 1978 to 2009. As an example for the recorded data, the empirical distribution function of ammonium based on different measurement campaigns during 1978 to 2009 is shown in Figure 2.7. It is therefore unclear how much of the observed temporal dynamics in water quality is due to changes in land-use and system dynamics caused by the political turnover, and how much is due to the measurement technique of each institution.
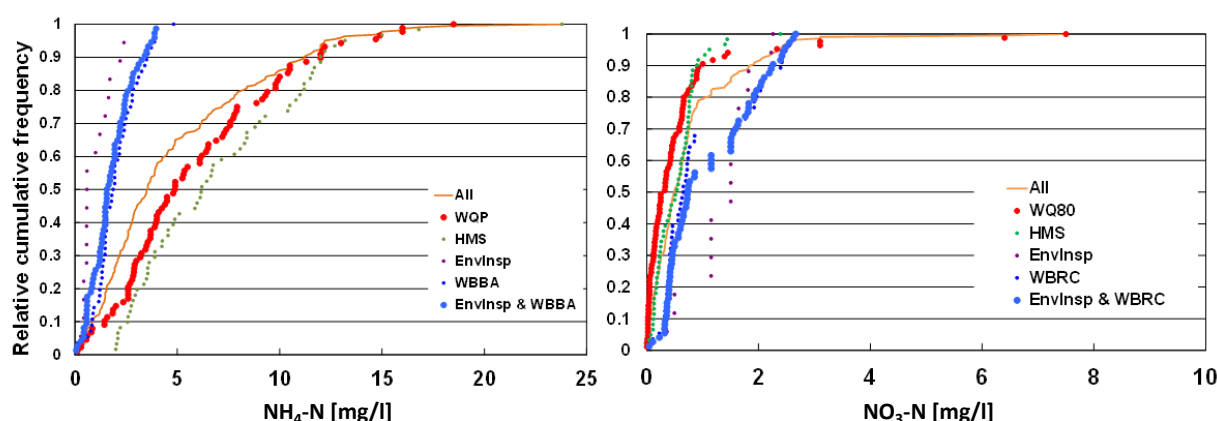
Fig 2. 7: Empirical distribution function of Ammonium-N and Nitrate-N daily measurements for the different monitoring campaigns. Legend: WQP=Water Quality Project (monitoring campaign: 1980–1990); HMS= Hydro-Meteorological Services (monitoring campaign: 1990–1995); WBBA=Western Bug Basin Authority (monitoring campaign: 1994–2008) and EnvInsp = Environmental Inspectorate (monitoring campaign: 2001–2008).

The period studied goes from 1978 to 2010. In this time, a significant politic change was experienced, which led to a series of changes affecting ultimately the watershed's hydrological processes and matter fluxes. The socio-economic modifications resulted in dramatic agricultural practice change with rapid land-use conversions. As a consequence fertilizer utilization decreased and forage was almost entirely eliminated (Fig 2.3).Further, the extensive slaughtering of livestock reduced the amount of available manure (*Stalnacke et al.,* 2003).

These changes are representative of the agricultural dynamics observed in many other countries in Eastern Europe undergoing similar transitions during this time period (*Mander et al.*, 2000; *Pekarova and Pekar,* 1996). Similar changes also occurred in the former German Democratic Republic, as the reunification of Germany led to fundamental structural changes in agriculture (*Meissner et al*., 1998). These studies show that the changes brought about by the political turnover inevitably affected the nutrient export from agricultural land to water bodies. Even though these changes are confirmed by statistics of fertilizer use in the region (Fig. 2.3), the expected water quality improvement on the parameter nitrate-N cannot be observed (Fig 2.8). This can be to a certain extent controlled by the residence time of the groundwater in an aquifer, which can range from months to decades, before discharging to the stream. If this would be the case, then the response to the minimal fertilizer application time period should be at least visible after a given time lag. In the study area, possibly, the time lag still hasn't been accomplished.
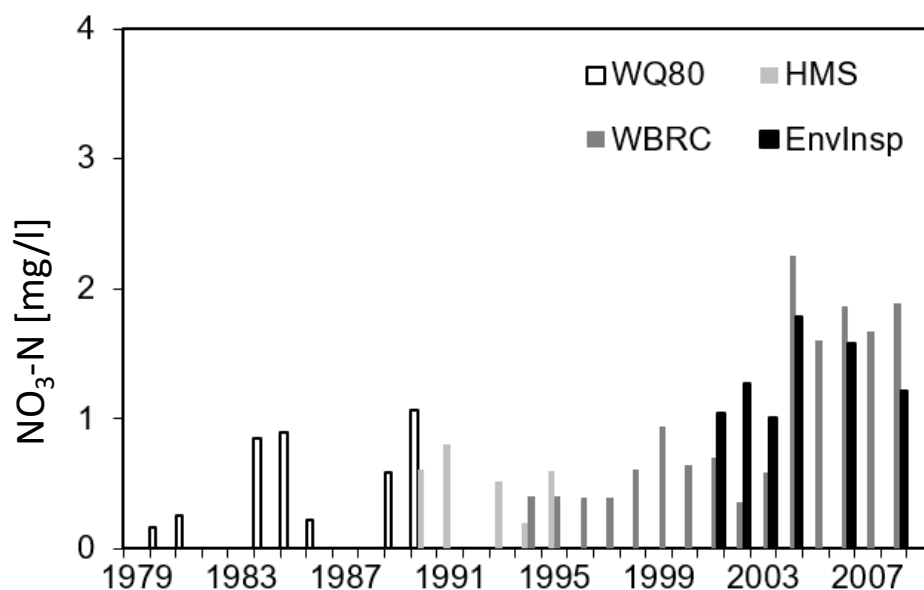
Fig. 2. 8: Water quality during the period 1979 - 2007. The graph shows annual mean concentrations of nitrate-Nat the Kamianka-Buzka outlet. Different monitoring campaigns. Legend: WQP=Water Quality Project; HMS = Hydro-Meteorological Services; WBBA=Western Bug Basin Authority and EnvInsp = Environmental Inspectorate.

Another possibility for this miss match could be caused by poor surveying statistics or by improved laboratory techniques or even both. Still, it is likely that in more recent years the continued reorganization of agriculture has led to increased fertilizer usage and therefore to higher nutrient concentrations.

2.2   Research location: Águeda watershed, Portugal

Located in north-central Portugal, the Águeda watershed (Fig. 2.9) covers an area of approximately 404 km². It merges into the Vouga River system, which has its coastal estuary at the city of Aveiro. The climate of the watershed is wet Mediterranean, with a wet period during autumn–spring (October–April), and a dry, warm period during the summer (June–September). Long-term mean annual rainfall is approximately 1400mmand long-term average monthly temperatures range from 19.8 °C in August to 5.8 °C in January (Leighton-Boyce et al., 2005).
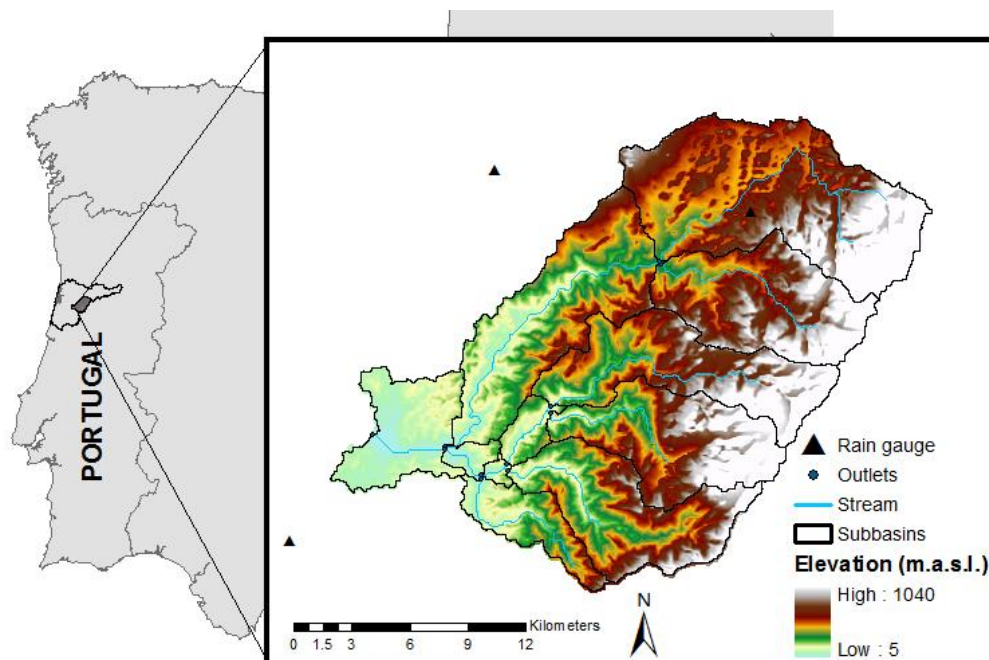
Fig. 2. 9: Location and elevation map of the Águeda watershed in north-central Portugal.

Altitude ranges from < 10 m asl at the watershed outlet, to >1000 m in the Caramulo Mountains. Slope profiles are generally convex-rectilinear and valley-side slopes angles typically around 20°, although 40° slopes are also frequent (Ferreira et al., 2000). According to the Corine Land Cover classification of 2006, almost 46 % of the area is covered by broad-leaved forest. This primarily consists of commercial forestry plantations of *Eucalyptus globulus* (*E. globulus*), planted as monocultures for paper pulp production which are harvested every 7–12 years. A full rotation cycle comprises 2–3 cuts, after which a new stand is planted (Santos et al., 2013) in terraces constructed by heavy machinery, not seldom mixing bedrock fragments and subsoil with the topsoil. New seedlings are generally left to grow unmanaged. Mixed forests (mixed stands of *E. globulus* and *Pinus pinaster*) cover 22 % of the watershed, followed by 14 % of complex agricultural systems (corn, vineyards, and pastures, often in terraced plots), 10 % of coniferous forest (*P. pinaster*), and 6% of transitional woodland-shrub (Fig. 2.10).
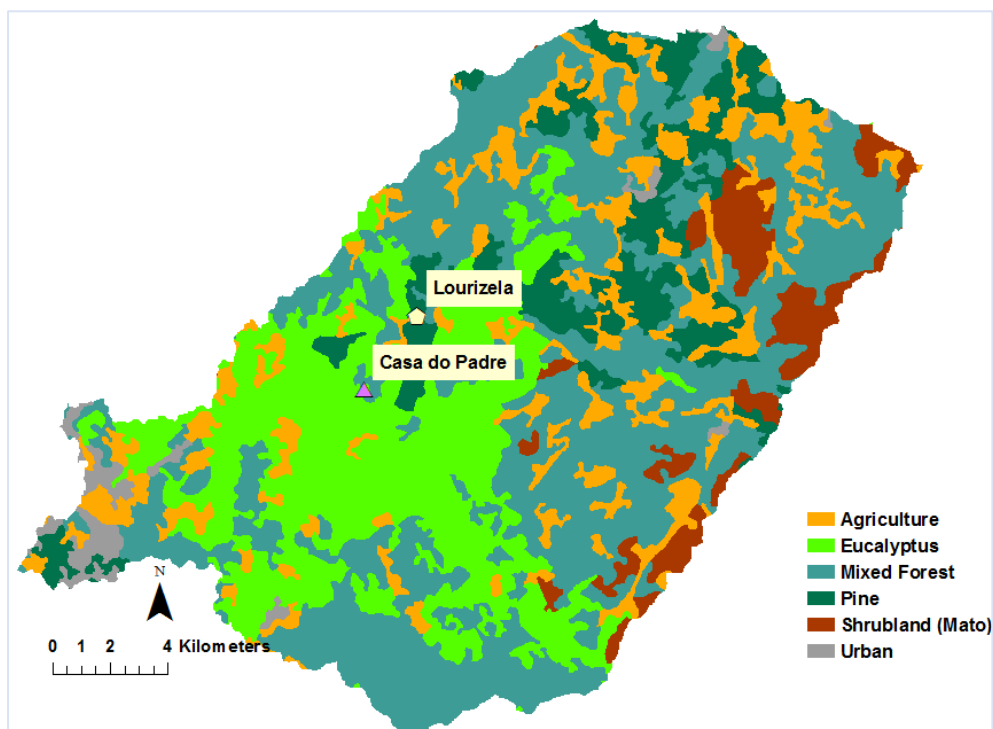
Fig. 2. 10: Land-use distribution on the Águeda watershed and location of the Casa do Padre and Lourizela sites for *E. globulus* and P. *pinaster* plantations, respectively.

The watershed is situated at the Hesperian Massif dominated by Pre-Cambrian metamorphic schists (Fig. 2.11) of the greywacke complex and Hercynian granites at higher altitudes. At lower elevations, and particularly in the floodplains of the main river valleys, the basal unit consists of bedded alluvial deposits, comprising large rounded quartz and quartzite pebbles in a poorly cemented sandy matrix (*Terry*, 1992).

Fig. 2. 11: Slope with *E. globulus* over schist bedrock at the Águeda watershed.

The productivity of the aquifers of the hard rocks of the *Hesperian Massif* is rather low. Studies regarding the capacity of the aquifers under the *Hesperian Massif* show an aquifer productivity ranging from 0.6 to 3 $L.s^{-1}km^{-2}$ (*Martins et al*., 2005). By contrast, the porous sediments show high productivity with a mean discharge of 40.1 $L.s^{-1}$ (*Mendonça et al.*1999). The groundwater depth follows the topographic features. In the valley, the groundwater table is located between 2 and 5 m below the surface and in higher elevated areas up to 150 m deep. In valleys, groundwater level fluctuations between the dry and wet season amounts 3 m and 5 m.

The mean groundwater recharge under both hard rock types amounts to 100 mm.yr⁻¹ year (PBH, 2011). Despite the low aquifer productivity, small-scale agriculture (Fig. 2.12) is highly dependent on groundwater resources for irrigation purposes. Frequently, the groundwater exploitation is uncontrolled, with drilling depths till 100-150 m and exploration up to 300 m (*Martins et al.*, 2005).

Fig. 2. 12: Typical small-scale farms in the Águeda watershed. Rural agricultural areas surrounded by *E. globulus* and *P. pinaster* trees (Photo: L. Bernard-Jannin, 2012).

The Águeda watershed, like the rest of Portugal, is prone to wild fires. Since 1980 the mean annual area burned in Portugal amounts to 1,070 km². This corresponds to around 1 % of the total area of the country and represents by far the highest fire incidence in Europe (*Nunes et al.*, 2005). On June of 1986, a wild fire burned down an area of 52 km² within the Águeda watershed, affecting 13 % of the river basin. Over the past 20 years an area of almost 126 km² of the watershed was burnt (Fig. 2.13). These disturbances have distinct effects on processes like erosion and runoff, having an impact on local water balances in both the short- and long-term perspective. Though the questions brought by disturbances as wild fires may

be scientifically appealing, the direct assessment of the impact of wild fire on water balance and sediment yield was not aim of this work.
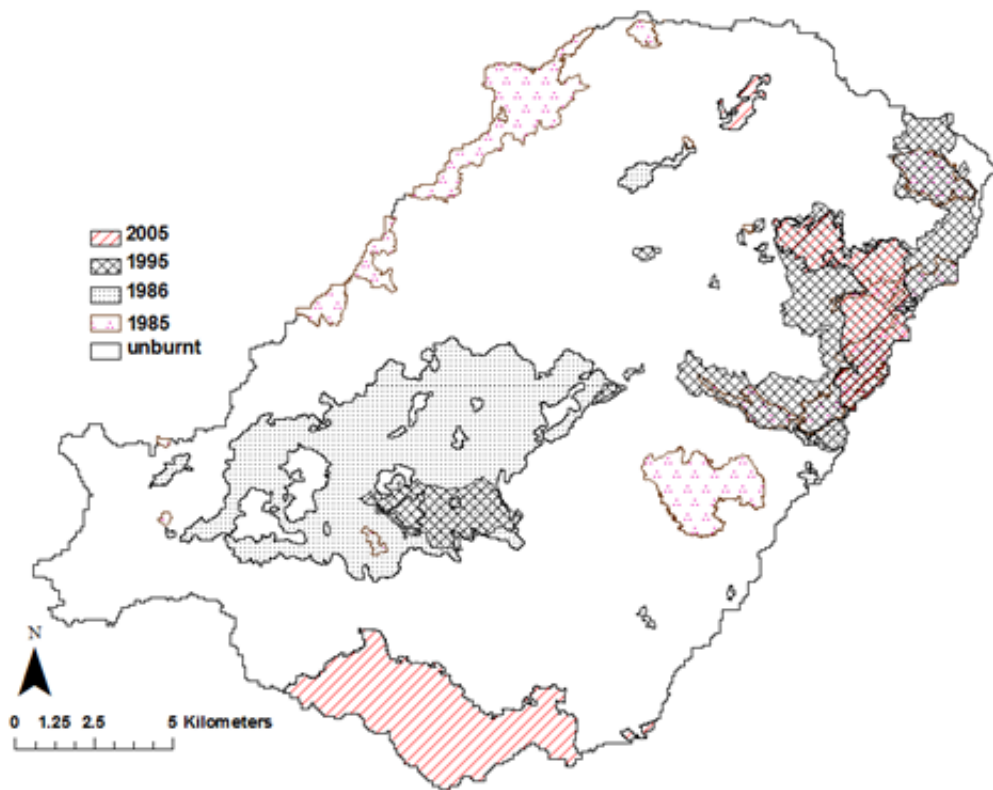
Fig. 2. 13: Areas burnt during the wild fires of 1985, 1986, 1995 and 2005. The extension of the burnt area amounts to 126 km^2 (with 278 km^2 unburnt). Source: ICNF (2015).

2.2.1 Soil data availability concerns

There is a limited amount of spatially distributed soil information available for northern Portugal, and much of the collected data is unpublished (*Pereira and Fitz Patrick,* 1995). According to the Portuguese soil classification system *(Cardoso*, 1974), the soils in the watershed are "Solos Litólicos" (Litholic soils).The available soil map consists of the FAO soil map from 1978, with a scale of 1:1,000,000. The Portuguese portion of this world map was described by *Cardoso et al.* (1973) within the 'Soil Map of Portugal'. According to this map, the soils within the Águeda watershed are mostly classified as Humic Cambisols over granite and schist as parent material. Later field-based soil observations (*e.g.*, *Pereira and Fitz Patrick*, 1995*; Leighton-Boyce et al*., 2005; *Santos et al*., 2013) do not fundamentally diverge

from the soil classifications indicated in the 'Soil Map of Portugal'. However, on steeper slopes, the soils have been described as shallow (30 cm total depth) Umbric Leptosols to Humic Cambisols (*e.g. Leighton-Boyce et al*., 2005; *Pereira and Fitz Patrick*, 1995; *Santos et al*., 2013). They have an A-horizon of 20 to 30 cm, textures ranging from sandy loam to silt loam, no B-horizon, and a high stone content ranging from 15 to 60% by weight. Organic matter content on the surface mineral soil layer ranges from 5–18% (*Leighton-Boyce et al*., 2005; *Keizer et al*., 2008; *Santos et al.,* 2013). On plateaus and in slope hollows, Dystric Cambisols to Humic Cambisols (Bh: FAO code) have been reported (*Terry*, 1992; *Santos et al.,* 2013). These soils have a B-horizon and are characterized by a silt loam to loamy sand texture, with a dark brown 0–20 cm surface mineral soil layer and an underlying 10 – 40 cm stony subsurface layer. The underlying bedrock-horizon is often a soft and weathered bedrock which the plant root can penetrate.
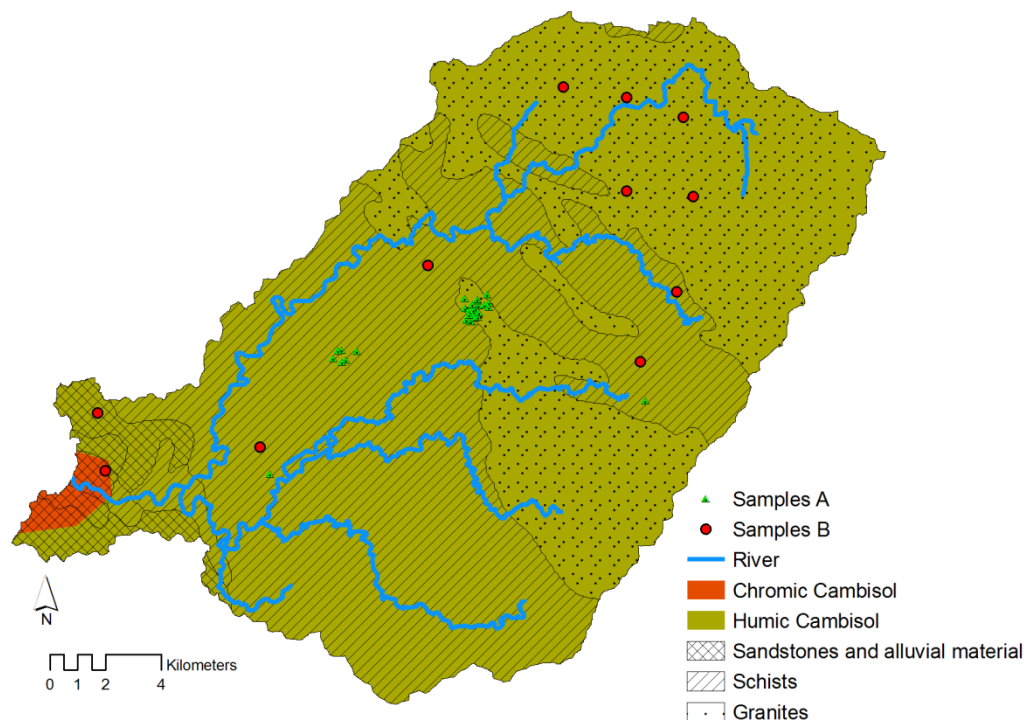
Fig. 2. 14: Soil map for the Águeda watershed clipped from the Soil Map of Portugal (*Cardoso et al*., 1973; Digital Environmental Atlas of Portugal). Samples A represent the locations of samples taken for previous projects in the same study area. Samples B were used to validate the SoLIM-based soil map.

Table 2. 1: Overview of published soil profile characteristics for the Água da watershed and profile information related to the Soil Map of Portugal.

FAO classification (1980)		Coverage	Hr	Sand (%)	Silt (%)	Clay (%)	Lower bound Depth (cm)	Stone content	Parent material	Source
Humic Cambisols		Água da watershed within the 1:1 000 000 Soil Map of Portugal	Ah	59	29	12	45	15*	Schist/ Granite/ Alluvial sands	Cardoso (1965)
			Bw	70	22	8	90	15*		
			Cv	52	38	10	140	60*		
Chromic Cambisol		Água da watershed within the 1:1 000 000 Soil Map of Portugal	Ap	70	21	9	22	22	Alluvial sands	Panagos (2006); Panagos et al (2012); ESDBv2 (2006)
			Bw	63	25	12	65	22		
			C	73	15	12	150	8		
Umbric Leptosols		Plot 40°37′51″N8°18′30″W	A	43	45	12	14	43	Schist	Santos et al. 2013; Gosch (2012)
Humic Cambisols		Plot 40°36′29″N; 8°19′59″W	Ah	29	47	24	24	18	Schist	
			Bw	18	59	23	40	14		
			C	24	57	19	>40	**		
Humic Cambisols		Plot 40°34′52″N; 8°21′42″W	Ah	20,9	64,0	15,1	27	44	Schist	Pereira and FitzPatrick, (1995)
			2Bw	6,1	74,3	19,6	50	21,1		
			2C	12,5	71,6	15,9	90	38,2		
Umbric Leptosols		Plot 40°35′30″N; 8°13′50″W	Ah	72,4	26,6	1,0	30	27	Granite	
			R	-	-	-	>30	-		
		Plot Falgorosa 40" 32' N, 8" 22' W	A	27,3	62,9	9,8	-	-	Schist	Thomas et al. (1999)
		Plot Falgorosa 40" 32' N, 8" 22' W	A	25,1	-69,7	5,2	-	-	Schist	
		Plot Lourizela 40" 38' N, 8" 19' W	A	55,1	40,4	4,5	-	-	Schist	
Umbric Leptosols		Plot Barrosa	A	27,8	58,4	13,8	-	-	Schist	

*- no value available, stone content based on the values for Portuguese Bh soils in the SPADE-2 databank (Hollis et al., 2006; Panagos et al., 2012)

**- high stone content (>60%)

This "softness" is often further enhanced due to soil preparation techniques (rip-plowing prior to planting), which may also explain the high stone content of the topsoil (*Doerr et al.,* 1996). At the watershed outlet, the soils are Chromic Cambisols (Bc: FAO code) to Humic Luvisols. These are deep sandy loam to loamy clay soils with a dark brown, 30 – 70 cm thick A-horizon followed by a reddish brown, 30 – 100 cm thick B-horizon. This study compiled and analysed existing soil data (on soil texture and profile depth) from 32 locations (Fig. 2.14 — samples A) collected by previous projects: IBERLIM (*Coelho et al., 1995a, b*), HIDRIA (*UA,* 2006), SILVAQUA (*Coelho et al.,* 2008), ERLAND (UA, 2008), RECARE (*WU*, 2013). Table 2.1 summarizes the soil profile characteristics observed in the Águeda watershed.

Soil water processes

During the dry season situations of soil water repellency (SWR) have been associated to the *P. pinaster* and *E. globulus* plantations, even under unburnt conditions for the study area (*e.g. Doerr and Thomas*, 2000*; Keizer et al.*, 2005; *Leighton-Boyce et al.,* 2005; *Santos et al.*, 2013) and Portugal in general (e.g. *Ferreira et al.*, 2000). SWR has been reported to alter the infiltration of water and solutes into the soil with important implications for plant growth, surface runoff and soil erosion (*Santos et al.*, 2013). Given this impact on the ecohydrologic behavior, the infiltration process was studied in order to improve the insights of the dynamics brought by the SWR behavior, in two paired-sites with *P. pinaster* and *E. globulus* plantations. This work was conducted jointly with the work reported by *Santos et al.* (2013) and with the work conducted on the supervised Master thesis of *Gosh* (2012).

The experiments conducted were:

- Laboratory analyses for texture, organic carbon, bulk density and water retention characteristics;
- Infiltration tests: the hydraulic conductivity in repellent and non-repellent conditions was measured using mini-disk and double-ring infiltrometers;

- Brilliant-Blue tracer was used to mark infiltration pathways in several soil profiles during soil wetting experiments in repellent and non-repellent conditions.

The two test sites were located in the central region of the Águeda watershed. The Casa do Padre site was dominated by *E. globulus* plantations and the Lourizela site dominated by *P. pinaster* (Fig. 2.10 – see labeled sites). In Casa do Padre the *E. globulus* seedlings were planted after the fire of 1986. These were *E. globulus* of third generation (being the third re-sprout after harvesting), with the last harvesting being in the past 8 years. At the Lourizela site the *P. pinaster* burned in 1991, being at the study time approximately 20 years old. Soils were Umbric Leptosols and Humic Cambisols developed on weathered schist on moderately steep slopes between 300 m and 500 m above sea level as reported in *Santos et al.* (2013).

Soil laboratory analysis

After profile description disturbed and undisturbed soil cores (five samples per diagnostic horizon) were extracted. Disturbed and undisturbed samples cores, with volumes of 100 cm^3, were analysed for organic carbon, texture, bulk density, and water retention characteristics. The water retention curves were determined according to the hanging water column method (*Dane and Hopmans*, 2002) for pF values from 0 until 2 while for values of pF 2 until 4,2 a pressure cell (Soil Moisture Equipment Corp., Santa Barbara, CA, USA) was used. These analyses were conducted during the dry summer season. The bulk density (ρ_b) was obtained by the dry weight/soil core volume.

Infiltration measurements

Top soil Infiltration rates were assessed using the Mini-disk Infiltrometer (MDI) and the double ring infiltrometer. The MDI is often used in the Mediterranean region because the instrument is easily transportable and it is easily fitted to make measurements on slopes due to its relatively small diameter (*González-Pelayo*, 2010). Ten repetitions were conducted in each study site under repellent (dry season – July 2011) and five repetition during non-repellent

conditions (wet season – December 2011) on the soil surface. During the field campaign in December (2011), at the top soil a repellent condition was still found at the *E. globulus* site. Since the soil at the *E. globulus* had further two diagnostic horizons with a non-repellent condition, differently from the *P. pinaster* site, three further infiltration measurements were conducted in each of the lower horizons. Mini-disk infiltrations at the *E. globulus* stand during a non-repellent situation was later on conducted by the team of University of Aveiro, and kindly made available for this work. At the *P. pinaster* site no further infiltration tests in depth were conducted, since the below C-horizon revealed a large amount of stones which hampered the mini-disk placement Infiltration measurements were performed under a pressure of -1.0 cm of water using the method proposed by *Zhang* (1997). This method measures accumulative infiltration in time, which is then fitted to the equation:

$$Inf = C1 \cdot t + C2 \cdot \sqrt{t} \qquad\qquad\qquad (eq.\ 3)$$

Where C1 (m s^{-1}) is related to hydraulic conductivity, C2 (m s^{-1}) is related to soil sorptivity and t(s) is the time. The hydraulic conductivity of the soil (k) is then computed from:

$$K = C1/A \qquad\qquad\qquad (eq.\ 4)$$

Where C1 is the slope of the curve of the accumulative infiltration vs. the square root of time, and A is a correction factor relating the van-Genuchten parameters for a given soil type to the suction rate and radius of the MDI. Since the soil texture was known, the value A was extracted from (DECAGON DEVICES, Pullman, WA, USA).

To assess the field saturated hydraulic conductivity further infiltration measurements using the double ring infiltrometer were also conducted. During repellent conditions five repetitions were done on the *E. globulus* site and two on the *P. pinaster* site. During non-repellent conditions only one double ring infiltration experiment was performed. The small amount of repetitions was brought by the difficulty of finding a suitable location for the installation of the device. These difficulties were mainly due the presence of superficial roots, large stones and slope

steepness. The rate of infiltration was determined as the amount of water per surface area and time unit that penetrates the soil. This was then calculated on the basis of the measuring results and the law of Darcy (Gregory et al., 2005).

Soil water repellency

On both repellent and non-repellent occasions both sites were investigated for SWR and soil moisture contents. In each occasion 5 repetitions in two depths of 2.5 cm and 7.5 cm were conducted. Additionally, three SWR measurements were conducted on the surrounding location of each infiltration measurement. The SWR measurement was carried out with the molarity of ethanol droplet (MED) test (King, 1981) which quantifies SWR as the lowest ethanol concentration permitting droplet penetration within 5 s (Moody and Schlossberg, 2009). Since SWR is strongly related to soil moisture content a time-domain reflectometry (TDR) measurement was done in parallel.

Tracer infiltration experiments

Soil water infiltration patterns were studied by applying the tracer "Brilliant Blue FCF" ($C_{37}H_{34}N_2Na_2O_9S_3$), because it is easily visible in most soils and has frequently been used as a dye tracer to stain flow pathways in porous media (e.g. *Flury and Flühler, 1995*; *Wahren et al.*, 2009). In addition, it has a low toxicity (*Flury and Flühler*, 1994) and a high mobility, due to its high solubility in water (200 gL^{-1}), low octanol-water partition coefficient ($K_{ow} < 10^{-4}$) and anionic characteristics (*Ketelsen and Meyer-Windel*, 1999).

The infiltration experiments under repellent conditions took place in July 2011 at both sites (*E. globulus* and *P. pinaster*). In the *P. pinaster* site, experiments under naturally occurring non-repellent conditions were made in December 2011, while at the *E. globulus* site non-repellent conditions had to be forced in March 2012 by adding a surfactant (Agri II wetting agent) at a concentration of 4 mL L^{-1} to the Brilliant Blue (BB) solution. Agri-II is a non-ionic surfactant

(supplied by Agri-Growth International, Inc., Canada), containing a blend of bio-degradable ingredients: ammonium laureth sulfate (56%); alpha pinene (3%); methanol (3%).

Plots of 2 m^2 without physical boundaries were prepared by removing the organic layer. Subsequently, the tracer (3 gL^{-1} BB) was applied to the surface of the plots (80 L, 60 min, intensity 40 mmh^{-1}) using a watering can. Within each plot of 2 m^2, the central area of 1 m^2 was excavated 2-3 days after the application of BB. The soil profiles were photographed and infiltration fronts were drawn by hand on transparent tracing paper. The tracing paper drawings were then superimposed with a grid with 10 cm x 10 cm cells and photographed again. These images were used for digitization and analysis of tracer profiles.

2.2.2 Stream flow and suspended load data availability concerns

The Águeda River is a left-hand tributary of the Vouga River. The Águeda River with a total course length up to Ponte Águeda of about 37 km follows the slope in SW direction. The drainage density of the watershed is very high, showing a fast response to precipitation events. The discharge starts decreasing in March and decreases until August and begins to increase with the rain season starting in September and October. Hydro-meteorological records for the Águeda watershed were compiled from the "Sistema Nacional de Informação de Recursos Hídricos" (SNIRH: *SNIRH*, 2014) database for period 1979 until 1999 for the gauge stations of Ponte de Águeda (watershed outlet) and Ponte Redonda. Streamflow data for Ponte de Águeda after the year 1999 has a very low quality, owing to the absence of an adequate stage-discharge curve during this period. Streamflow for Ponte Redonda presented a large number amount of gaps and measurements artifacts. This gauge was deactivated on the year 2000.

SNIRH also recorded total suspended solids (TSS) data. This data is a monthly point measurement data from April 1989 to November 2005 at Ponte de Águeda and from 2001 to 2012 at Ponte Redonda (*SNIRH*, 2014). Noticeable is the fact that the TSS measurement start during a period where no simultaneous streamflow measurement is conducted.

2.3   Soil data preparation for model use

2.3.1 SOLIM

The Soil Land Inference Model (SoLIM) (*Zhu*, 1997, 1999; *Zhu and Mackay*, 2001) provides a set of tools for predictive digital soil mapping under the SoLIM framework (http://solim.geography.wisc.edu). The framework utilizes the spatial relationship between the soil feature to be predicted and environmental variables to derive a map of the likelihood of the occurrence of each soil feature across the watershed (*Zhu and Mackay*, 2001). According to *Zhu* (1999) there are two basic types of knowledge, which can be used to establish the relationships between the soil information to be derived and its environmental variables, which, are considered for computing the similarity. The first type of knowledge describes the environmental conditions under which an instance of a particular soil would typically occur, while the second type of knowledge describes how the similarity value will change as the environmental conditions deviate from the typical environmental conditions (*Zhu*, 1999). The SoLIM framework consists of three major components: (i) a similarity model for representing soils as a continuum; (ii) a set of automated inference techniques for mapping soils using the similarity model; and (iii) a set of procedures for deriving soil information products from the similarity model (*Zhu and Mackay*, 2001). A complete description of the SoLIM model can be found in *Zhu et al.* (2007).

2.3.2 The Dobrotvir watershed

The approach was built upon the idea that if the relationship between each soil and its specific environment is known, it can infer which soil might be at each location on the landscape by assessing the environmental conditions at that point. In order to understand how the individual soil classes are associated with environmental conditions, elevation, slope, aspect, landscape position (*METI and NASA*: ASTERGDEM, 2009), and land use (*Schanze et al.*, 2012) the pixel

frequency distribution was derived by environmental conditions within the soil unit polygons from the available soil map. For this purpose the statistical tool, KnowledgeMiner, belonging to the SOLIMsolutions5.0 software package, was used. In addition, local specialists contributed their expertise to further supplement the data. This understanding allowed the establishment of relationships for each soil class/environmental condition pair. The soil distribution was then carried out by implementing a soil-land-inference model (SoLIM) (*Zhu*, 1997, 1999; *Zhu and Mackay*, 2001) where a set of speculative techniques constructed under fuzzy logic linked the characterized environmental conditions with the extracted relationships to infer the spatial distribution of soils (*Zhu and Mackay*, 2001). A spatially continuous similarity value (fuzzy membership values) map was then obtained for each soil unit. The combination of the similarity value maps allowed the construction of a new soil map. This result was validated with information from the 34 mapped sites. A common way to gather information about the continuous soil landscape variation is to construct a catena soil landscape (*Milne*, 1935) model. The Catena model implies an agreement of the soil pattern with a landform crossing from the hilltop to the valley bottom along topo sequences. In our research, 17 soil samples were taken along a north to south transect (Fig. 2.15). It then became possible to identify the five predominant soil units along the transect present at the fragmented soil map of the region. This procedure allowed particularly the investigation of soils under forest.
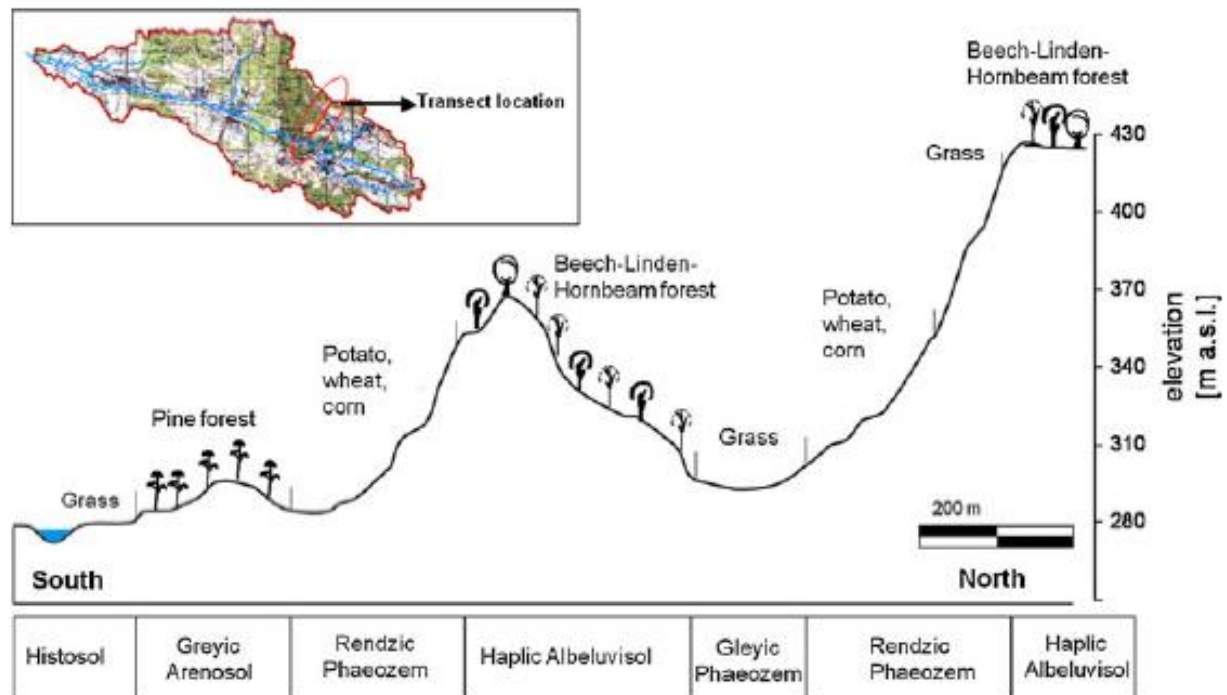
Fig. 2. 15: Location of the investigated transect and soil units distribution along the landscape model. Annotations are in accordance with the FAO-WRB soil classification.

2.3.3 The Águeda watershed

For comprehension purposes the "effective soil depth" is understood as the top soil layers (A and B horizons), which are relevant for water storage and runoff-erosion processes. To create a map of the potential distribution of effective soil depths, the effective soil depths were conceptually divided into three depth classes: (1) shallow: < 30 cm; (2) intermediate: 30–80 cm; and (3) deep: >80 cm. Next, the spatial characterization of effective soil depths was done by assessing how each of the three soil-depth classes change with the following five environmental variables: elevation *(METI and NASA*: ASTER GDEM, 2009), slope angle, plan curvature (slope, and plan curvature were derived with spatial analyst extension of ArcGIS 9.3 software from the elevation raster), land cover (*Corine Land Cover*, 2006), and parent material (*Atlas Digital do Ambiente*: Carta Litológica, 1982). These variables were selected based on field observations at the 32 above-mentioned locations (samples A on Fig. 2.14), and combined with local expert knowledge to establish and extrapolate the relationships to the

watershed where few locations had been studied. Elevation was used to distinguish effective soil depths on the upper portions of the topo sequence (summits, shoulders) from those on the lower portions (backslopes, footslopes, and drainage ways). Slope gradient is especially important for characterizing the steep backslope positions. The plan curvature data layers were used to map effective soil depths that can be separated by concavity or convexity, thus, indicating the likelihood of sediment deposition. Figure 2.16 illustrates the relationship between effective soil depth, landscape position, vegetation, and geology; which represents the knowledge of the implemented soil–landscape model used in the SoLIM approach.

Depth class	Intermediate	Intermediate	Shallow	Intermediate	Deep	Intermediate	Shallow	Deep
Landscape position	Summits	Slope shoulders	Steep backslopes	Intermediate footslopes	Flat terraces	Nose slopes	Backslopes	Footslopes to drainage ways
Geology	Schists, granites	Schists, granites	Schists, granites	Schists, granites	Schists, granites	Schists, granites	Schists, granites	Schists, granites, alluvial deposits

Fig. 2. 16: Conceptual toposequence showing the variation in soil depth classes along an idealized hill slope and associated landscape position, land cover and geology used for the environmental descriptions.

SoLIM-based soil map validation

A continuous similarity map (*i.e.,* "fuzzy membership map") was obtained for each effective soil depth class. In the next step, the fuzzy membership map was "hardened" by assigning the effective soil depth class with the highest membership value to each pixel. In the last step, the

final soil map was created by combining the effective soil depth map with the geological map. The newly derived soil map shall be from this point on referred to as SoLIM-based soil map. The SoLIM-based soil map was then validated at 11 randomly selected locations (Fig. 2.14 — samples B). Validation was done for profile depth, landscape position, land cover, and bedrock geology.

2.4 Eco-hydrological model implementation

2.4.1 SWAT-Model

The hydrological model SWAT (Soil and Water Assessment Tool: *Arnold et al*., 1998, version 2009) was applied to simulate the water balance and matter exports of the study watersheds. SWAT is a process-oriented, semi-distributed and continuous hydrological model. It was designed to simulate the impact of various agricultural management practices on water, sediment, and nutrients in large and complex watersheds, over long periods of time (*Arnold et al*., 1998; *Neitsch et al.,* 2005). The main components of SWAT include water fluxes, climate/weather, and land management. A full description of the model can be found in Arnold et al. (1998) and *Neitsch et al.* (2009). Within the model, soil water storage, surface runoff, crop growth, and nutrient fluxes are simulated for each so-called Hydrological Response Unit (HRU). HRUs are the basic computation units, where it is assumed that soil, land use, and slope are homogeneous. The model's hydrological components consist of surface runoff, percolation, lateral flow, groundwater, evapotranspiration, and channel transmission loss. Surface runoff is estimated using a modification of the Soil Conservation Services (SCS) curve number method (*SCS*, 1972) where daily curve number is a function of plant evapotranspiration. In SWAT, the soil profile is subdivided into multiple layers where the processes of infiltration, evaporation, plant water uptake, lateral flow, and percolation to lower layers occur (*Lam et al*., 2010). Potential evapotranspiration was estimated according to the Penman-Monteith method in the Dobrotvir watershed and Hargreaves method in the Águeda

watershed. The model utilizes as basic soil properties for each layer the individual fractions of sand, clay, and silt, thickness, hydraulic conductivity, bulk density, available water capacity (SWAT terminology for plant available water), and soil organic matter content. Plant available water is the difference between water content at field capacity and at permanent wilting point (pF 4.2). The majority of soil management practices can be simulated in SWAT through direct changes in parameter values (*Ulrich and Volk*, 2009). Many studies have used SWAT to assess the effects of land-use change and management practices (*e.g.*, *Shanti et al.*, 2001; *Ulrich and Volk*, 2009; *Lam et al.*, 2010). The SWAT model monitors five different pools of nitrogen (N) in soils: two inorganic (ammonium, NH_4^+, and nitrate, NO_3^-) and three organic; fresh organic N associated with crop residue and microbial biomass, and active and stable organic N associated with soil humus (*Ulrich and Volk*, 2009). Nitrogen is added to the soil through fertilizer, manure or residue application, fixation by bacteria, and precipitation (*Neitsch et al.*, 2002). Nitrogen losses occur through plant uptake, transport with surface runoff, lateral flow, percolation and with eroded sediment (*Neitsch et al.*, 2002; *Ulrich and Volk*, 2009). SWAT is a flexible tool for scenario simulation that allows the implementation of a wide variety of conservation practices and other best management practices (BMP), such as fertilizer and manure application rate and timing, cover crops (perennial grasses), filter strips, conservation tillage, irrigation management, flood prevention structures, grassed waterways, and wetlands *Gassman et al.* (2007). In SWAT, sediment yield for each HRU is estimated by the Modified Universal Soil Loss Equation (MUSLE; *Williams,* 1975).This equation was modified from the universal Soil Loss Equation (USLE; *Wischmeier and Smith* 1978) where the rainfall energy factor is replaced with a runoff factor. This update of equation improves sediment yield prediction by considering runoff as a function of antecedent moisture condition as well as rainfall energy (*Neitsch et al*, 2011). Sediment routing is regulated by the processes of deposition and degradation. Deposition occurs when the upland sediment load is larger than the transport capacity of the channel and degradation occurring when it is smaller (Bieger et

al., 2012). The transport capacity of a channel segment is calculated as a function of peak channel velocity (*Arnold et al.* 2011).

2.4.2 Model implementation in the Dobrotvir watershed

2.4.2.1   Model set-up

The Dobrotvir watershed was divided into 20 sub-basins. For the period until 1980 - 1991, a traditional agricultural management scheme was assumed. Agricultural areas sum up to 48% of the watersheds area. The agricultural HRUs where distributed by five crop rotation groups (according to FAO, 2005; *Pospelova* (1997), *Pospelova and Schinke* (1997)) in order to assure a realistic spatial crop distribution in the watershed (Table 2.2). These crop rotations have as predominant cultures winter wheat, sugar beet and corn silage (Department of Statistics for the Lviv Region, 2013, *FAO*, 2005). Since no accurate cultivation statistics were available for this time period the management schemes were distributed through all sub-basins.

Table 2. 2: Crop rotation schemes applied to the agricultural lands in the Dobrotvir watershed model.

Year	Crop rotation				
1	Sugar beet	Pasture	Winter wheat	Sugar beet	Spring barley
2	Spring barley	Winter wheat	Winter wheat	Corn silage	Potato
3	Corn silage	Winter wheat	Potato	Pasture	Sugar beet
4	Pasture	Potato	Sugar beet	Winter wheat	Corn silage
5	Winter wheat	Sugar beet	Corn silage	Winter wheat	Pasture
6	Winter wheat	Corn silage	Pasture	Potato	Winter wheat
% of arable land	22	19	25	10	24

Conventional disk bedder and field cultivator operations were applied. During the decades of the 1970's and the 1980's a cultivable land expansion with grain (mostly winter wheat) and technical crops (mostly sugar beet) occurred (*Pospelova,* 1997). This unregulated expansion hindered the correct management of crop rotations. To maintain yields and compensate for the degrading soil fertility loss, large amounts of fertilizers were applied mineral-N fertilizer amounts have been reported to range during this period from 140 kg N ha^{-1} to 250 kg N ha^{-1} (*Pospelova*, 1997; *WDC*, 2008; Department of Statistics for the Lviv Region, 2013). Organic fertilizer application was also largely used during this period with ranges going from 3 ton.ha^{-1} to 20 ton.ha^{-1} cattle manure (*Pospelova,* 1997; *FAO*, 2005) for winter wheat and until 40 ton.ha^{-1} cattle manure for sugar beet (*Pospelova and Schinke*, 1997). In the simulated crops a fresh manure use of 20 ton.ha^{-1} was allowed for winter wheat and sugar beet, this corresponds to a total of around 100 kg N ha^{-1}.The management operations for the different crops growing can be viewed in Table 2.3. A pasture crop was introduced in the rotation to reproduce a non-managed fallow land year between corn silage and winter wheat.

The forest management was assumed to be close-to-nature. As in other groundwater-influenced lowland regions, drainage systems are important landscape features, which have a major impact on hydrological flow pathways (*Stone and Krishnappan*, 2002). *Kiesel et al.* (2010) show the importance of taking such systems in hydrological modelling by comparing how flow components were affected through the incorporation of drainage in the model setup. Drainage system distributions in the study watershed were analysed by *Terekhanova* (2009).

Based on this spatial distribution, new agricultural and pasture land-use classes with a drainage marker were created for better model calibration. Slopes were divided into three classes: until 6 %, between 6 and 12 %, and above 12 %. Point source effluents were used as input data for the simulation to represent the five wastewater treatment plants present in the watershed. Point-source effluents were used as annual estimated averages for flow and N loadings based on a correlation with population data according to Helm (2010) and Terekhanova et al. (2009).

Table 2. 3: Operation schedules for the growing crops in the Dobrotvir watershed.

Year*	Crop	Operation	kg Nha^{-1}	Time period**
0		Tillage (disk bedder)		2W.AUG
0		Fertilization - fresh manure	100	2W.AUG
0	Winter wheat	Planting		2W. SEP
1		Fertilization - elemental N	60	1W.MAR
1		Fertilization - elemental N	50	1W.APR
1		Fertilization - elemental N	30	1W.JUN
1		Harvest and kill		1W.AUG
0		Tillage (disk bedder)		1W.OCT
0		Fertilization - fresh manure	100	2W.OCT
1		Tillage (field cultivator)		1W.MAR
1	Sugar beet	Planting		2W.MAR
1		Fertilization - elemental N	120	2W.MAR
1		Harvest and kill		2W.SEPT
0		Tillage (disk bedder)		1W.OCT
0		Fertilization - fresh manure	40	2W.OCT
1		Tillage (field cultivator)		1W. APRL
1	Corn silage	Planting		2W. APRL
1		Fertilization - elemental N	100	1W.MAR
1		Harvest and kill		2W.AUG
0		Tillage (disk bedder)		2W.AUG
0		Fertilization - fresh manure	40	2W.AUG
1		Tillage (field cultivator)		1W.MAR
1	Spring barley	Planting		1W.MAR
1		Fertilization - elemental N	100	2W.MAR
1		Harvest and kill		2W.JUL
0		Tillage (disk bedder)		1W.NOV
1		Tillage (field cultivator)		2W. MAR
1		Fertilization - elemental N	120	2W.MAR
1	Potato	Planting		2W. APRL
1		Harvest and kill		2W.SEPT

* - the markers 0 and 1 denote the year change

** - 1W: first two weeks of the month; 2W: last two weeks of the month. The target date for the operation was either the 10th or the 20th of the Month. Specific dates were adjusted to exclude days with precipitation before or after.

Table 2.4 presents the input data used by the model in the Dobrotvir watershed. Further constrains to the modelling process are due to that the presence of only one precipitation station within the study area, and the lack of information available regarding to the karst aquifer underneath the watershed.

Table 2. 4: Input data used by the model in the Dobrotvir watershed

Data	Year	Resolution	Source
Digital Elevation Model	-	30 m	Meti and NASA: ASTER GDEM (2009)
Land cover	1989	15 x 15 m	Landsat-7 ETM+, cf. *Schanze et al.* (2012)
Soil	-	1: 200,000	Krupskyi M.K. L'viv Land Planning Institute
Climate data (temperature, precipitation, wind speed, humidity, sunshine duration)	1971-2010	Time series – daily values	*ECA&D* (2010) and *NOAA* (2011), Climate Station University L'viv
Stream flow	1980-1998; 2006-2010	Time series – daily values	Hydrometeorological Services L'viv
Water quality	1978-2009	Daily values – irregular periodicity	Cf. Fig. 2.8
Sewage disposal	1979-1991	Annual averages	Vodokanal L'viv

2.4.2.2 SWAT model calibration and validation

Since significant changes in nutrient fluxes occur after 1991 with the collapse of large-scale organized agriculture, model calibration and validation was conducted for the period until the dissolution of the Soviet Union, from 1980 to 1985 and from 1986 to 1990, respectively.

Calibration and validation of the water balance was conducted, from 1980 to 1985 and from 1986 to 1990 respectively, using data from the gauge at Kamianka-Buzka. The Sequential Uncertainty Fitting, ver. 2 (SUFI-2) procedure of *Abbaspour* (2007) was used for calibration and sensitivity analysis, which has been shown by numerous studies to be an efficient method for watershed model calibration (*Abbaspour et al.*, 2007; *Schuol et al.*, 2008; *Faramarzi et al.*, 2009).

Due to data reliability issues (*cf.* 2.1.2.2) nutrient fluxes were limited to the simulation of nitrate-N loads. The punctual concentration data available revealed a bad correlation with the observed discharges, so that the construction of an artificial time series, for auto-calibration, was not feasible. The limited amount of observed nitrate data makes application of an

objective function to the simulation output infeasible, therefore after manual calibration for the period 1980-1985, verification was conducted for the periods 1990-1999 and 2001-2011 by plotting the measured data against the simulated time series. An assessment of the nitrogen cycle at the basin and HRU scale was done.

Statistical criteria

To evaluate model performance, three widely used objective functions were utilized (*Legates and McCabe*, 1999; *Krause et al.*, 2005; *Moriasi et al.*, 2007): Coefficient of Determination (R^2; *e.g. Colin Cameron and Windmeijer*, 1997); Nash–Sutcliffe Efficiency (E, *Nash and Sutcliffe*, 1970), the Nash–Sutcliffe efficiency with logarithmic values (LnE: *Krause et al.*, 2005). The R^2 is in statistics the proportion of variance of the dependent variable which is predictable from the independent variable and normally ranges between 0 and 1. In cases where negative R^2 values arise then the mean of the observed data provides a better fit then the fitted function. Parameter E indicates how well a model simulates the observed data as the sum of squared errors between simulated and observed values. The optimal value of E is 1 (*Nash and Sutcliffe*, 1970) and is calculated as:

$$E = 1 - \frac{\sum_{i=1}^{n}(O_i - P_i)^2}{\sum_{i=1}^{n}(O_i - \bar{O})^2}$$
(eq. 5)

with O observed and P predicted values. This objective function tends to emphasize the fit to peak flows in a time series and deemphasize low flows (*Legates and McCabe*, 1999; *Bekele and Nicklow*, 2007). To provide a better measure of low flow fit, *Krause et al.* (2005) suggested the use of LnE, where E is calculated with logarithmic values of O and P. With this calculation runoff values the peaks are flattened and the low flows are kept more or less at the same level, resulting in an increased influence of low flows compared to peak flows (*Krause et al.*, 2005).

2.4.2.3 Intervention options from agriculture and forestry

For the simulation of management options in rural areas at the Dobrotvir watershed for the mitigation of N pollution three scenarios where developed. The first scenario was developed with the intent of reducing the nitrogen input into water bodies from agriculture by reducing the yearly total fertilization application by 15%. The levels of fertilization obtained with this reduction are in agreement with the *KTBL*- Faustzahlen für die Landwirtschaft (2009) and the guidelines of the "Umsetzung der Düngeverordnung" (*Albert et al.*, 2007). In the following this scenario will be mentioned as "15NReduction". A second fertilization reduction scenario was developed by reducing the fertilization amount by 25%. This scenario should create an extreme situation to the model, where nitrate-N reductions should in any case occur, as given the opportunity to assess crop yields under different N situations. This scenario was named "25NReduction".

The third scenario was built with the intent of providing an alternative land use for abandoned agricultural lands (also called marginal lands). In this scenario the of a short-rotation coppice (SRC) plantation of a generic poplar was simulated. SRC crops of fast-growing woody biomass production represents the good source of alternative energy with the potential to replace to a certain extent the usage of fossil fuel, especially for heating purposes. This goes is in agreement with the commitment of the European Council to achieve by 2020 at least a 20 % reduction in greenhouse gas emissions as compared to 1990 while raising the share of renewable energy sources by 20 % (*Directive* 2009/28/EC).

Though the Ukraine is not an EU member, the country has signed the "New Climate Agreement" (*United Nations*, 2015) in New York on 22 April 2016 to slow down the increase of average annual temperatures and replacing the traditional energy sources with renewable ones, including bioenergy and biomass for power (*SEEMLA*, 2016a). According to the REN21 UNECE Renewable Energy Status Report (*UNECE*, 2017) by 2014 the Ukraine obtained around 4% of its energy from renewable sources, even though the share is far from the target,

according to the UNECE report, the Ukraine is a country with high acceptance to the use of renewable energy sources.

In addition to the net CO_2 emission, SRC crops require a reduced chemical input compared to traditional agricultural lands (*Tubby and Armstrong*, 2002). SRC crops are very well suited at taking up nitrogen and are ideal for tackling nitrate pollution. Nitrate retention levels of SRC are larger than for grassland or arable land, even during the winter months due to high uptake of SRC crops (*Haycock and Pinay*, 1992). Short rotation coppices can be grown successfully on a wide range of sites but very shallow and waterlogged soils are best avoided. The prolonged SRC cultivation, especially for very short rotation periods (3 to 5 years), requires an environmentally-friendly fertilization concept. A nutrient recycling method from grey water has been reported (*Aronsson et al*., 2000; *Aronsson and Bergström*, 2001) as being suitable for both plant nutrition and treatment of waste water. A possible negative aspect to the establishment of SRC plantations is the substantially higher water use than that of traditional agricultural crops or grasslands(*e.g. Petzold et al*., 2011).Other authors suggest that SRC in non-water limited sites do not affect the regional water cycle (*Fischer et al*., 2013; *Bloemen et al*., 2017). Despite some risks (especially reduction of groundwater recharge), the targeted use of SRC provides possibilities to control and regulate water and matter fluxes in the landscape. For example, erosion control, water retention in the area (developed root systems decrease surface runoff generation due to increased infiltration), carbon sequestration, and retention of nutrients in the soil (*e.g. Feger et al*., 2010; *Wahren et al*., 2015).

This scenario (SRC) assessed the possible N reduction by replacing in selected marginal agricultural areas the land-use with generic poplar trees fertilized with sewage sludge (Table 2.5). Criticism may arise by attempting to include the application of sewage sludge to SRC crops, since several preconditions need to be gathered, from legislation point of view to the infrastructure needed to carry out such a fertilization activity. Still, several authors (*e.g. Dimitriou and Rosenqvist*, 2011; *Dimitriou and Aronsson*, 2011;) report on the positive effects of applying treated wastewater or sewage sludge to SRC plantations on plant growth while

allowing near to zero leaching of nutrients to groundwater. From an IWRM perspective the scenario contributes to the integration of different sectors *e.g.*: urban water management, economical benefits from biomass production or alternative water treatment.

In the Ukraine around 30 % of the arable land is potentially marginal land (*SEEMLA*, 2016a) mostly due to degradation, abandonment and contamination. *Baumann et al*. (2011) studied the farm abandonment in the L'viv Oblast since the break of the Soviet Union and derived rates up to 50 % farmland abandonment. For this scenario 16% of the watershed (436 km^2) area were declared as suitable marginal lands for SRC crops.
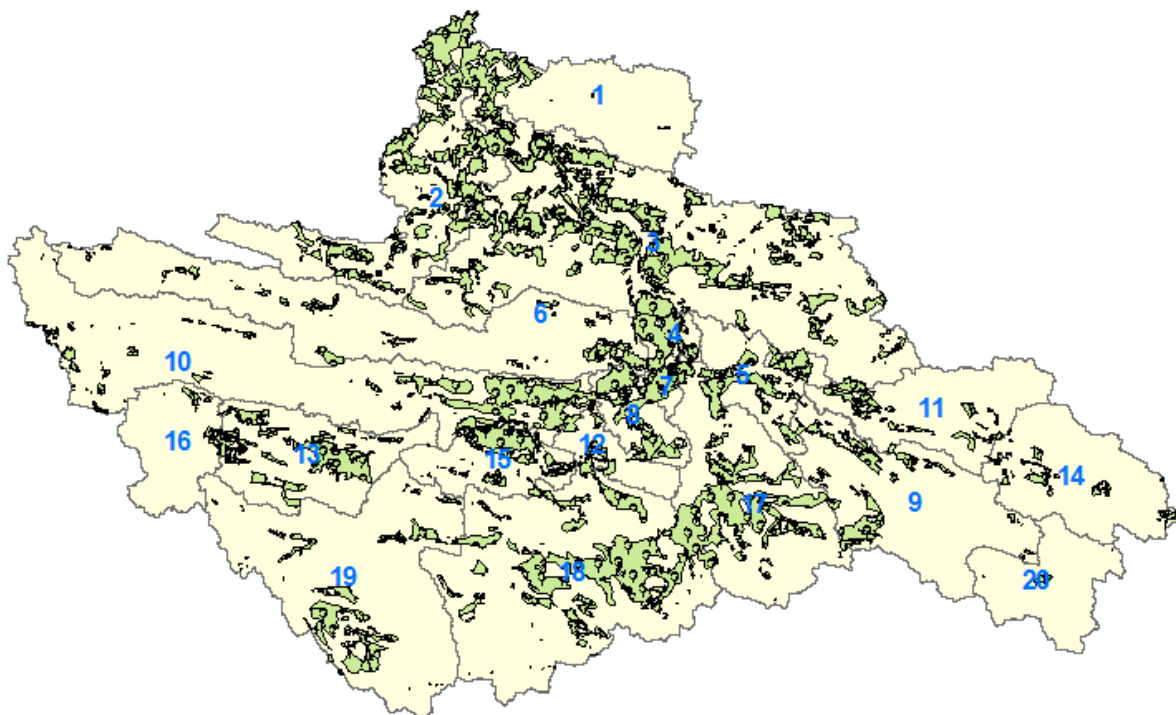
Fig. 2. 17: Short rotation coppice (SRC) crops distribution in the Dobrotvir watershed. Green areas mark the suitable land for SRC plantations.

This is a maximum scenario which, makes use of all suitable areas, while keeping the threshold of land abandonment. These areas have gentle slopes (until 6 %), an agricultural land-use and soil types such as Gleyic Phaeozem, Greyic Arenosol and Endogleyic Arenosol due to the observed deep profiles, sandy loam to silty loam textures, low organic matter content and pH from 6 to 7 (Fig. 2.17).

Several authors reported benefits of fertilization to SRC crops (*e.g. Brown and van den Driessche*, 2002; *Georgiadis et al.*, 2017). Several countries (*e.g.* UK, Denmark, Sweden – *DEFRA*, 2004; *Hall*, 2003; *Aronsson et al.*, 2000) suggest application rates of 70-100 kg N ha^{-1}yr^{-1} since these should on the one hand be beneficial for crop growth, while not resulting in excessive nitrate-N leaching once the crop is established During the month of May a sewage sludge application, with a total N amount of 70 kg N ha^{-1} was included.

Table 2. 5: Nutrient composition of sewage sludge fertilizer included to the SWAT database (Source: IWAS Project; *Helm et al.*, 2013).

Nutrient	Content (fraction)
Fraction of Mineral N (NO3 and NH4) in fertilizer (kg min-N/kg fertilizer)	0.097
Fraction of Mineral Pin fertilizer (kg min-P/kg fertilizer)	0.017
Fraction of OrganicN in fertilizer (kg org-N/kg fertilizer)	0.011
Fraction of OrganicP in fertilizer (kg org-P/kg fertilizer)	0.002
Fraction of Mineral N in fertilizer applied as ammonia (kg NH3-N/kg min-N)	0.8

2.4.3 Model implementation in the Águeda watershed

2.4.3.1   Model setup

For the Águeda watershed, two separate SWAT projects were created, differing only in the soil input data: (1) SWAT-BASE, using the existing 1:1,000,000 soil map; and (2) SWAT-SOLIM, using the SoLIM based soil map. Both soil maps were used to derive the soil parameters needed as input for water balance modelling with SWAT. Table 2.1 provides the different profile information used in the two SWAT projects. The soil profile information used in the model setup include a C-horizon, which represented a fractured bedrock layer where the fraction of soil is very low and is distributed in unconnected pockets. This addition allowed for a better representation of belowground plant biomass development and interflow processes. In SWAT-SOLIM a soil class differentiation by material was done, Humic Cambisols over granite and alluvial sands material were characterized according to Cardoso

(1965), while Humic Cambisols over schist were characterized according to Gosch (2012). Soil hydraulic properties were completed with PTFs according to Nunes (2007) and Gosch (2012). For both projects the watershed was divided into 11 sub-basins (Fig. 2.9). For the SWAT-BASE project, a total of 264 HRU were derived, whereas the SWAT-SOLIM project had a total of 587 HRUs, with the change in the amount of HRUs being due to the higher number of soil classes in SWAT-SOLIM. The combination of the different soil input data and their HRU composition each represent a distinct "model structure". Thresholds for the HRU definition were left at zero %. Both projects utilized: climate from the "Sistema Nacional de Informação de Recursos Hídricos" (SNIRH, 2014) stations ("Campia", "Oliveira do Bairro", and "Pessegueiro do Vouga"); topography (METI and NASA: ASTER GDEM 2009), and Corine land use (CLC, 2006). The mountain hydro-geological system of the Águeda watershed is believed to consist of fractured media with perched groundwater tables, which contributes only a negligible amount to groundwater flow (Coelho et al., 1995a, b).

Table 2. 6: Input data used by the model in the Águeda watershed

Data	Year	Resolution	Source
Digital elevation model	-	30 m	METI and NASA: ASTER GDEM (2012)
Land Cover	2006	1:100 000	AEA: Corine Land Cover (*CLC*, 2006)
Soil	1973	1:1000 000	*Cardoso et al.* (1973)
Climate data (precipitation, temperature wind speed, humidity, sunshine duration); Stream flow	May.1979 - 1996	Daily values	*SNIRH* (2014) -climate stations: "Campia", "Oliveira do Bairro", and "Pessegueiro do Vouga" Stream flow gauge: "Ponte de Águeda" , "Ponte Redonda"
Total suspended solids	1992 – 1996 2001 - 2012	Daily values at monthly time step	*SNIRH* (2014) – gauge "Ponte de Águeda", "Ponte Redonda"

Therefore, a deep impermeable layer was specified for the areas with schist and granite geology, and assumed to be present at 1 m below the soil column. For areas with alluvial sands as parent material no deep impervious layer was specified, since the groundwater table is assumed to be located between 5 to 15 m below the surface (*PBH*, 2012). An identical management scheme was applied to both projects, with a 12-year rotation scheme for *E. globulus*. On arable land, monoculture corn and intra crop rotation of potato and winter pasture (*PBH*, 2012) were simulated. Table 2.6 gives the input data used in SWAT.

2.4.3.2   SWAT model calibration and validation

The two SWAT projects were calibrated and validated using streamflow data from the watershed outlet at "Ponte de Águeda" (SNIRH, 2014). Due to data limitations, two periods with continuous average daily discharge measurements were selected. The longest period, from 1991 until 1995, including wet, average, and dry years was taken for calibration. A shorter (from May to1979 until 1981) independent period was taken for validation of the model outputs at the watershed outlet. To avoid the impacts of initial parameter values on model assessment, a warm up period of two years was set before calibration and validation periods and not included in the analysis. Auto-calibration was conducted using a Monte-Carlo based — Latin Hypercube sampling approach.

For the parameters shown in Table 2.7, the parameter uncertainty bounds were used to generate the 5000 parameter sets for the auto-calibration process (Latin Hypercube sampling *n*=5000). During the auto-calibration procedure, parameter replacement is done independently, without interactions between consecutive parameter substitutions.

After the streamflow calibration, sediment yield calibration was done for the best hydrological fitting parameter set with the SWAT-SOLIM model. The best parameter set was again validated for the gage „Ponte Redonda" for the time period 1993 until 1995 to ensure a fitted water balance at the start of the sediment assessment.

Table 2. 7: SWAT parameter description, lower and upper bounds.

Parameter	Parameter Description[1]	Lower Bound	Upper Bound	Initial value
SURLAG[s]	Surface runoff lag coefficient	0	3	4
SOL_AWC[r]	Available water capacity of the soil layer (mm/mm)	-0.15	0.15	0.13-0.30
SOL_K (no rock)[r]	Saturated hydraulic conductivity (mm/hr)	-0.15	0.15	58 - 79
SOL_K (rock)[s]	Saturated hydraulic conductivity (mm/hr)	100	1000	58 - 79
CH_N1[s]	Roughness coefficient n	0.01	0.3	0.014
CH_K1[s]	Effective hydraulic conductivity (mm/hr)	0	100	0
ALPHA_BF*[s]	Baseflow alpha factor (days)	0.001	0.99	0.048
GW_DELAY*[s]	Delay time for aquifer recharge (days)	0	31	31
GW_REVAP*[s]	Groundwater revap coefficient	0.02	0.2	0.02
GW_QMN*[s]	Threshold depth of water in shallow aquifer for return flow to occur (mm)	0	200	0
RCHRG_DP*[s]	Deep aquifer percolation coefficient	0	0.25	0,.05

1 - Detailed description is available at http://www.brc.tamus.edu/swat/swatdoc.html (Neitsch et al., 2009).

s - Parameter is replaced by direct substitution.

r - Initial parameter value is multiplied by (1+ a given value).

*-The parameter was differentiated for the 3 bedrock geologies in the watershed.

Given the limited amount of available observed data, only a simple model calibration and verification was feasible against the existing discrete TSS observations for the Ponte de Águeda gauge (1992-1996). The Sequential Uncertainty Fitting, ver. 2 (SUFI-2) procedure of *Abbaspour* (2007) was used for calibration and sensitivity analysis of modelled sediment against the punctual observed data.

The calibration parameters are listed in Table 2.8. Sediment routing method was the simplified Bagnold equation (*Bagnold*, 1977; CH_EQN=1) so that the maximum amount of sediment which can be transported is a function of the peak channel velocity. Channel bed degradation can be adjusted for stream bed erodibility and cover (*Neitsch et al.*, 2011).

Table 2. 8: SWAT parameter description for sediment yield, lower and upper bounds.

Parameter	Parameter Description[1]	Land cover	Lower Bound	Upper Bound	Initial value
ADJ_PKR	Peak rate adjustment factor for sediment routing in the sub-basin (tributary channels).	All	0.5	2	0
PRF_BSN	Peak rate adjustment factor for sediment routing in the main channel.	All	0	2	1
SPCON	Linear parameter for calculating the maximum amount of sediment that can be retained during channel sediment routing.	All	0.0001	0.01	0.0001
SPEXP	Exponent parameter for calculating sediment retained in channel sediment routing.	All	1	1.5	1
CH_COV1	Channel erodibility factor.	All	1	20	0
CH COV2	Channel cover factor.	All	1	20	0
USLE_K	USLE Soil erodibility factor	All	0.1	0.3	0.29
USLE_C	Minimum value of USLE C factor for water erosion (factor)	Pasture	0.05	0.15	0.003
		Corn	0.07	0.3	0.2
		Potato	0.07	0.3	0.2
		P. pinaster	0.0001	0.003	0.001
		E. globulus	0.0001	0.03	0.1
		Mediterranean shrub	0.003	0.05	0.004
USLE_P	Support practice factor	Pasture	0.8	0.9	1
		Corn	0.6	0.9	1
		Potato	0.8	0.9	1
		P. pinaster	0.8	0.9	1
		E. globulus	0.6	0.9	1
		Mediterranean shrub	0.8	0.9	1

The ranges for the sediment calibration, particularly USLE parameters were based on past research conducted on the region and from soil erosion studies conducted at European scale (*Panagos et al.,* 2014, 2015a, b). *Panagos et al* (2014) states for northern Portugal a USLE_K value between 0.2 and 0.3. The calibration interval, of this parameter, was allowed to go until values of 0.1 in order to take into consideration deviation brought by soil organic matter, soil

structure and high infiltration capacities along roots and stone fissures. For USLE_C the ranges for the calibration parameter were derived from *Panagos et al.* (2015 a b). Since *E. globulus* was an agroforestry system higher values of USLE_C were allowed. Panagos et al. (2015b) reports values of USLE_P for northern Portugal to present values between 0.6 and 0.9.

Further model verification for the daily sediment yield values was done for the Ponte Redonda gauge (2001-2012). Since no discharge measurements were available, the observed data was used to estimate daily sediment yield values with simulated discharge, which was then compared with the sediment yield modelled by SWAT. To confirm model outputs a HRU-based assessment of results was done.

2.4.3.3   Statistical evaluation criteria and ensemble definition

To evaluate model performance three widely used objective functions were utilized (*Legates and McCabe*, 1999; *Krause et al.*, 2005; *Moriasi et al.*, 2007): Nash–Sutcliffe Efficiency (E, *Nash and Sutcliffe*, 1970), the Nash–Sutcliffe efficiency with logarithmic values (LnE, *Krause et al.*, 2005), and the Root Mean Square Error-Observation Standard Deviation Ratio (RSR, *Singh et al.*, 2004). E and LnE measures are explained in chapter 2.4.2.2.

RSR is calculated as the ratio of the Root Mean Square Error and standard deviation of measured data, as shown in Eq. (2):

$$RSR = \frac{\left[\sqrt{\sum_{i=1}^{n}(O_i - P_i)^2}\right]}{\left[\sqrt{\sum_{i=1}^{n}(O_i - \bar{O})^2}\right]} \qquad \text{(eq. 5)}$$

RSR has an optimal value of 0, and incorporates the benefits of error index statistics and includes a scaling/normalization factor (*Moriasi et al.*, 2007). For each SWAT project, an ensemble of the 10 best-fitting parameter sets was identified, the median streamflow

(ensemble median) and the ensemble stream flow spread (max–min) were calculated. Overall model performance assessment was done for each SWAT project for the ensemble median. Further assessment of streamflow time series was conducted by visual inspection of the daily hydrographs and flow duration curves. For the sediment yield calibration only the R^2 statistical index was used due to the limited amount of observed data.

2.4.3.4   Intervention options from agriculture and forestry

Watershed management options involve introducing best management practices (BMPs) to reduce soil erosion and sediment transport. Two intervention options were developed for the Águeda watershedand are depicted in Table 2.9. The first intervention option (management scenario) explored the efficiency of residue management and zero tillage (RESTILL). Residue management refers to the handling and utilization of plant and crop residues. Particularly, the application of mulch from forest residues has been investigated in the watershed in micro-plots as a way of reducing runoff in post-fire situations (*Prats et al*. 2012). The expansion of this operation from the punctual post-fire management to the yearly executed operations on agricultural areas should not bring great constrains. Since SWAT does not allow residues from one HRU (*e.g.* forest) to be applied on another HRU (*e.g.* agricultural land), this management scenario was conducted by changing the harvest efficiency (HARVEFF) to 10 %. Thus, 90 % of the yield biomass is left on the ground. The following scheduled operation is then a Zero tillage operation (Zero till in till.dat file), where 75 % of the residue is left undisturbed. Zero or minimum tillage practice that the ground is worked very little or not at all before the seed is sown.There is evidence that zero tillage systems may bring benefits to the farmer (in particular on smallholder farms) since crops can be sown almost immediately the previous crop has been harvested while time and financial means are saved (*Rawson and Macpherson*, 2000; *Van Herwaarden et al.,* 2003). Problems as *i.e.* low seed germination and frequent use of herbicides for weed control under the employment of this technique may occur. For the

purposes of the present work the scenarios assessment disregards agricultural productivity and pesticide utilization.

Table 2. 9: Intervention options for the Águeda watershed and SWAT parameterization.

Scenario	Description	Parameter	Applied to HRU	Calibration value	Modified value
BASE	Calibrated simulation for sediments	-		-	-
RESTILL	Efficient residue management and zero tillage	HARVEFF (.mgt)	Corn & Potato	0 (default)*	0,10
		TILL_ID (.mgt)	Corn Soil: Schist Deep & Granite Deep Slope: 0 - 10	1	4
TER	Optimal terrace conservation state	USLE_P (.mgt)	*E. globulus*	0,8	0,2
RESTILL+TER	Simultaneous application of both intervention options	**	**	**	**

* - A value of zero is assumed by the model has a value to be ignored and all yield is removed from the field.
** - As described above

The second intervention option relates to the conservation state of the terraces for *E. globulus* plantations (TER). Terraces are traditional techniques for soil conservation. However, ploughing for terrace construction for new plantations has been found to produce high overland flow and erosion rates for western Mediterranean standards, particularly during the first year after terrace building (*Cerdà et al*., 2009; *Fernandéz-Raga et al*., 2010; *Martins et al*. 2013). The simulation of such single events is difficult and not an aim of this work. Of greater interest for this work is the possible different behavior of the established terraces. *Shakesby et al.* (1994) and *Malvar et al.* (2011) reported sediment losses decline rapidly after rip-ploughing for terrace construction. The authors attributed this to the formation of a protective stone lag, and to the subsequent development of vegetation and litter cover. Still the quality of the implemented terraces should be considered as poor. For this intervention option terraces under *E. globulus* are replaced with reverse-slope bench terraces. For this, the parameter USLE_P was set to 0.2 (*Wischmeier and Smith*, 1978; *Panagos et al*. 2015b).

A third scenario (RESTILL+TER) simulation was evaluated including both developed intervention options.

3.   RESULTS

3.1   Bridging the soil information gap

3.1.1 Western Bug headwaters sub-watershed test site

3.1.1.1   Soil texture transformation

The data set obtained from sampling the soil pits was used to evaluate the accuracy of the procedure developed by *Rousseva* (1997) to transfer data between different soil texture schemes and to test the suitability of different PTFs that were used to predict plausible soil water retention values. The soils of the data set vary in a wide range of organic carbon (0.22–6.66 M %), bulk density (1.00 to 1.53 g cm^3) and soil texture. According to the USDA classification scheme the soil texture can be classified as sand (5 soils), loamy sand (1 soil), sandy loam (1 soil), loam (5 soils), silt loam (7 soils), and sandy clay loam (2 soils). Figure 3.1a shows that equations [1] and [2] are well suited to fit measured cumulative particle size distributions of various textures. The texture data measured according to *Katschinski's* (1956) texture scheme was fitted. Using the obtained parameters (a, b, m, n), equation (1) and (2) was employed to transform *Katschinski's* (1956) texture scheme to the texture scheme used in Germany. In Fig. 3.1 b, the transformed texture data are compared with the texture data independently, measured according to the soil texture scheme used in Germany. The fit was considered valid in the majority of cases.
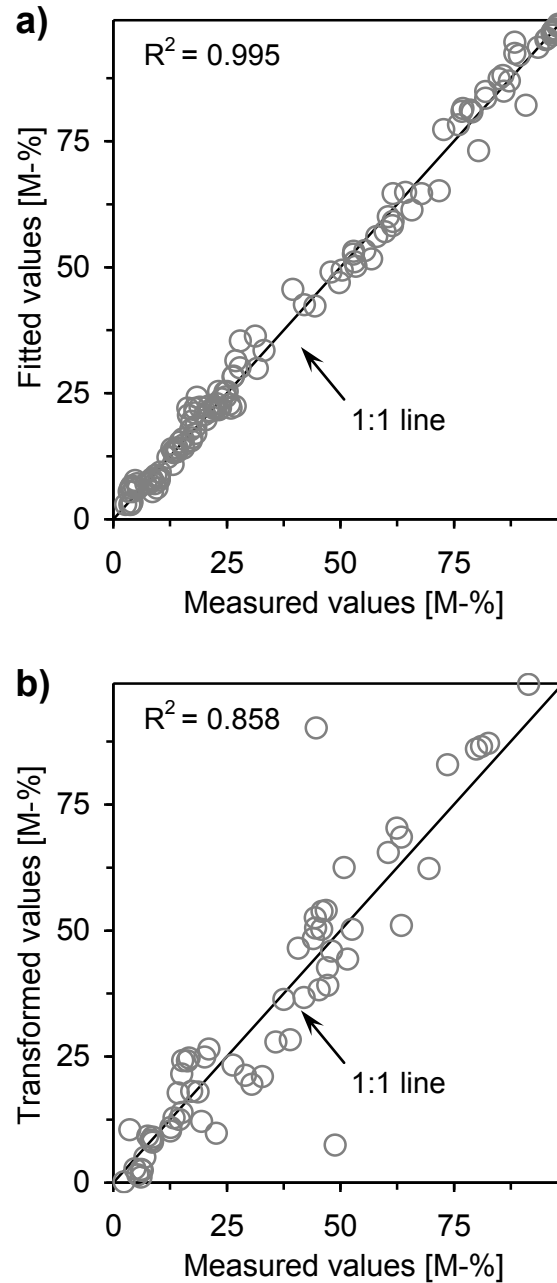
Fig. 3. 1: **a**) Fitted vs. measured values of soil particles for 21 soil horizons from eight sites of the headwater sub-basin (Western Bug watershed, western Ukraine). The soil particle distribution was measured according to *Katschinski's* (1956) particle size limits (1, 5, 10, 50, 250, and 1,000 µm) and fitted to Eq. (1 or 2). **b** Transformed versus independently measured values of soil particles for the same horizons as in Fig. 3.1 a. The soil particle distribution was measured according to the German particle size limits (2, 6.3, 20, 63, 200, 630 and 2000 µm). The transformed values were calculated according to the German texture classification scheme using Eq. (1 or 2) and the parameters obtained by the fit shown in Fig. 3.1 a. In Fig. 3.1 b, the amount of the fraction of clay (particles <2 µm), silt (the sum of particles with a diameter finer than 6.3, 20, and 63 µm), and sand (the sum of particles with a diameter finer than 200, 630, and 2,000 µm) are presented.

3.1.1.2   Pedotransfer functions

A total of 13 horizons from eight soil profiles in the headwater watershed region were used for the prediction of soil water retention by means of different PTFs. In Figure 3.2, water content measured at field capacity at $\log10|h/\text{ cm}|$ = 2.0 and the measured plant available water capacity were compared with the corresponding values estimated using PTFs. The results reveal that all PTFs produced valid estimates of water content at field capacity. However, only the PTF of *Wösten et al.* (1999) estimated the available water capacity with high accuracy. The estimates based on the PTF of *Wösten et al.* (1999) were considered justifiable as the soil texture data measured according to *Katschinski's* (1956) soil texture scheme that had to be converted to USDA texture scheme. The approach of *Wösten et al.* (1999) was applied using the original texture data from *Katchinski's* texture scheme to estimate the available water capacity (prediction not shown). The soil texture data did not reduce the accuracy of the prediction of plant water available when comparison to the prediction based on USDA soil texture. Similar results were reported by *Walczak et al.* (2006) and *Nemes and Rawls* (2006). *Walczak et al.* (2006) illustrated an approach for the prediction of soil water retention curves based on soil data from Spain. They tested its validity for differing soils from Poland. No significant differences in the accuracy of the predicted soil water retention data were detected, although the particle size distributions used in the contrasting systems of Spain (sand: 20–2,000 µm, silt: 2–20 µm, clay: <2 µm) and Poland (sand: 10–1,000 µm, silt: 2–10 µm, clay: <2 µm) were significantly different. *Nemes and Rawls* (2006) evaluated the impact of different representations of the particle size distribution and soil water retention. They found no evidence that using different silt/sand boundaries (20, 50, 63 µm) will result in a significant loss of estimation accuracy. However, it was concluded that using an interpolated soil texture data poses fewer risks when compared to a PTF than using measured data with an incorrect silt/sand boundary.
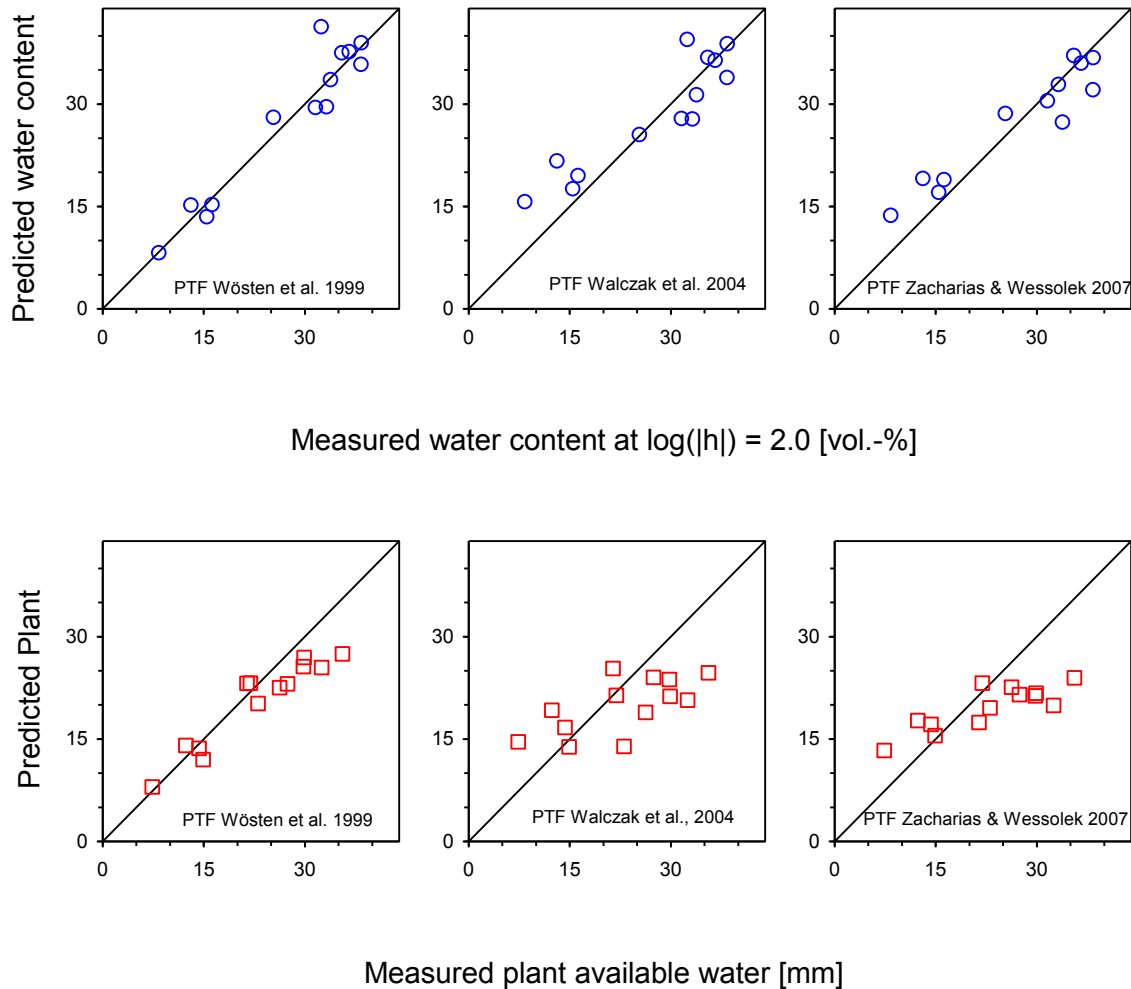
Fig. 3. 2: Measured vs. predicted volumetric water content at log (|h|) = 2.0 (blue circles), and measured versus predicted plant available water (red quadrates) for three different pedotransfer functions (PTF). Thirteen soil horizons of eight sites of the headwater sub-watershed (Western Bug) were examined. Plant available water represents the difference in water content at log (|h|) = 2.0 and water content at log (|h|) = 4.2, where h = pressure head.

3.1.1.3 Soil unit digital mapping

From the 17 samples taken along the soil transect Rendzic Phaeozem soil type was found under agriculture fields on south- southwest steep to toe slopes on calcareous substrates. These soils are generally shallow with a dark humus rich surface horizon (mollic horizon) overlaying carbonated rock. Depending on the relief position, the thickness of the mollic horizon may vary between 30 cm at steep middle slopes and 70 cm at toe slopes. Haplic Albeluvisol was mainly found under beech/linden/hornbeam forests on elevated to steep slope sites. Albeluvisols from loess are characterized by a clay illuviation horizon, which may hinder

root development and drainage. Gleyic Phaeozems occurred predominately under grass on intermontane depressions or valley bottoms where a high wetness index could be observed. The Gleyic Phaeozems formed on loess and in contrast to the Albeluvisols, the deeper layers are more compacted which amplifies stagnant water formation. Greyic Arenosols are well drained, weakly podzolised sandy soils which were mainly found under pine forests in flat slope areas.

Formation of organic soils (Histosols) takes place under the influence of groundwater. Thus, Histosols occur on smooth slope and valley bottom areas, mostly under grass or agriculture fields. The upper peat layers was strongly decomposed, whereas, deeper layers were dominated by sedge and reed peats. From the field survey and fragmented map analysis, a soil landscape model could be derived, which was then used as a base for the SOLIM run. In the new SOLIM derived soil map, five soil units were distributed over 204 km^2 of the headwater's watershed (Fig. 3.3).

The soil landscape model led to the prevalence of Haplic Albeluvisols in high elevation areas and northern slopes, Rendzic Phaeozems were distributed over agricultural land and steep slopes, Greyic Arenosols were prevalent under pine forested areas on flatter regions near the river areas, Gleyic Phaeozems occurred on wet valley bottoms and Histosols on flat river vicinities. Overall, the Haplic Albeluvisols dominated, covering 43 % of the watershed, Rendzic Phaeozems covered approximately 26 %, Greyic Arenosols covered around 16 %, and Gleyic Phaeozems and Histosols covered 8 % and 7 %, respectively. Of the 34 mapped sites, SOLIM inferred the soil unit correctly at 31 sites (91 %).

The mapped transect, covering the transitions between major landscape units, such as ridge top to valley bottom and distance to river, was also accurately reproduced.
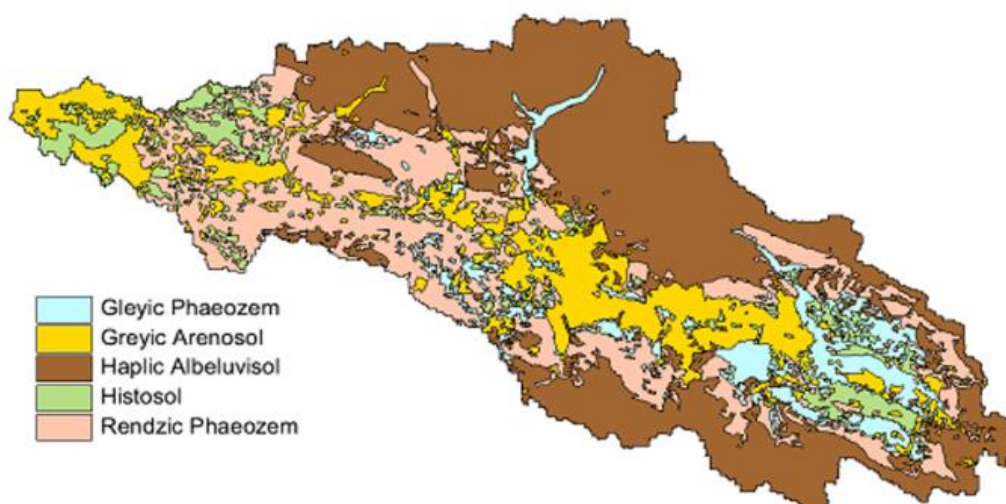
Fig. 3. 3: Distribution of soil units over the headwater sub-basin of the Dobrotvir watershed.

A second SOLIM run was conducted for the whole Dobrotvir watershed, to fill the gaps of the 1:200 000 scale soil map. For this, the five analysed soil units were distributed in gap areas. The resulting soil map of the Dobrotvir watershed (Fig. 3.4) shows a distribution of following soil units: Haplic Albeluvisol (39 %), Gleyic Phaeozem (19 %), Chernozem (13 %), Greyic Arenosol (12 %), Gleyic Albeluvisol (7 %), Histic Gleysol (5 %), Rendzic Phaeozem (3 %) and Histosol (3 %). No verification of the gap filling was possible for the Dobrotvir watershed.
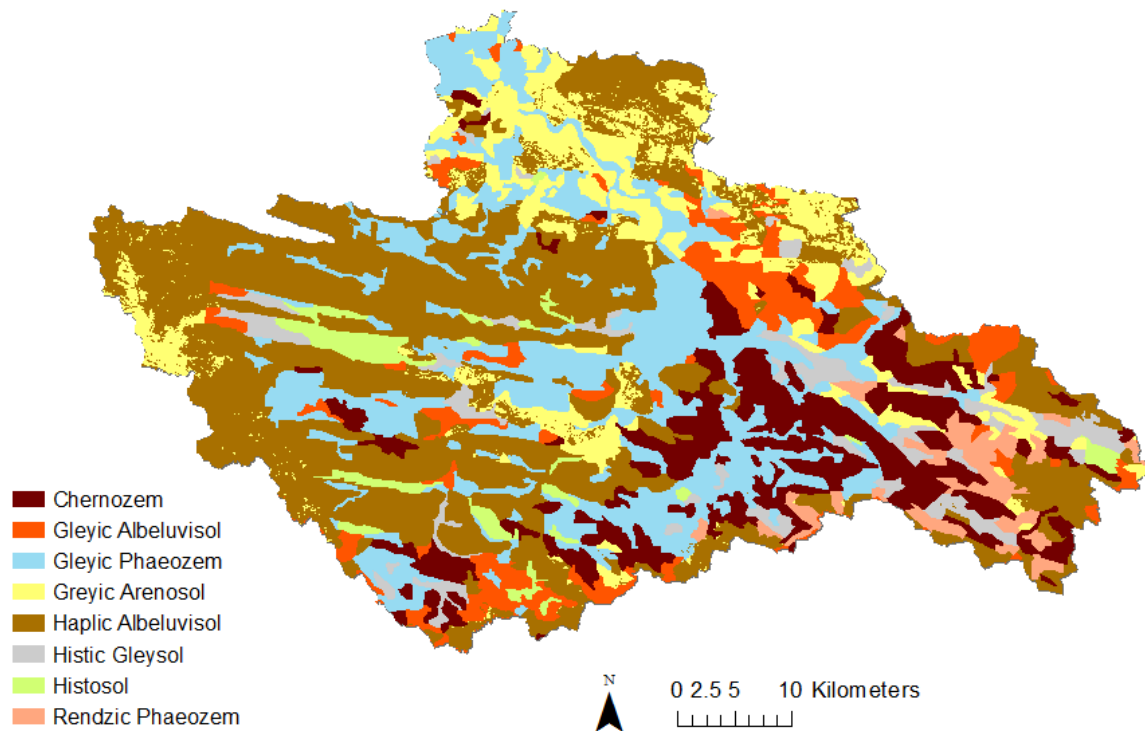
Fig. 3. 4: Distribution of soil units over the Dobrotvir watershed.

3.1.1.4   Plant-available soil water

The amount of soil water available for plants depends on soil structure, texture, and the depth of the root system. However, under humid conditions not all of the available plant soil water stored in the root zone will be extracted by plant roots (*Breda et al.* 1995; *Schwärzel et al.* *2009b*; *Guswa*, 2010). The calculation and evaluation of the amount of potentially available soil water, based on maximum root depth, may lead to a misinterpretation of the quality of a soil with respect to its productivity. Therefore, the concept of effective rooting depth was introduced by *Renger and Strebel* (1980). It was assumed that within the effective rooting depth all plant available water, which is equivalent to the difference in soil water content between field capacity and permanent wilting point, can be taken up. Thus, the effective rooting depth depends on the species and the soil and may be deduced from the depth function of soil water content in groundwater free soils at the end of the growing season in years with high evaporation demand and little precipitation (*Renger and Strebel*, 1980;

McKeague et al. 1984). Therefore, the effective root depth is generally less than the maximum root depth. Estimates of effective root depths for the main land-use types, including crops, grasses, conifers, and broadleaves, in relation to soil texture and bulk density can be found in *Boden AG* (2005). These estimates were used to calculate site-specific plant-available soil water, disregarding capillary rise of water from groundwater, for the investigated soils (Table 3.1).

Table 3. 1: Texture dependent potential available water capacity (AWC) related to maximum root depth in accordance to soil type, landform position, land use, and effective root depth of the headwater sub-basin of the Dobrotvir watershed.

Soil type	Landform position	Land use	Effective root depth (dm)	Potential AWC related to maximum root depth (mm)
Gleyic Phaeozem	Intermontane depressions/valley bottoms	Grass	5	90
		Crop	7	130
		Pine forest	12	205
Greyic Arenosol	Flat plains	Grass	5	85
		Crop	7	115
		Pine forest	12	155
		Deciduous forest	12	155
Haplic Albeluvisol	Slopes	Grass	8	205
		Crops	10	260
		Pine forest	15	415
		Deciduous forest	15	415
Histosol	River near plains/valley bottoms	Grass	4	110
		Crops	6	185
Rendzic Phaeozem	Upper slope/plateaus	Grass	3	80
		Deciduous forest	5	125
	Middle slope/steep slopes	Grass	3	80
	Toe slopes	Grass	5	125
		Crop	7	170

The spatial distribution of plant available soil water within the headwater watershed is presented in Fig. 3.5. The different land-use types taken into consideration were pine forest, grassland, crops, and broadleaf trees, including oak, beech, hornbeam and linden. For the Rendzic Phaeozem soil unit, a further slope differentiation was conducted with the division into upper slope/plateaus, middle slope/steep slope, and toe slope. Overall, nearly two-thirds

of the study area (59 %) was characterized by high to extremely high amounts of plant available soil water. Maximum values for soil water availability were achieved for Haplic Albeluvisols under forested areas, whereas minimum values were observed for Rendzic Phaeozem under grasslands on upper to middle slopes.
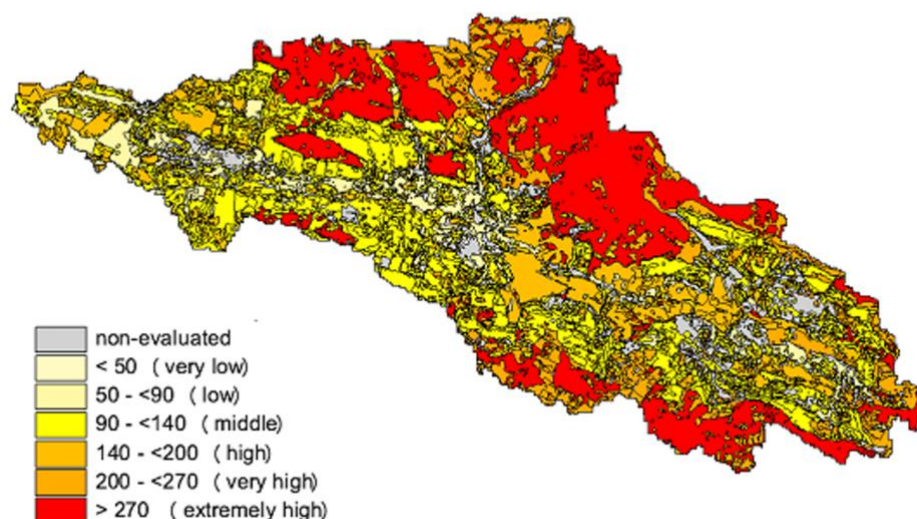
Fig. 3. 5: Spatial distribution of plant available soil water over the headwater sub-basin of the Dobrotvir watershed, disregarding capillary rise from groundwater.

3.1.2 Águeda watershed test site

3.1.2.1 Soil data assessment

Soil laboratory analysis

The results of the texture analysis for both study sites, Casa do Padre (*E. globulus*) and Lourizela (*P. pinaster*), can be seen in Table 3.2. The soils were described as being a Humic Cambisol with three horizons and a depth of 51 cm on the eucalypt site. On the pine site the soil was classified as Umbric Leptosol with an A-horizon over a C-horizon of weathered

bedrock with a depth of 22 cm. The large amount of stones on the C-horizon in Lourizela did not allowed the collection of samples.

Table 3. 2: Site characteristics for the Humic Cambisol in Casa do Padre site and Umbric Leptosol in Lourizela site.

		Lourizela	Casa do Padre		
Horizon		A	A	B	C
Thickness	[mm]	140	200	140	170
Clay	[%]	12,9	24,5	23,5	19,2
Silt	[%]	53,6	57,5	59,2	57
Sand	[%]	34,2	18	17,3	23,8
N	[%]	0,23	0,41	0,38	0,15
C	[%]	4,3	7,0	5,8	2,2
C/N		18,9	17,2	15,4	14,7

Silt was the predominant particle size in both sites and horizons. The greater difference in terms of particle size was the sand content in the pine site. The C/N ratio is similar in both sites, being as expected higher at the top soil as on the lower horizons of the eucalypt site. The low C/N values are within the expected for fertile soils, e.g. Chernozem C/N <10.

From the water retention curve the statistical values, saturation water content (Sat), field capacity (Fc), wilting point (Wilt. P.), dry bulk density (Bd), and plant available water capacitiy (PAWC) were determined (Table 3.3). Porosity was calculated from the bulk density and using a particle density of 2,65 g.cm^{-3} (silica). Taking further in consideration the fitted pF curves (Fig. 3.6) it is noticeable that both sites soil A-horizons (HA) show a similar median saturation and field capacity, whereas Lourizela shows a larger amount in narrow macropores. In Casa do Padre the B and C horizons (HB and HC) show similar hydraulic characteristics. These results may indicate that the different water retention capacity of the sites is less governed by the tree type, in the case *E. globulus* and *P. pinaster*, but by the soil profile depth and landscape characteristics.

Table 3. 3: Site characteristics for the Humic Cambisol in Casa do Padre site and Umbric leptosol in Lourizela site. The values given represent the median of sampling and in parenthesis the mean absolute deviation from the median.

| Horizon | | Lourizela | Casa do Padre | | |
		A	A	B	C
Sat	[mm]	63	88	84	95,2
	m3/m3	0,45 (0,031)	0,44(0,049)	0,59(0,040)	0,56 (0,021)
Fc	[mm]	32,2	46	43,4	56,1
	m^3/m^3	0,23 (0,016)	0,23 (0,031)	0,31 (0,018)	0,33 (0,020)
Wilt. P	[mm]	9,8	28	15,4	22,1
	m^3/m^3	0,07 (0,029)	0,14 (0,050)	0,11 (0,033)	0,13 (0,040)
Bd	[g cm^{-3}]	0,99 (0,012)	0,7 (0,05)	0,94 (0,072)	1,21 (0,032)
PV		0,63 (0,012)	0,74 (0,018)	0,64 (0,028)	0,54 (0,012)
PAWC	[mm]	22,4	18	28	34

Sat - saturation water content; Fc - field capacity; Wilt. P - wilting point; Bd - dry bulk density; and PAWC - plant available water capacitiy.
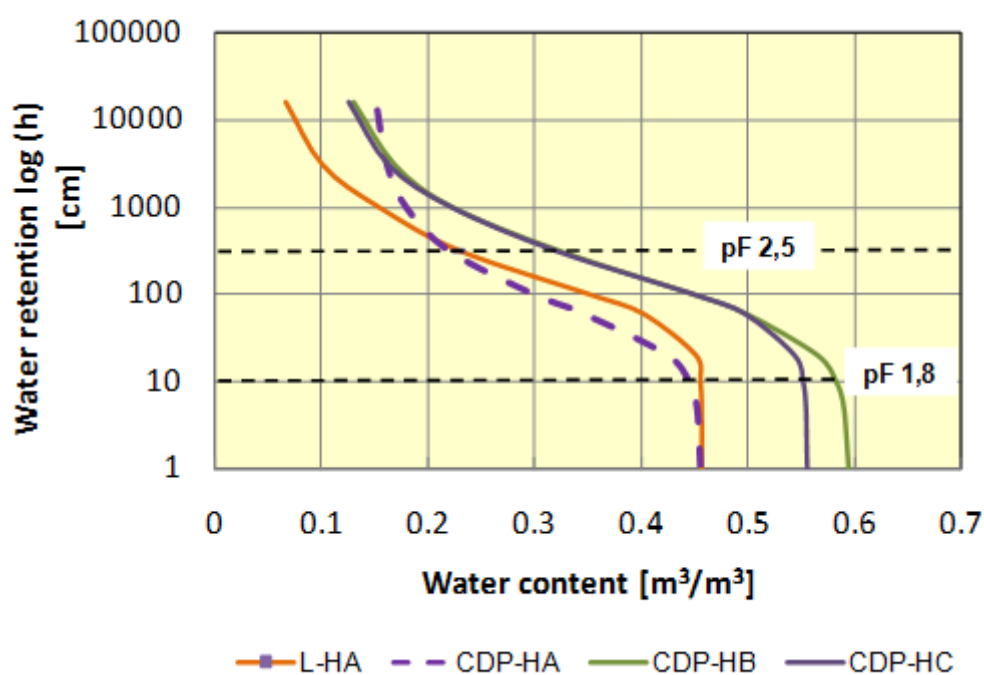
Fig. 3. 6: Water retention curves for the study sites Casa do Padre (CDP) and Lourizela (L).

Soil hydraulic conductivity and soil water repellency

As described in chapter 2.2.1.1 top soil infiltration rates were assessed using the MDI and the double ring infiltrometer. These methods allow the measurement of, respectively, the soil matrix near saturation hydraulic conductivity ($K_{(near-sat)}$) and the saturated hydraulic conductivity (K_{sat}). The measurements for both sites and in both repellent and non-repellent conditions are given in Table 3.4. The contrasting values of $K_{(near-)sat}$ and K_{sat} give indication on the relevance of macropores and soil cracks (along stones and roots) on the water infiltration pathways. Soil matrix infiltration may be further hindered by the soil water repellency, which, is bypassed while using the double ring infiltrometer, due to the large presence of macropores. There were several difficulties while conducting the field experiments during the summer season (repellent), due to conditions of no infiltration with the MDI and not reaching steady state with the double ring infiltrometer. Thus, the sample size taken into the assessment was with three samples rather short and may not be representative. Both soil water repellency and soil moisture reflect the expected pattern, with higher SWR classes while decreasing soil moisture content. The infiltrometry in Casa do Padre on non-repellent condition was not conducted at the same time as in Lourizela, due to an unexpected SWR presence reaching the Ethanol class 8 while SMC was 12 %. On this occasion (winter season) $K_{(near-sat)}$ at the top soil was 0,1 mmh^{-1}, a similar value to the one obtained during the warm season field survey. The opportunity to conduct further infiltrometry on during this survey was taken. Infiltration with the MDI was conducted at the depths of 20 cm and 40 cm. The values of ($K_{(near-sat)}$ where respectively 5,5 and 6,3 mm.h^{-1} while SWR Ethanol class was 0 and SMC was 31% and 45 % respectively. These values comply with the ones found later after repellency was broken at the top soil. From the comparison of both repellent and non-repellent seasons it is observable that infiltration rates increase with decreasing SWR class, except for K_{sat} in Casa do Padre during the non-repellent season. This may be a result of site heterogeneity and small replicate number.

As *Santos et al.* (2013) reported, on a study where these measurements were also included, the eucalypt study site (Casa do Padre) showed a higher SWR spatial heterogeneity in terms of sampled depth, over a 12-month period. According to this work these differences in spatial heterogeneity between the two sites could be related to the greater resistance of the soil under Eucalypt than Pine to the breaking of SWR.

Table 3. 4: Soil hydraulic conductivity (Ksat), soil water repellency (SWR) and soil moisture content (SMC) for the study sites Lourizela and Casa do Padre.

		Lourizela	Casa do Padre
Repellent	Soil matric $K_{(near-)sat}$ (mm/h)	0,25	0,11
	Ksat (mm/h)	126	284
	SWR 2,5 cm (Ethanol class)	7	8
	SWR 7,5 cm (Ethanol class)	7	7
	SMC 2,5 cm, (% vol.)	2	4
	SMC 7,5 cm, (% vol.)	4	6
Non-repellent	Soil matric $K_{(near-)sat}$ (mm/h)	0,7	6,4
	Ksat (mm/h)	265	186
	SWR 2,5 cm (Ethanol class)	0	4
	SWR 7,5 cm (Ethanol class)	0	0
	SMC 2,5 cm (% vol.)	16	15
	SMC 7,5 cm (% vol.)	18	15

Tracer infiltration experiments

With the tracer infiltration experiments no quantitative evaluation was strived, rather a qualitative understanding of the infiltration paths was intended. Figure 3.7 shows 4 of the 12 analysed profiles from the BB tracer infiltration experiment. Under pine, it is to point out that the locations within the study site Lourizela chosen for the repellent and non-repellent experiments revealed a strong difference in soil depth. During repellent conditions bedrock was found at 20 cm depth and for the non-repellent condition bedrock was at 40 cm depth. Under repellent conditions a smaller dye coverage was observed. The infiltration patterns

under repellent and non-repellent conditions were comparable: after a 5 cm wetting from the water flows preferentially, mainly following root channels and along rocks. The impoundment at the profile bottom occurs due to the presence of bedrock, which then leads to lateral flow. The main difference is the flow connectivity shown under non-repellent conditions. This observation was present in all analysed profiles. The non-connectivity observed could be due to the presence of a hydrophobic region, an increased number of macro pores, or both.

The observed BB impoundment at the eucalypt site may support the findings of *Santos et al.* (2013) where SWR was broken bottom-up possibly due to the presence of macropores and preferential flow pathways. On Lourizela, under *P. pinaster*, the smaller profile depth and the existence of a wetting front (due to a thicker humus layer) may have led to an increased profile homogeneity and to a top-down breaking of SWR.
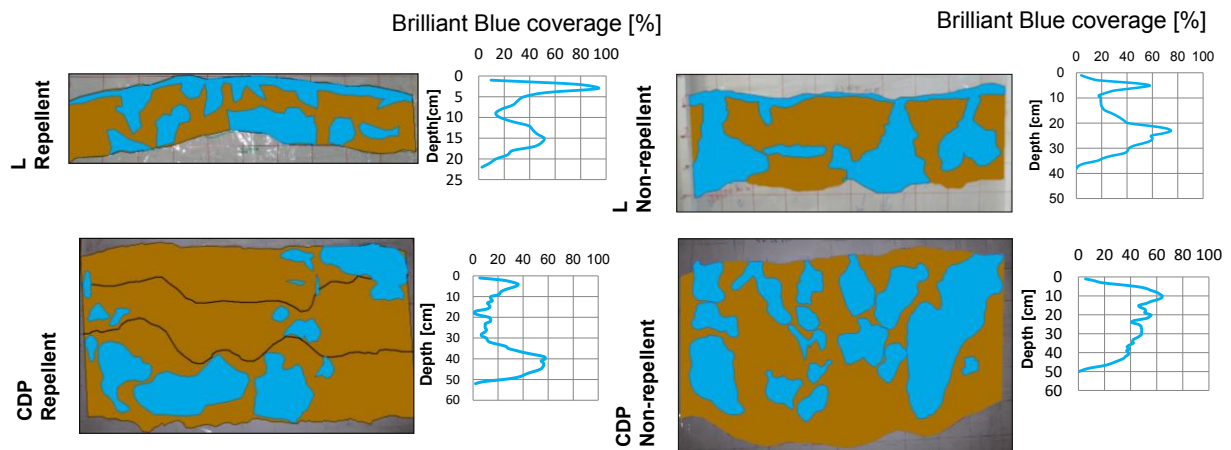
Fig. 3. 7: Digitized dye profiles and corresponding Brilliant Blue coverage for both study sites under repellent and non-repellent conditions. With L: Lourizela study site and CDP: Casa do Padre study site.

Under eucalypt, the infiltration pattern under repellent and non-repellent conditions appeared to be different, with a BB coverage increasing along the profile under repellent conditions while decreasing along the profile under non-repellent conditions. Under repellent conditions, tracer coverage increased steadily until reaching a maximum at c. 40-50 cm, this could be due to hydrophobic conditions and/or macro pores closer to the soil surface, and water accumulation

above the bedrock at the profile bottom. In non-repellent conditions, however, the maximum coverage was between 10– 20 cm and 40 cm, decreasing with depth; in this case, the breaking of hydrophobicity in the soil layer could have led to a greater contribution, of soil matrix on the surroundings of macropores and root channels, to water flow in the profile. Similarly to Lourizela under non-repellent conditions, a pathway connectivity was observed in Casa do Padre study site. The average results of the assessed profiles are shown in Figure 3.8.
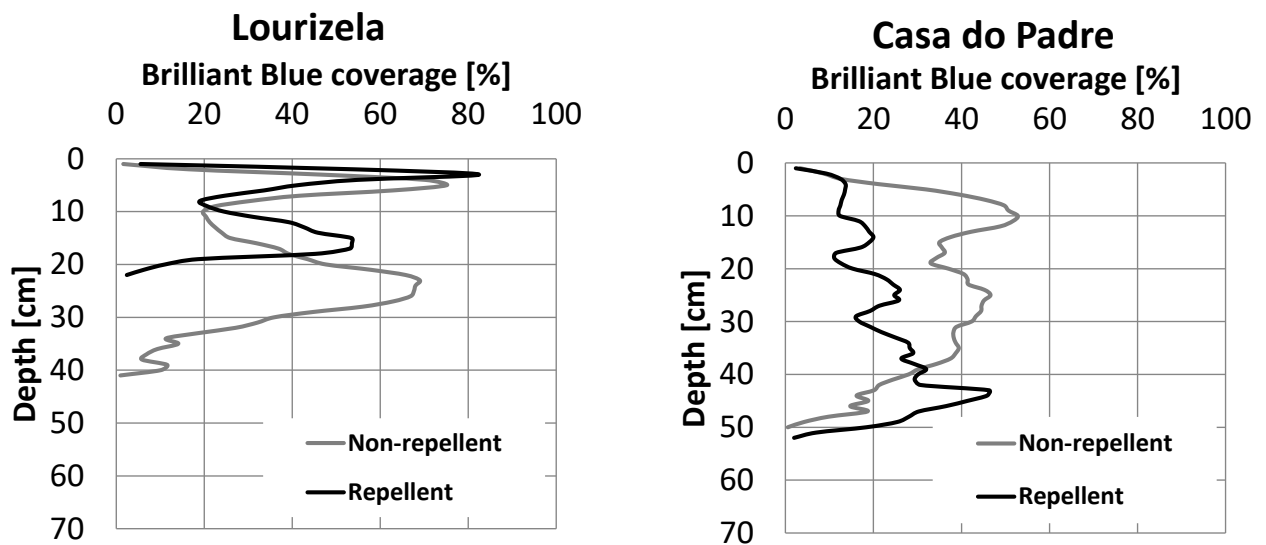
Fig. 3. 8: Infiltration experiments. Average dye coverage profiles distribution (%) in 1 cm depth increments in pine and eucalypt, in repellent conditions and non-repellent conditions. Each profile is the average of three profiles (12 profiles in total).

These interpretations should be taken with care, however, due to the higher clay content of the eucalypt site (24%) when compared with that of the pine site (12%). *Ketelsen and Meyer-Windel* (1999) concluded that increasing amounts of clay increase BB adsorption in the soil matrix. In that study soils with a clay percentage >12 % showed a high BB adsorption. However, the authors also concluded that organic carbon seems to inhibit BB adsorbtion to clay particles. Thus, inferences on water flow through the soil should be done carefully when comparing different soils. In this case, the comparison between non-repellent and repellent conditions should be feasible.

3.1.2.2 SoLIM-based soil map

The SoLIM-based soil map (Fig. 3.9) markedly enhances the spatial heterogeneity in effective soil depth compared to the original, 1:1,000,000 map, as it comprised a total of 8 soil units opposed to the two units of the original map. The predominant effective soil depth class is the intermediate class (30–80 cm), covering a total of 53% of the area, of which 23 % is over granite and 30 % over schist. Shallow soils were mainly found on steep slopes (>20°) under pine plantations. These cover a total of 22 % of the watershed, of which 15 % over schist and 7 % over granite. Deep soils were found on alluvial sands parent material, on areas with negative plan curvature values (such as valley bottoms and convergent slopes), and on agriculture terraces (where soils are assumed to have a homogeneous effective soil depth). Deep soils cover a total of 25 % of the watershed. From the 11 locations that were sampled to validate the SoLIM effective soil depth predictions, 8 exhibited the predicted effective soil depth. From the three mismatches, two could be ascribed to a wrong classification of land cover in the Corine-2006 map. The field survey showed that a pine plantation had been misclassified as an agricultural field. If the correct land cover would have been introduced in SoLIM, the correct depth class would have been obtained for both locations. In the last unmatched sample, a profile with > 90 cm depth was described, while this work derived an intermediate effective soil depth (30–80 cm). While the number of samples used to validate the SoLIM-based soil map was low, it was beyond the scope of this work to predict with high accuracy the watersheds effective soil depths. The SoLIM-based soil map gives nonetheless, a good representation of the soil profile depth variation.
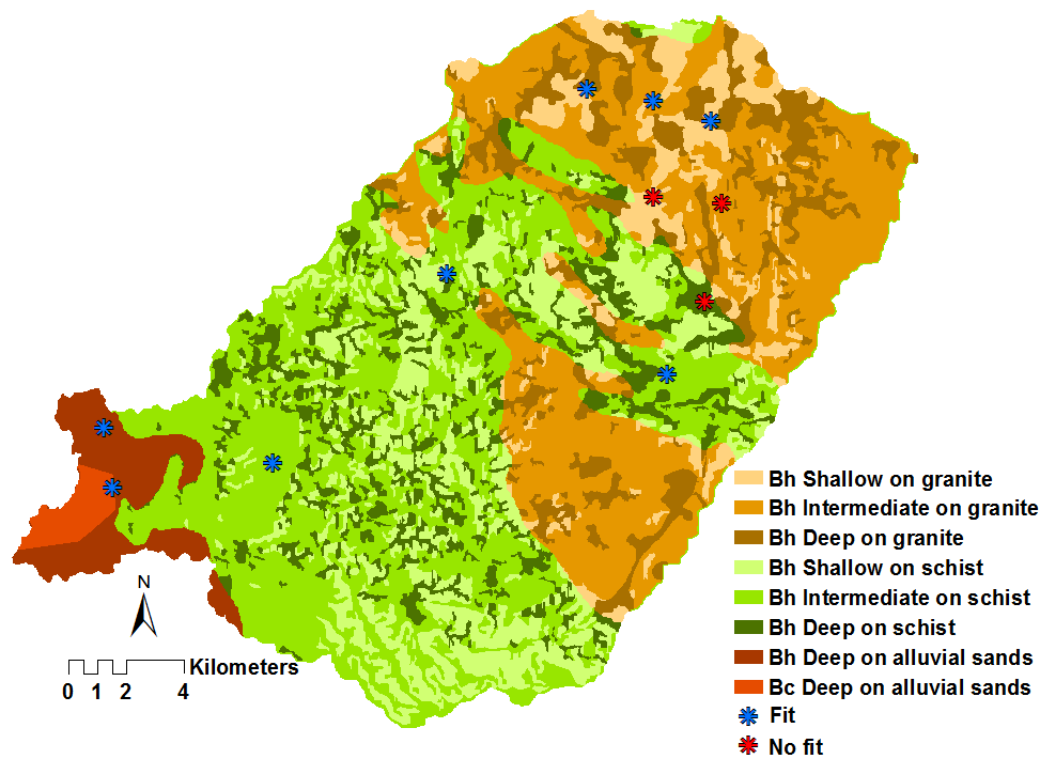
Fig. 3. 9: SoLIM-based soil map for the Águeda watershed; Bh are Humic Cambisols and BC are Chromic Cambisols; validation points: "Fit" — points where profile depth was correctly predicted; "No-fit" — point where profile depth was not correctly predicted.

3.2   Eco-hydrological modelling with SWAT

3.2.1 The Dobrotvir watershed

3.2.1.1   Hydrological modelling

Calibration parameters and sensitivity analysis

As described in Chapter 2.4.2.2 calibration and sensitivity analysis was done according to the procedure of *Abbaspour* (2007).The parameter controlling groundwater flow from the shallow aquifer to the reach was the most sensitive parameter in model calibration, followed by the

groundwater delay time parameter. The importance of the groundwater parameters is not surprising due to the hydrogeological characteristics of the watershed. Similar results have been found in previous SWAT studies dealing with groundwater influenced watersheds (*Holvoet et al*., 2005; *Schmalz and Fohrer*, 2009; *Kiesel et al.,* 2010). In the SWAT model, water balance is represented by several storage volumes, including: canopy storage, snow, soil profile, shallow aquifer, and deep aquifer (*Eckhardt et al.*, 2002). Therefore, it is reasonable that parameters directly related to storage components will have a high sensitivity. Soil related parameters were given values according to previous field campaigns. Further ranges for the selected parameters were based local expert knowledge, and literature review (*e.g.*, *Spruill et al*., 2000; *Terekhanova*, 2009*; Ulrich and Volk*, 2009).
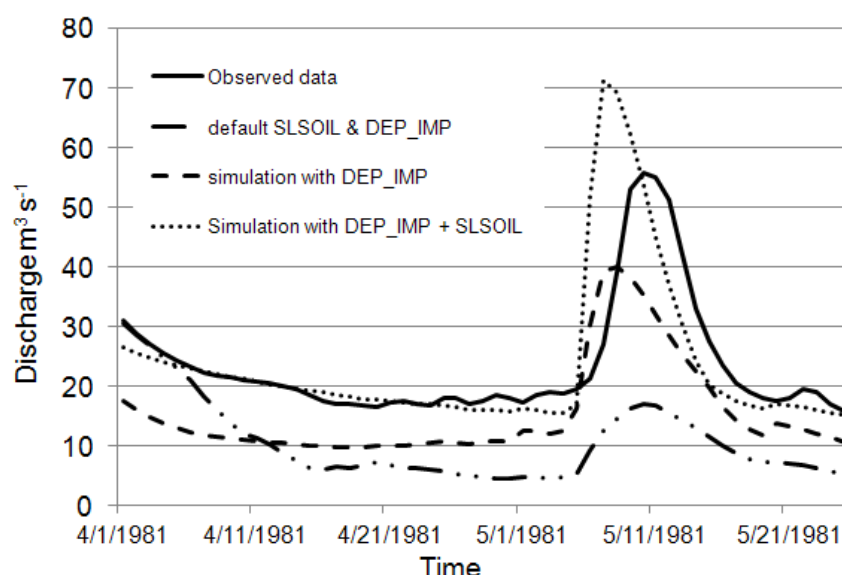
Fig. 3. 10: Comparison of three model runs during the calibration process: default values for the parameters SLSOIL and DEP IMP; DEP IMP = 1500 (mm) and DEP IMP = 150 (mm) + SLSOIL = 20 (m). DEP IMP = Depth of impervious layer for perched water tables in mm; SLSOIL = Slope length for lateral subsurface flow in m.

As shown in Fig. 3.10, significant improvement in model performance occurred when parameters were included to account for the "Depth of impervious layer for perched water tables in mm" (DEP IMP) and "Slope length for lateral subsurface flow in m" (SLSOIL). Inclusion of these parameters allows for representation of a perched water table which enables the regulation of water percolating out of the soil profile. The default parameterization of SWAT

assumes slope length for lateral subsurface flow to be equal to the average sub-basin slope length; however several studies have shown the importance of adequately parameterizing slope length (*e.g. Spruill et al*., 2000; *Lenhart et al*., 2002).Therefore the SLSOIL parameter was further adjusted in this study, producing a more reliable base and interflow simulation, and resulting in a better estimation of vertical and lateral soil flow.

For the auto-calibration of the water balance the parameters listed in table 3.5 were included based on the sensitivity analysis. The t-stat value provides a measure of sensitivity whereas the P-value determines the significance of the sensitivity (*Abbaspour*, 2007).

Table 3. 5: SWAT parameters used for calibration, fitted values and sensitivity statistics (downward sensitivity increase).

Parameter (SWAT IO 2009 manual)	Fitted value	t-Stat	P-value
Minimum snowmelt rate (mm H_2O/°C day)	1.555	0.029	0.976
Groundwater recession coefficient (days)	0.114	0.117	0.906
Time to drain soil to field capacity (hours)*	24	0.362	0.717
Lateral flow travel time (days)	29	-0.413	0.679
Threshold depth of water in the shallow aquifer for movement to the unsatured zone to occur (mm H_2O)	202	0.421	0.673
Plant uptake compensation factor	1	-0.455	0.649
Maximum snowmelt rate (mm H_2O/°C day)	8.2	-0.616	0.537
Snow melt base temperature (°C)	-0.8	0.766	0.443
Depth to impervious layer in soil profile (mm)	259	1.156	0.247
Initial SCS runoff curve number for moisture condition II **	0.161	-1.515	0.129
Depth to subsurface drain (mm)*	722	-1.800	0.072
Capillary rise coefficient	0.12	-1.862	0.063
Drain tile lag time (hours)*	10	-2.318	0.021
Soil evaporation compensation factor	0.23	2.927	0.003
Groundwater recession coefficient for bank storage (days)	0.421	3.106	0.001
Effective hydraulic conductivity in the main channel (mm/hr)	74	-3.645	0.000
Minimum snow water content that corresponds to 100% snow cover (SNOCOVMX) (mm H_2O)	116	3.704	0.000
Fraction of snow volume represented by SNOCOVMX that represents 50% snow cover	0.3	-3.903	0.000
Depth of impervious layer for perched water tables (DEP_IMP) (mm)	902	7.738	0.000
Slope length for lateral subsurface flow (SLSOIL) (m)	14	-13.323	0.000
Maximum canopy storage (mm H_2O)	6	21.029	0.000
Groundwater delay time (days)	447	-21.871	0.000
Threshold depth of water in the shallow aquifer for return flow to occur (GWQMN) (mm H_2O)	510	-31.012	0.000

*only applied to drained HRU's

** Initial parameter value is multiplied by (1+a given value) (Abbaspour, 2007).

Water balance

Table 3.6 provides the major average annual water balance components during the calibration period at the watershed outlet and as well as the observed average annual discharge and actual evapotranspiration (Et = Observed precipitation − Observed discharge). The simulated total annual water discharge was reproduced by the model. Possibly the difference between both Et values was given by a compartment which is not being taken into consideration in the observed values, as for example the karst system in which the watershed is located. Comparing the modelled results with those obtained by *Pluntke et al.* (2014) the relative components (surface runoff, Lateral flow, Groundwater) contribution is in agreement.

Table 3. 6: Major water budget components at the gauge Kamianka-Buska during the calibration (1980–1986) period.

Average annual values (mm)	Simulated	Observed
Precipitation	686	686
Surface runoff Q	26	
Lateral soil Q	78	
Groundwater (Shallow Aquifer) Q	94	
Total discharge	221	217
Et	419	469[a]
Pet	625	

[a]Et = Observed precipitation – Observed discharge

The comparison between of observed and simulated monthly medians also largely reproduce the watersheds water balance (Fig. 3.11). The shift observed in the months March and April, may be the result of a slower snowmelt response in the system than within the model setup, as snowmelt is a slow and gradual process when compared to rainfall runoff.

Figures 3.12a and b show the results of calibration and validation respectively. Both Nash-Sutcliffe Index (NS) and Coefficient of Determination (R^2) for the calibration (NS = 0.46, R^2 = 0.52) and validation (NS = 0.51, R^2 = 0.47) periods indicate a reasonable fit of the water balance. The relatively low NS and R^2 might be due to the fact that there was only one precipitation station inside the watershed, as several studies have indicated that an under-

representation of spatial rainfall variability may result in added model uncertainty (*Kirsch et al.*, 2002; *Inamdar and Naumov*, 2006; *Strauch et al.*, 2012).
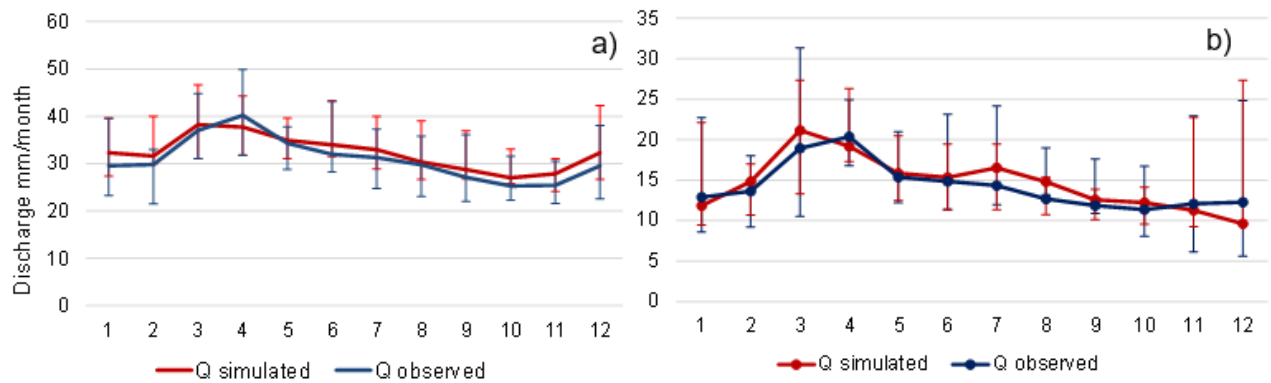
Fig. 3. 11: a) Comparison of monthly median observed and simulated discharge during the calibration (1980-1985) in the Dobrotvir watershed at the gauge Sasiv. b) Comparison of average month observed and simulated discharge during during the calibration (1980-1985) in the Dobrotvir watershed at the gauge Kamianka-Buska. Bars show the monthly value spread.

For example, the over estimation of the peak flows may be a consequence of a localized precipitation event occurring near the gauge, which was incorrectly taken as representative of conditions over the entire watershed in terms of extent, duration, or intensity. In such cases, an improvement in precipitation input data would clearly allow better model performance. The calibration of base flow was both time consuming and complex in this study, and was not successful in some cases, as shown in Fig. 3.12.

A significant source of the difficulty in calibration may be the very long storage times present due to the hydrogeological characteristics of the watershed (*i.e.* karst aquifer). Figure 3.13 and b show the Autocorrelation Function (ACF) (*Venables and Ripley*, 2002) of observed and simulated discharge values for a time lag of 30 (Fig. 3.13a) and 550 days (Fig. 3.13b) respectively. It can be seen from Fig. 3.13 that there was still a significant correlation after 30 days, and only after 550 days did the ACF enter the range of the 95 % confidence interval about zero. The slowly declining values in the correlogram may be indicative of a long-range autocorrelation in stream flow, although the source of this autocorrelation is not certain

(*Szolgayov´a et al.*, 2012). One possible explanation for this behavior is the presence of a hydrologic system with a very large storage component, which is consistent with previous findings of high long-term ACF in a karst system by *Fiorillo and Doglioni* (2010).
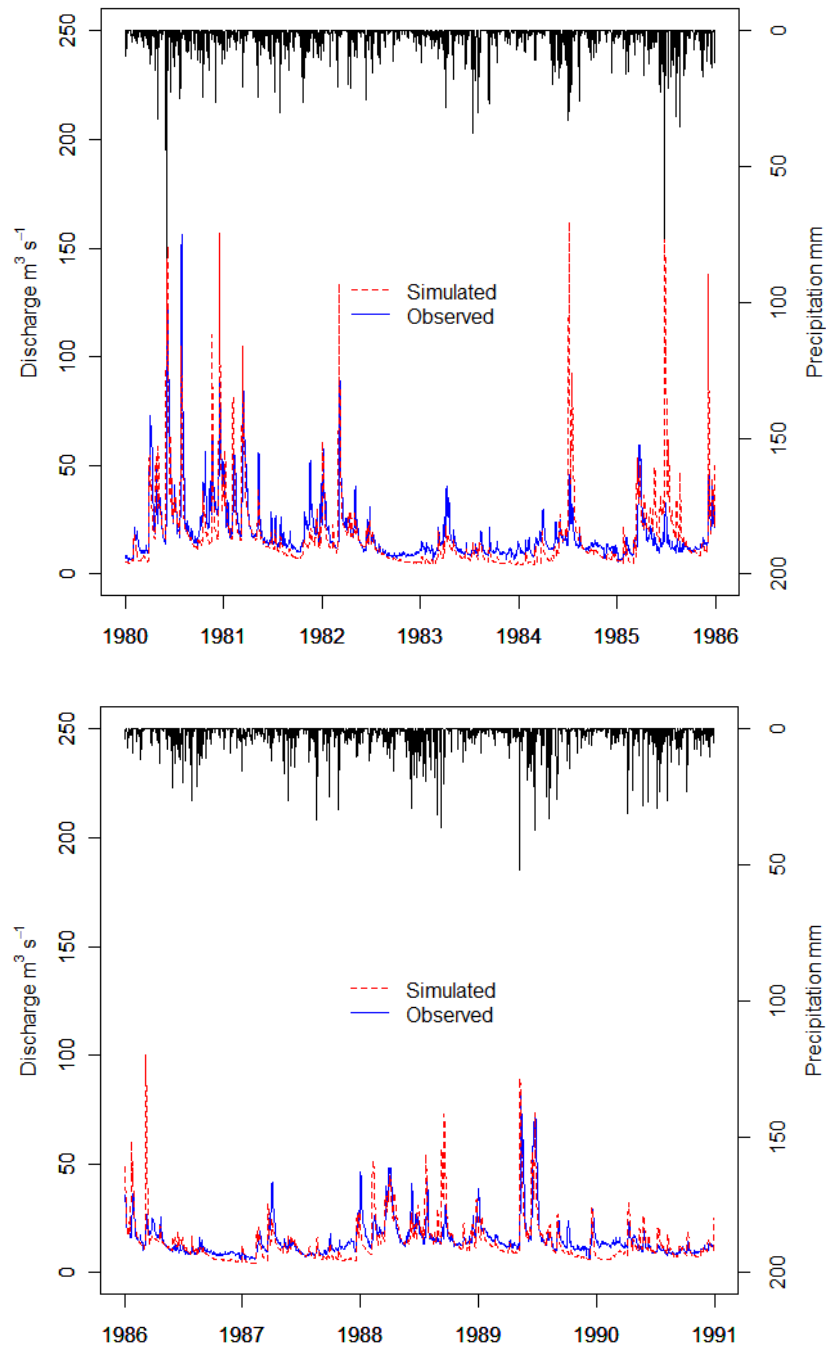

Fig. 3. 12: Above: Comparison of daily observed and simulated discharge during the calibration (1980-1985) in the Dobrotvir watershed at the gauge Kamianka-Buska (R^2=0.52, NS=0.46). Below: Comparison of daily observed and simulated discharge during the validation period (1986-1990) in the Dobrotvir watershed at the gauge Kamianka-Buska (R^2=0.47, NS=0.51).
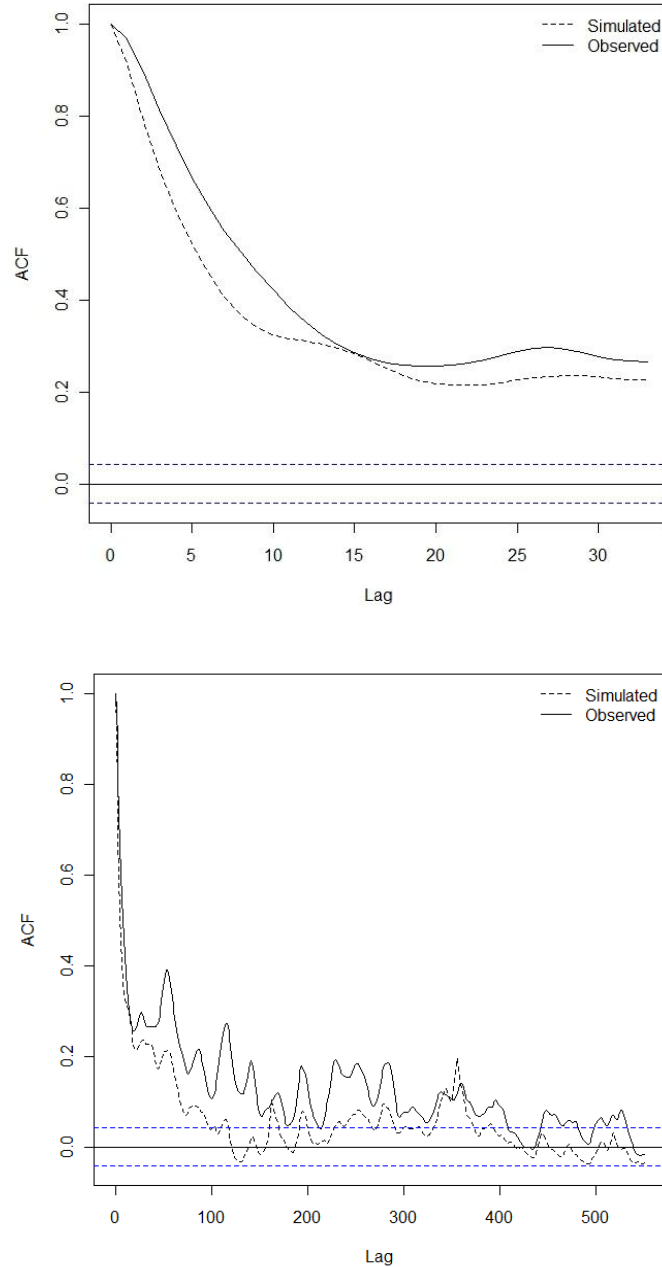
Fig. 3. 13: Autocorrelation Function (ACF) of daily observed and simulated discharge values, during the calibration period 1980 to 1985, for the gauge Kamianka-Buzka, Dobrotvir watershed, for a time lag of (above) 30 days and (below) 550 days. Dashed lines depict the 95 % confidence intervals.

Crop yields

As a result of the calibration, the default radiation use efficiency (BIO_E) of each crop was in increased from 39 to 45 (kg ha^{-1})/(MJ.m^{-2}). The harvest index (HVSTI) was also set to 0.7 for grain cultures and to 1.25 for potato and sugar beet according to the manual since the harvested portion is belowground. No biomass or harvest targets were pre-fixed. Optimum

and base growth temperatures of each crop had been adjusted during the pre-processing stage and were not further calibrated. The comparison between the mean annual observed and simulated crop yields for the period 1980–2010 is presented in Figure. 3.14. Due to data scarcity the entire period of available data was take for comparison, rather than only the calibration period. The observed statistics are annual averages from the L'viv Oblast (Department of Statistics for the L'viv Region, 2013). For the period 1980-1984 only the 4 years average was available.
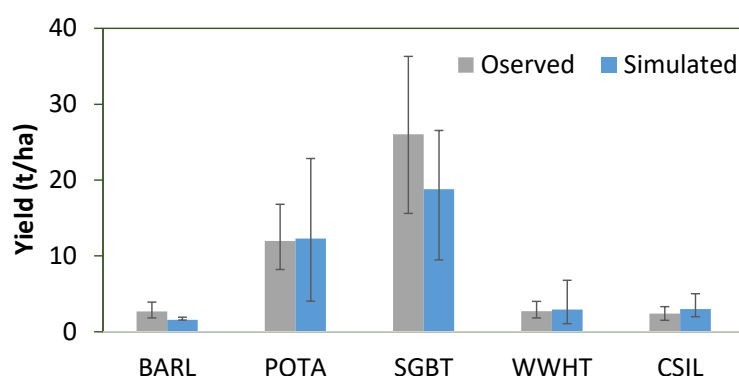
Fig. 3. 14: Observed and simulated average annual crop yields for the period 1980 – 2010 (observed Barley values were listed as "cereal other than wheat").

The simulated average annual yields are within the reported values, except for sugar beet which was underestimated. The annual variability of yields was larger than the observed values, except for spring barley. However, given the data available for both management optimization and yield calibration, the crop yield simulation was considered satisfactory.

3.2.1.2   Nitrate-N calibration and evaluation

After manual calibration for the period 1980-1985, verification was conducted for the periods 1990-1999 and 2001-2011 by plotting the measured data against the simulated time series. An assessment of the nitrogen cycle at the basin and HRU scale was done. Manual calibration of nitrate-N fluxes was done by fitting the parameters listed in Table 3.7. Clearly the

parameters controlling the denitrification process (CDN and SDNCO) were the most sensitive of the calibrated parameter group.

Table 3. 7: SWAT parameters used for calibration, fitted values and sensitivity statistics.

Parameter	Range	Fitted value
Nitrate percolation coefficient (NPERCO)	0 – 1	0.05
Rate for humus mineralization of active organic nutrients (CMN)	0.0001 - 0.003	0.0003
Denitrification exponential rate coefficient (CDN)	0 – 3	0.3
Nitrogen uptake distribution parameter (N_UPDIS)	0 - 100	90
Residue decomposition coefficient RSDCO	0.02 - 0.1	0.1
Denitrification threshold water content (SDNCO)	0 – 1	0.87

The basin wide annual nitrate-N averages (Table 3.8) show a relatively large denitrification value, which may occur due to the watershed lowland characteristics and the value is within the range estimated range of 18 to 46 N kg.ha^{-1}.a^{-1}(Hofstra & Bouwman, 2005) for poor drained upland crops with an annual N input of 150-225 N kg.ha^{-1}.a^{-1}. This is further supported by the average low C/N ratios of 15 which give the soil a low N retention status, which could favor leaching.

Table 3. 8: Basin wide average annual values for nitrate-nitrogen for the calibration period.

Process	Nitrate-N kg.ha^{-1}.a^{-1}
Fertilization	114.1
Denitrification	31.3
Plant uptake	68.9
NO3 Lateral flow (Lat. + Tile)	3.2
NO3 Leached	5.1
NO3 in Surface runoff	1.7

Figure 3.15 provides the nitrate modelling results for stream nitrate-N loading. Model outputs, for the time periods 1980-1986, 1990-1999 and 2001-2011, show a reasonable model behavior in terms of temporal dynamics and fitting of low exports while peak loading are overestimated. Reasons for this overestimation may be model failure as sampling timing, since

the peaks may have been missed by campaign. Smaller loading peaks could have been achieved at the costs of denitrification, by fitting the parameter CDN a larger value.
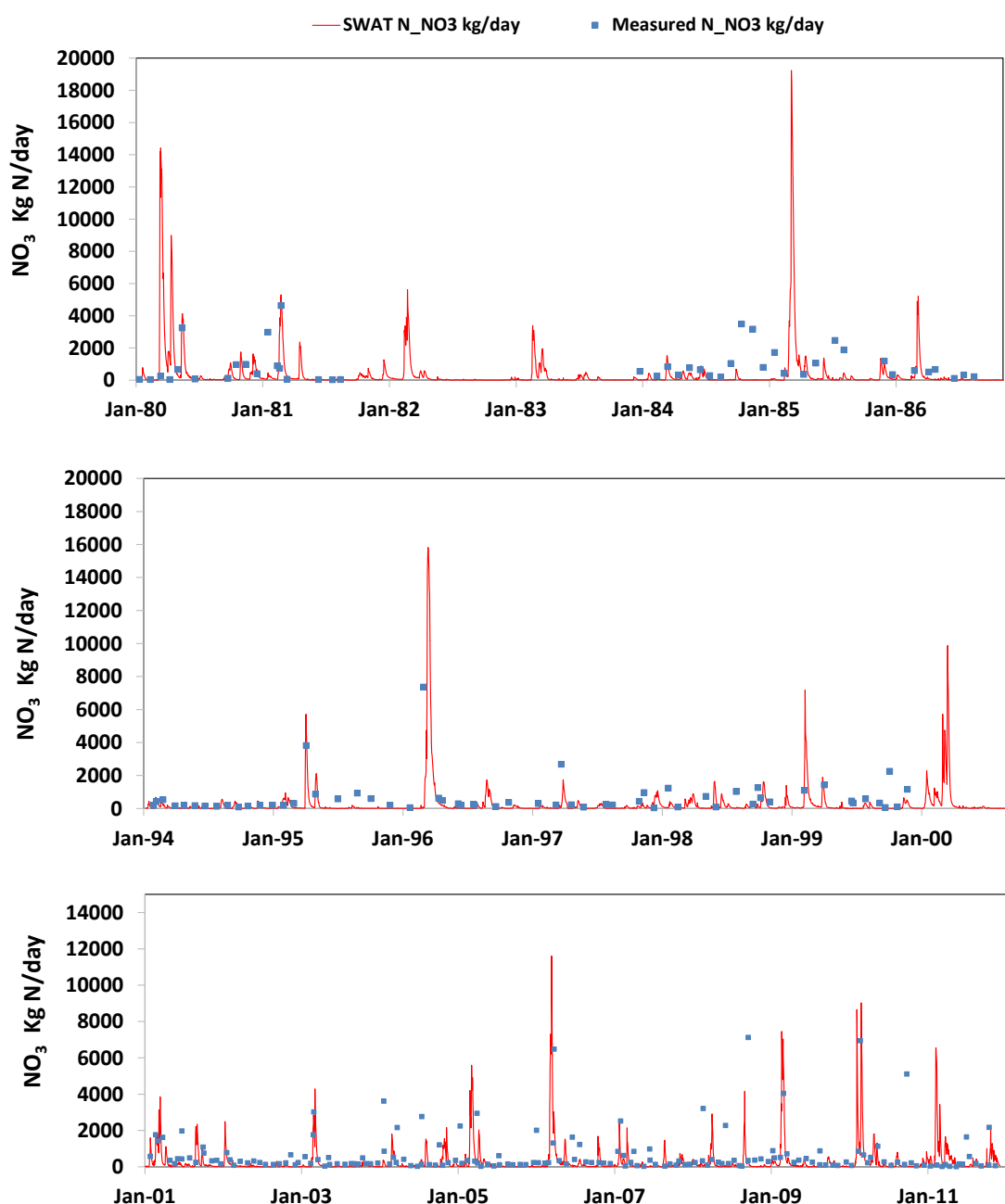
Fig. 3. 15: Simulated and observed nitrate-N loads for the periods of 1980 - 1986; 1994 – 2000 and 2001 – 2011 for gauge Kamianka-Buska.

This would however have increased the denitrification values up to 80 kg ha^{-1} a^{-1}, which is not reasonable. Other SWAT model application in the Northern Ukraine (*Osypov et al.,* 2017) resulted in good performances for the simulation of nitrate-N at the outlet, however, no reference is made to the process of denitrification. In general, SWAT studies give special focus to the achievement of statistical performance indexes as NSE and R^2. Such reference performance indexes, as shown by (*Moriasi et al.,* 2007) are valuable tools for model evaluation, however, on a situation of scarce and uncertain data a greater weight should be given to the representation of internal N cycling.

To examine internal cycles of nitrate-nitrogen in the watershed rates of denitrification and plant uptake were investigated. Figure 3.16 shows N plant uptake and denitrification after a fertilization operation on a winter wheat area (HRU 823) during the year 1982. Plant uptake starts within 24h of application and within the following 6 days 32 kg N.ha^{-1} is taken up. On day 6 with the increase in soil moisture denitrification starts while plant uptake decreases. During this vegetation period, in this HRU, a total of 140 kg N.ha^{-1} are added by fertilization, 122 kg N.ha^{-1} are taken up by the plant and 26 kg N.ha^{-1} are denitrified.
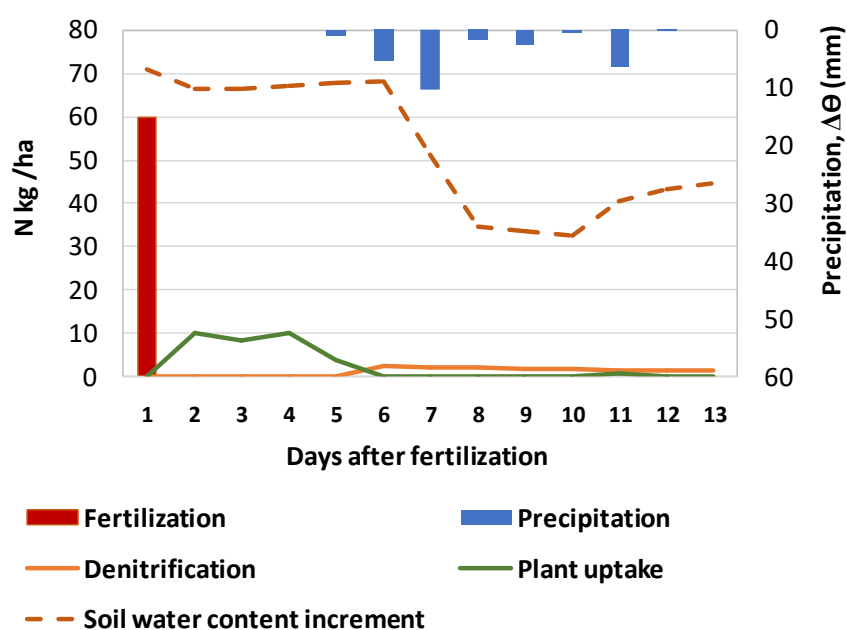
Fig. 3. 16: Denitrification and plant N uptake of winter wheat after fertilization with 60 kg N.ha^{-1}.

The cumulative N plant uptake is shown in Figure 3.17. Plant uptake occurs mainly during the 10 days after fertilization, producing a "stair" shaped curve instead of the expected smooth S-shaped curve through the different stages of vegetative growth. This could be as already described by (*Pohlert et al.*, 2005) due to the lack of a sink limitation for the simulated nitrate uptake, which leads to the accumulation of a deficiency which is promptly mitigated when the nitrate pool in the soil is refilled by fertilization.
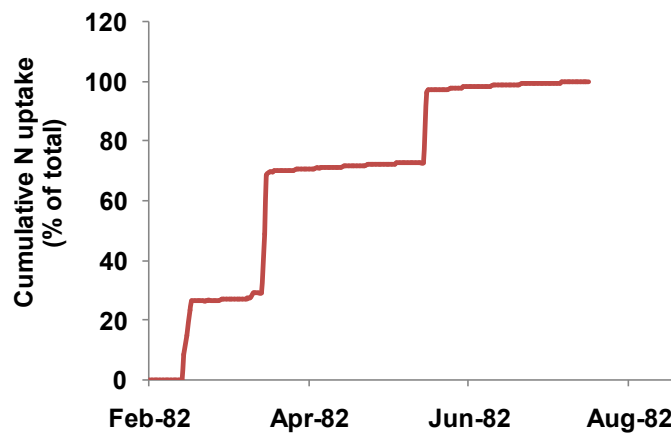
Fig. 3. 17: Cumulative N plant uptake of winter wheat during the growing season of 1982.

Given the uncertainties, both on the parameterization as on the data for calibration, this model set up was kept and it is assumed to represent the overall system nitrate-N tendency. This model application is on the following referred as "Baseline" scenario. In Figure 3.18 a) average annual stream loads of nitrate-N for the calibration period 1980-1985 can be observed. In this simulation head water sub-basins have a clearly lower nitrate pollution, which increases with the river course and reaches the maximum at the outlet. In Figure 3.18 b) the average annual sub-basin nitrate-nitrogen exports to stream are displayed. Here it can be seen a stronger spatial variation, as exports range from 0.7 until 7.3 kg N $.ha^{-1}.a^{-1}$. The sub-basin at the outlet, with larger forested area reveals lower exports along with sub-basin 13 on the west of the watershed. Sub-basin 13 is mainly dominated by urban areas (L'viv city). Since urban management practices which may lead to N pollution (other than waste water treatment plants) were not focus of this work and, therefore, not included in the simulation.
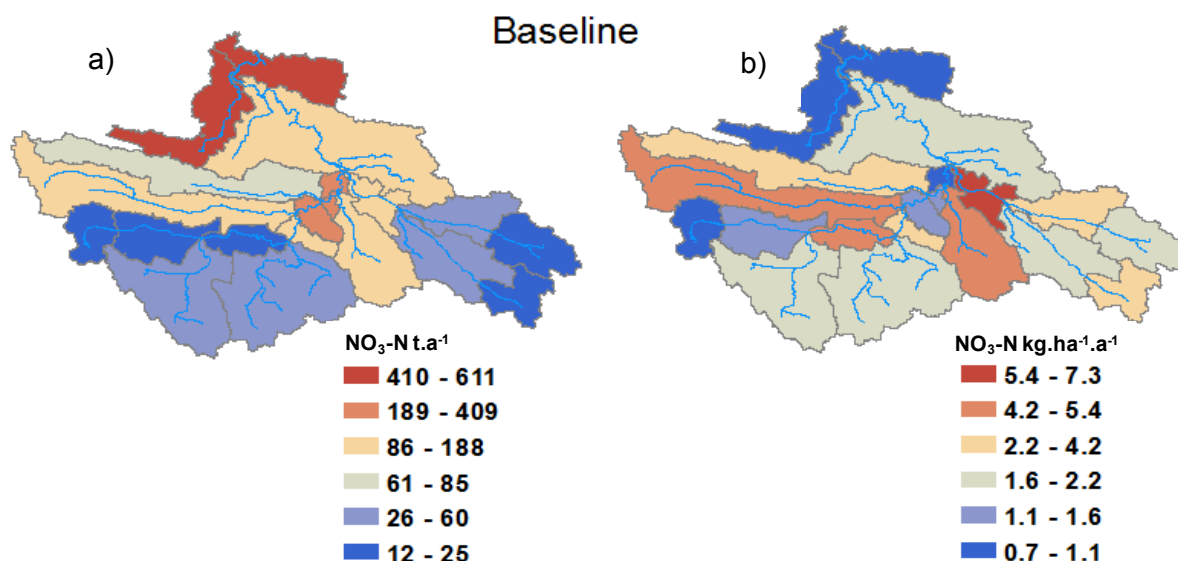
Fig. 3. 18: Baseline simulation for the parameter nitrate-nitrogen for the calibration period. a) Average annual stream loads in ton.a^{-1}. b) Average annual sub-basin exports in kg.ha^{-1}.a^{-1}.

3.2.1.3 Intervention options impact on nitrate exports

The aim of the scenario building was to assess interventions options for the agricultural areas which would reduce the nitrate-N export of these areas. The constructed scenarios with the aim of reducing nitrate-nitrogen pollution in the Dobrotvir watershed were: i) reduction of the applied fertilizer by 15% (15NReduction); ii) reduction of the applied fertilizer by 25% (25NReduction); and iii) alternative agro-forestry of SRC for biomass production (SRC). Given the limitations of the Baseline scenario the assessment of the scenarios was rather conducted for the rate of change than for actual absolute values. Figure 3.19 depicts possible reduction rates by the different scenarios. The 15NReduction scenario presents predominantly reduction rates that range between 10.3 until 23.1 %, while sub-basin 13 most likely due to the small percentage of agricultural land, shows a reduction between 5.0 until 10.2 %. The scenario 25NReduction shows overall larger reduction potentials, with most sub-basins having a reduction between 16.8 until 35.9 % and one sub-basin reveals the highest reduction class 36.0 until 49.6 %. The SRC scenario shows the most differentiated results. This scenario shows both sub-basins with the largest reductions as with the smallest. This was to be

expected since fraction of SRC suitable areas differs greatly from one sub-basin to the other (Fig. 2.17).
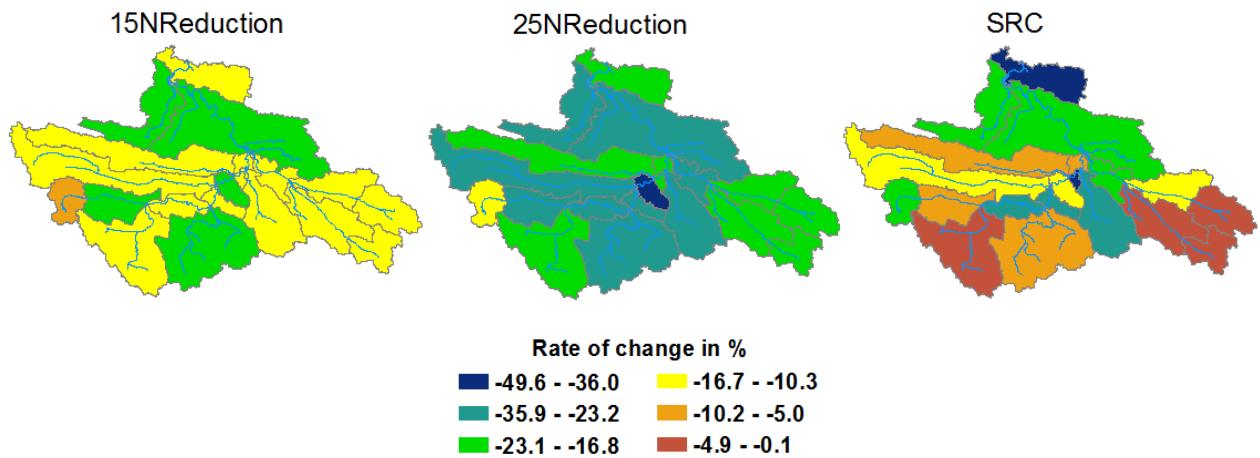
Fig. 3. 19: Sub-basin nitrate-N export rate of change (in %) relative to the Baseline simulation as given in Fig. 3.18.

For the two fertilization reduction scenarios the impacts on crop yield were assessed (Fig. 3.20). In both cases lower yields were obtained. In the scenario 15NReduction yield was reduced by approximately 5 %, whereas scenario 25NReduction obtained simulated yield reductions between 10 to 25 %. The winter wheat simulated production presented the strongest losses. This may imply that, although this scenario shows the largest nitrate-N export reductions for the entire watershed, its implementation potential may not be economic feasible and requires a more exact site evaluation beforehand.

The SRC scenario may have other implications for the watershed, which derive from the greater water demand of SRC species, particularly from the growing poplar plantations in the simulation. Figure 3.21 shows the relative change of the main water balance components simulated with the SRC scenario. The water balance component revealing the largest change was surface runoff, which was expectable due to the larger water uptake from the soils and increased infiltration. The increased water uptake can also be noticed in the increased actual evapotranspiration and reduced lateral + tile flow, groundwater flow, total aquifer recharge and water yield at the outlet.
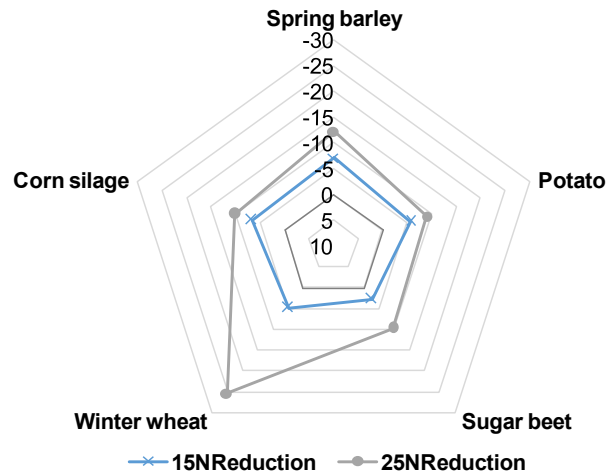
Fig. 3. 20: Simulated yield reduction (rate of change in %) from the fertilization reduction scenarios "15NReduction" and "25NReduction" relatively to the Baseline scenario for the main crops growing in the Dobrotvir model.

However, except for surface runoff, the values oscillate between the positive 2 % and negative 4%. Since the watershed is not water limited and to a large extent groundwater fed, this scenario could bring the positive effects of reduction of N exports without endangering water supply to other activities.
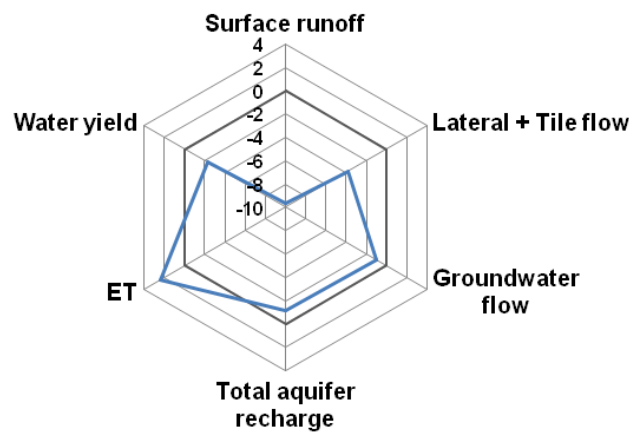
Fig. 3. 21: Relative change (rate of change in %) of the main water balance components simulated with the SRC scenario in relation to the Baseline scenario for the calibration period.

Similar observation can be made for the direct HRU comparison of the Baseline and SRC scenarios (Fig. 3.22). For these HRUs an increase of actual evapotranspiration can be seen

as a decrease in groundwater recharge, lateral + tile flow, groundwater flow and surface runoff.

These results are in line with those found by *Mwangi et al.* (2016) and *Petzold et al.* (2010).
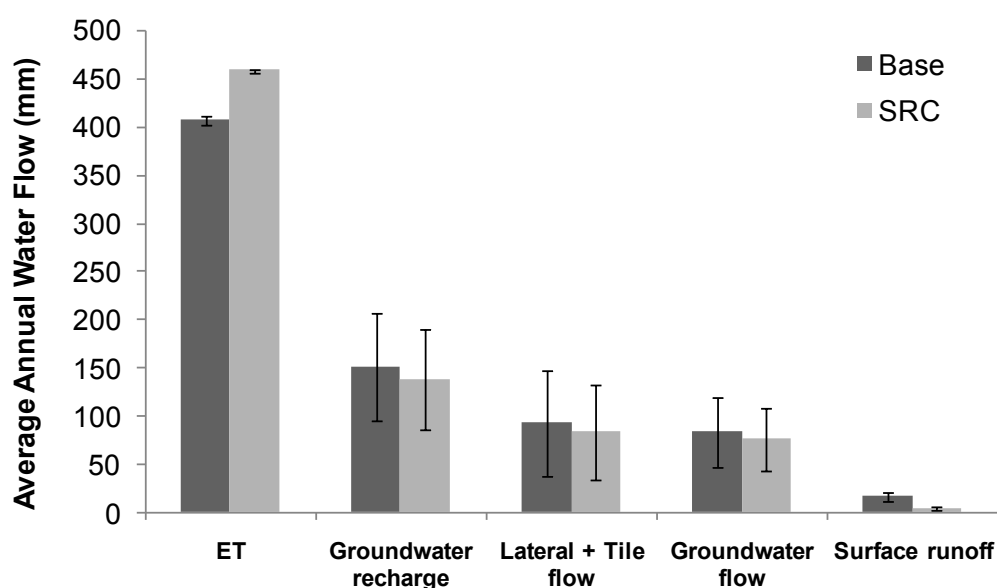
Fig. 3. 22: HRU-based comparison of the main water balance components for the Baseline and SRC scenarios.

From the direct HRU assessment it was also possible to observe a clearly reduced export to stream and leaching of nitrate-nitrogen (Fig. 3.23). This was expectable since along to the reduced fertilization application in these areas, the reduced flows should further hinder N pollution.
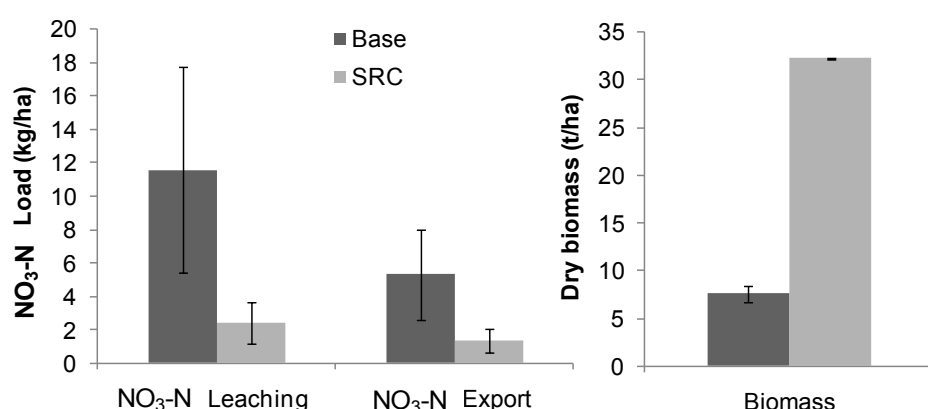
Fig. 3. 23: HRU based comparison of the nitrate-nitrogen leaching, export to stream and simulated biomass for the Baseline and SRC scenarios.

During the SRC scenario a first agriculture crop was replaced by a generic poplar, which was harvested after 4 years. The accumulated aboveground dry biomass of the generic poplar produced 33 ton.ha^{-1}, which makes an average of 8.25 ton.ha^{-1} a^{-1}. This value is lower than the economic optimum of 12 ton.ha^{-1} (*Schwarze and Röhrich*, 2006), however still within the range of economic feasible of 8 to 12 ton.ha^{-1} a^{-1}. The feasibility of this scenario is demarked by the existence of innovative ongoing research projects funded by the European Union as the SEEMLA ("Sustainable exploitation of biomass for bioenergy from marginal lands" H2020 Grant nr. 691874; *SEEMLA*, 2016b) where SRC plantations are being investigated in western Ukraine for energy purposes and the ongoing EU BBI-JU project, Dendromass4Europe ("Securing Sustainable Dendromass Production with Poplar Plantations in European Rural Areas"; Grant nr 745874; *D4EU*, 2017), where dendromass production from different poplar hybrids is being assessed. Still, these research projects do not focus on N pollution mitigation, but on the economic value of the agro-forestry plantations.

3.2.2 The Águeda watershed

3.2.2.1   Hydrological modelling

Calibration parameter ensemble

The range of values for the ensemble created for each SWAT project are provided by Table 3.9, while the parameter description can be found in Table 2.7. On the SWAT-SOLIM ensemble, a reduction of the parameter ranges can be observed for most parameters. The largest reductions occurred for GW_DELAY (delay time for aquifer recharge) for granite and schist parent material, and for GW_QMN (threshold depth of water in shallow aquifer for return flow to occur) for schist parent material, amounting to reductions of 26, 22, and 19 %, respectively. The values for GW_DELAY (ranging from 5 to 30 days) indicate the delay between water exiting the soil profile and entering a shallow aquifer. The perched groundwater

tables (aquifer that occurs above the regional water table, in the vadose zone) could lead to a wide range of parameter values, since GW_DELAY depends on the depth of the water table and on the hydraulic properties of the geologic formations. The larger GW_QMN values for the granite and schist parent material than for the alluvial sands material appear to be reasonable, since return flow from groundwater to the stream promptly occurs in groundwater near areas. Overall, the reduction in the ranges of the values for the groundwater-related parameters potentially indicates that the model structure of SWAT-SOLIM is better able than SWAT-BASE to describe the interaction between the vadose zone and groundwater. Improved soil variation representation should result in a more constrained parameter range, and therefore reduced parameter uncertainty and improved parameter identifiability. In the case of the SOL_AWC (soil available water capacity) parameter, the range of values was 10% wider for SWAT-SOLIM than SWATBASE. This may be related indirectly to the difference in soil spatial heterogeneity. The final parameter ensemble ranges were large for both projects, which may indicate that the parameter values obtained from calibration were affected by factors such as correlations amongst parameters and/or a lack of parameter sensitivity (*Wagener et al*., 2003; *Wagener and Kollat*, 2007). *Beven and Freer* (2001) argue that equifinality is inherent to systems where components cannot be specified independently, such as in environmental modelling and that rather than seeking to identify a single optimal parameter set, it was suggested that the search should focus on model structure and parameter space. *Shen et al.* (2012) and *Strauch et al.* (2012) also indicated that the initial number of parameter sets (Latin Hypercube sampling n) used in a SWAT calibration may affect their value ranges. Regardless, the ensemble simulations provide a good prediction of the water balance for both model structures, while providing an indication of parameter uncertainty (which would not be apparent if only a single parameter set was used).

Table 3. 9: Calibrated parameter minimum and maximum for both model ensembles. For parameter descriptions see Table 2.7

Parameter	SWAT-BASE Ensemble			SWAT-SOLIM Ensemble		
	Minimum	Maximum	Best Fit	Minimum	Maximum	Best Fit
SURLAG	0.00	0.06	0.0079	0.00	0.02	0.0071
SOL_AWC	-0.10	0.14	0.12	-0.14	0.13	0.13
SOL_K (no rock)	-0.15	0.15	0.02	-0.15	0.13	-0.05
SOL_K (rock)	114.16	277.44	147.47	127.69	278.22	237.40
CH_N1	0.01	0.26	0.14	0.01	0.25	0.06
CH_K1	9.37	89.36	29.75	9.37	71.83	58.71
ALPHA_BF[a]	0.05	0.88	0.33	0.14	0.92	0.17
ALPHA_BF[b]	0.04	0.98	0.28	0.20	0.98	0.67
ALPHA_BF[c]	0.16	0.69	0.16	0.16	0.72	0.51
GW_DELAY[a]	1.49	30.33	3.63	3.63	24.42	24.42
GW_DELAY[b]	1.06	30.09	18.53	4.90	27.16	10.87
GW_DELAY[c]	1.10	30.53	15.09	4.26	30.53	8.66
GW_REVAP[a]	0.05	0.20	0.17	0.02	0.17	0.06
GW_REVAP[b]	0.03	0.18	0.18	0.03	0.18	0.18
GW_REVAP[c]	0.02	0.17	0.02	0.02	0.17	0.09
GW_QMN[a]	6.00	176.05	176.05	43.58	176.05	57.94
GW_QMN[b]	6.30	199.04	144.87	26.38	185.86	154.54
GW_QMN[c]	1.16	43.58	10.41	1.16	18.15	4.28
RCHRG_DP[a]	0.01	0.24	0.19	0.02	0.22	0.22
RCHRG_DP[b]	0.02	0.24	0.20	0.03	0.25	0.23

[a] - For areas with parent material granite.
[b] - For areas with parent material schist.
[c] - For areas with parent material alluvial sand.

Water balance

Table 3.10 lists the major average annual water balance components during the calibration period at the watershed outlet and relates these to the observed average annual discharge and actual evapotranspiration (Et = Observed precipitation − Observed discharge). When analyzing the water balance components the following differences stand out: 1) an increase of surface runoff was observed in SWAT-SOLIM in relation to SWAT-BASE. This trend is consistent with the expected water holding capacity of the soils, which is directly related to the effective soil depth. The soils used in SWAT-SOLIM are faster saturated and overland flow will occur more quickly. 2) An increase in lateral flow was observed in SWAT-SOLIM in relation to SWAT-BASE. Such a result was expected since in SWAT lateral flow occurs whenever the

water content of the soil exceeds its water content at field capacity. 3) A reduction of actual evapotranspiration was observed in SWAT-SOLIM in relation to SWAT-BASE. Such a trend is in agreement with the observations for surface runoff and lateral flow. This value is also in compliance with those observed from the difference between annual average precipitation and total water yield.

Table 3. 10: Major water budget components of both model ensembles and observed total discharge at Ponte de Águeda during the calibration (1991–1995) period.

Average annual values (mm)	SWAT-BASE	SWAT-SOLIM	Observed
Precipitation	1483	1483	1483
Surface runoff Q	131	211	
Lateral soil Q	507	569	
Groundwater (ShalAq) Q	29	7	
Total discharge	667	789	760
Et [a]	781	690	683[a]
Pet	1033	1033	

[a] Et = Observed precipitation – Observed discharge

Streamflow

The values of the statistical evaluation criteria used for the assessment of the simulated daily stream flow by the two SWAT projects are provided in Table 3.11. During the calibration period (1991–1995), both projects indicate a good agreement between measured and simulated stream flow (*Moriasi et al*., 2007). This indicates that the structural differences between the projects were overcome during the calibration process. Nevertheless, SWAT-SOLIM ensemble median shows better fitting (E = 0.60; LnE = 0.78; RSR = 0.61) and a smaller spread (max–min) of statistical evaluation criteria. For the validation period (1979–1981), higher model performances were achieved for the ensemble median of both projects. This may be due to the characteristics of the stream flow time series, which lacked an extreme wet year as it was present in the calibration time series (*i.e.*, 1995). Also despite the higher maximum objective function values, the ranges of values during the validation period were larger than

those of the calibration period. Figs. 3.24 and 3.25 show the fit between the simulated and measured daily discharge for both SWAT-BASE and SWAT-SOLIM, as well as for the calibration and validation period. SWAT-BASE shows a larger spread of the simulated discharge, particularly during stream flow recessions, which may indicate that the model structure does not permit fast enough stream flow routing. Furthermore, SWAT-BASE failed to simulate the first peaks in streamflow after the dry summer season, which may be due to the presence of a storage component in the model that does not actually exist and, which likely indicates an overestimation of effective soil depth in the SWAT-BASE project. After the dry season, this storage needs to be filled first before stream flow can be produced. The same model behavior can be observed during the validation period.

Table 3. 11: Median, minimum and maximum statistical evaluation criteria, of both model ensembles stream flow outputs, to the observed discharge of Ponte de Águeda: model calibration (1991-1995) / model validation (1979-1981). E is the Nash–Sutcliffe Efficiency; LnE is the logarithmic of the Nash–Sutcliffe Efficiency; and RSR is the ratio of the Root Mean Square Error and standard deviation of measured data

Index		SWAT-BASE	SWAT-SOLIM
E*	Median	0.59/0.60	0.60/0.64
	Min	0.51/0.47	0.55/0.58
	Max	0.62/0.64	0.64/0.65
LnE*	Median	0.76/0.87	0.78/0.86
	Min	0.72/0.27	0.75/0.71
	Max	0.82/0.90	0.80/0.88
RSR**	Median	0.63/0.61	0.61/0.58
	Min	0.71/0.73	0.67/0.62
	Max	0.62/0.61	0.60/0.58

The SWAT-SOLIM ensemble results reveal a narrower spread and a better fit to the stream flow recession curves. Furthermore, SWAT-SOLIM succeeded in simulating the first post-summer peak flows during both the calibration and validation period. However, SWAT-SOLIM also simulated a (non-existent) peak in stream flow following the first post-summer

precipitation event. The mismatch may be related to a model underestimation of interception, for example by the litter layer, as according to Leighton-Boyce et al. (2007), eucalypt litter may intercept 3mmcm^{-1} of litter depth. Alternatively, accelerated infiltration by preferential flow in water repellent soils may also play a role, especially in eucalypt stands. Soils under eucalypt in the region are well-known to develop extreme water repellency during the dry summer season (*e.g.*, *Doerr et al*., 2000; *Ferreira et al.,* 2000; *Keizer et al.*, 2008; *Santos et al*., 2013). *Santos et al*. (2013) and *Vieira et al.* (2014) emphasized that addressing soil hydrophobicity in hydrological/erosion models may potentially improve the understanding of the process of infiltration, wetting-up and breaking of soil water repellency after the summer season.

SWAT may be underestimating infiltration capacity during the dry season, suggesting that the curve number method for surface runoff generation could be adapted to account for preferential flow following dry weather conditions. Overall, the model performance was satisfactory for both parameter ensembles and for both calibration and validation period.

Since for the sediment was not carried out for all parameter sets of the SWAT-SOLIM ensemble, a further water balance validation was done for the best fitting parameter set. Figure 3.26 shows thefit between the simulated and measured daily discharge for the gage Ponte Redonda for the period 1993 until 1995. The overall system performance was satisfactory, although peak discharges are underestimated. This can result from a misrepresentation of the precipitation pattern, since these sub-basins do not have a rain gauge in the proximities. The same model behavior as in the ensemble assessment is observed.
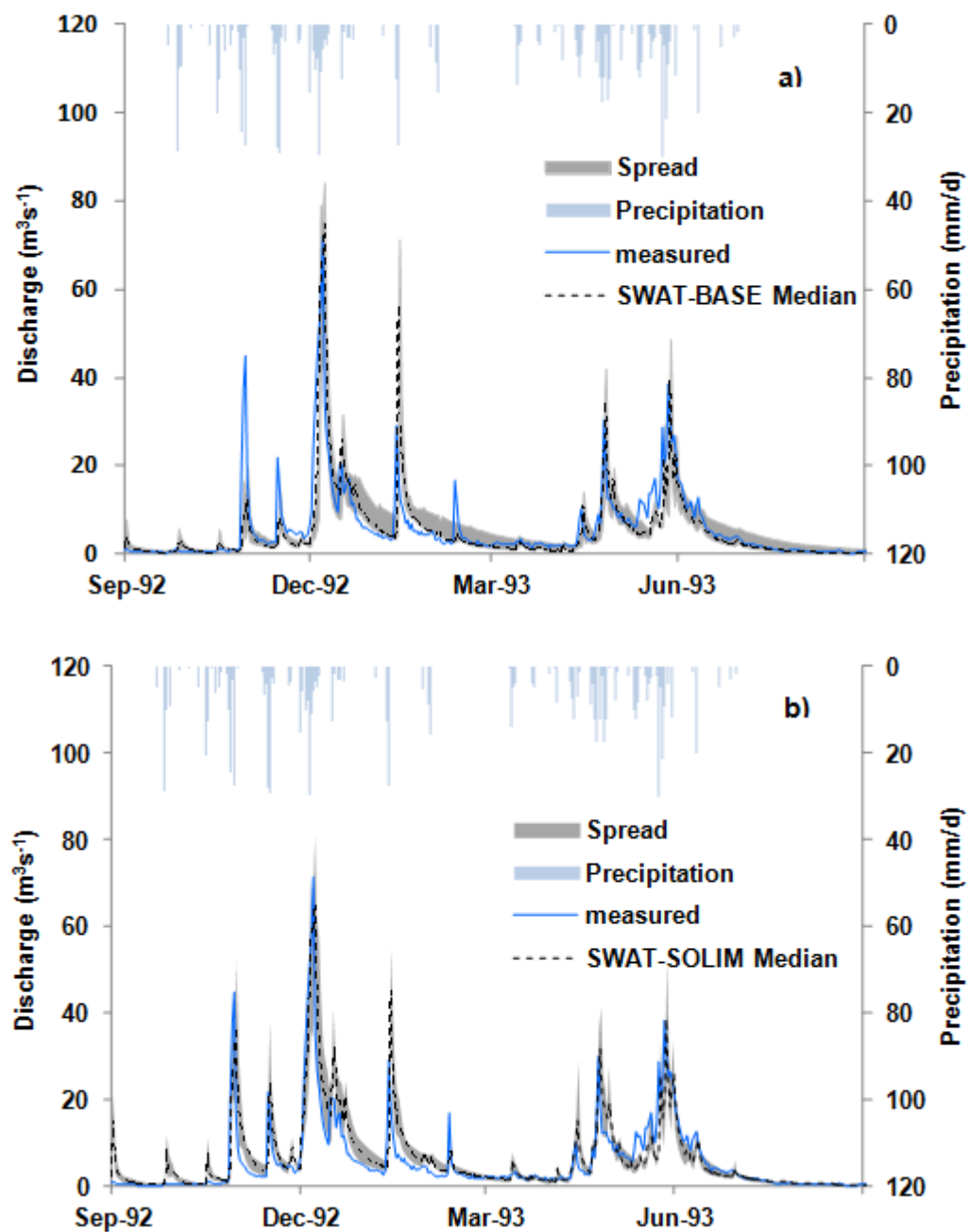
Fig. 3. 24: Measured and simulated daily discharge at the Águeda watershed outlet, Ponte de Águeda, for the calibration period (1991–1995). a) Results of the SWAT-BASE ensemble. b) Results of the SWAT-SOLIM ensemble. Statistical evaluation criteria, of both model ensembles are to be found in Table 3.11.
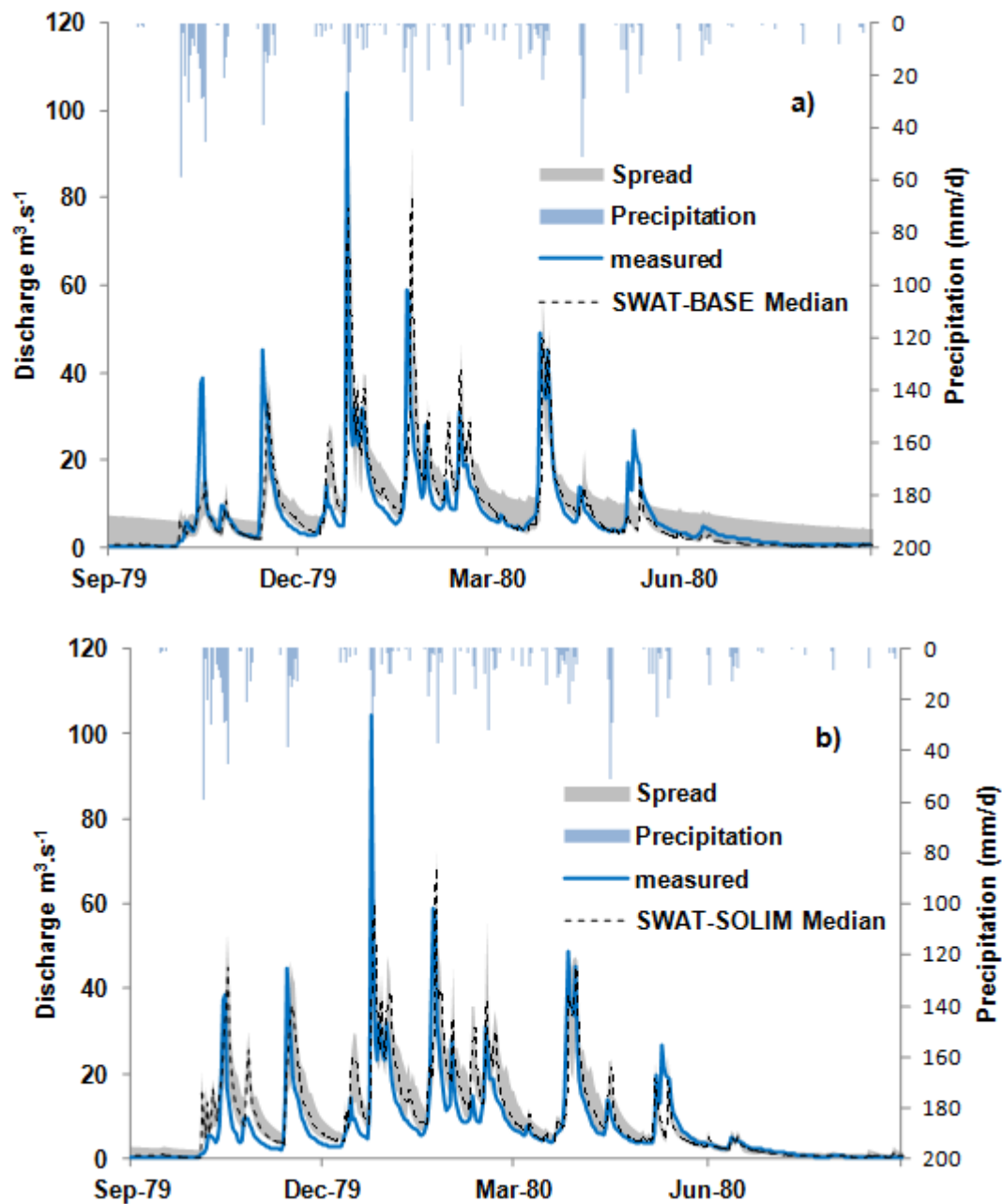
Fig. 3. 25: Measured and simulated daily discharge at the Águeda watershed outlet, Ponte de Águeda, for the validation period (May 1979–1981). a) Results of the SWAT-BASE ensemble. b) Results of the SWAT-SOLIM ensemble. Statistical evaluation criteria, of both model ensembles are to be found in Table 3.11.
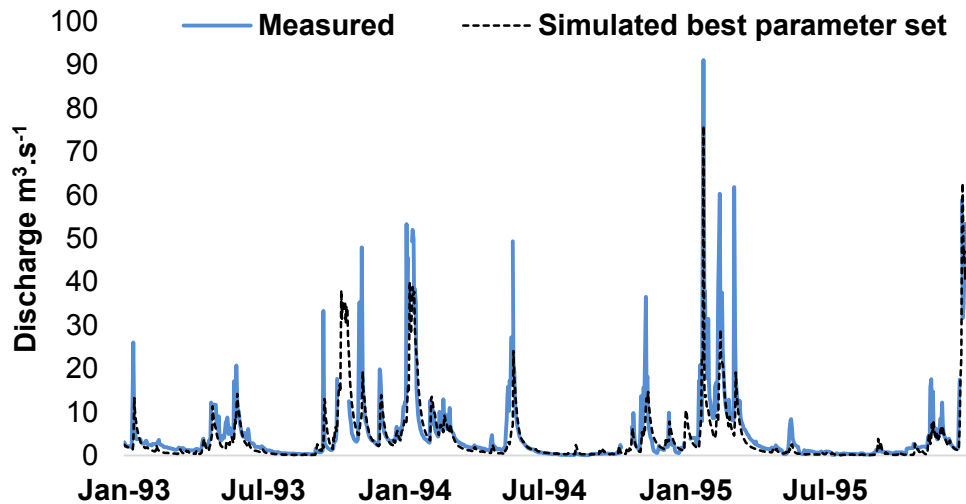
Fig. 3. 26: Measured and simulated daily discharge at the Águeda watershed gage Ponte Redonda, for the period 1993-1995. Simulated data obtained from the best fitting parameter set. R^2:0,63; LnE=0,62.

HRU-based assessment

Figure 3.27 provides an example of the plant available water for four representative HRUs. These consist of eucalypt plantations on granite-derived Humic Cambisols with different depths on steep slopes (>18°). The SWAT-BASE project predicts that the soils dry out during August, whereas the SWAT-SOLIM predicts that this occurs by mid- June, at least in the case of the shallow and intermediate effective soil depths. It is likely that SWAT-BASE does not correctly simulate temporal patterns in soil water availability for the shallower and intermediate soils, although it does for the deeper soils. Given the wide spread occurrence of soil water repellency in the study watershed when soils become dry, SWAT-SOLIM would suggest an earlier establishment of water repellency and associated changes in rates of infiltration and leaching of solutes due to preferential water movement (Blackwell, 2000). In a case of management scenario assessment, neglecting the timing of soil water repellency establishment, would lead to biased conclusions.

The differences of spatially differentiated runoff components predicted by the two SWAT projects can be seen from the example of the contribution of precipitation to surface runoff

generation (surface runoff coefficient) in Figure 3.28. SWAT-SOLIM predicts larger surface runoff coefficients than SWAT-BASE for more than 67 % of the watershed. Overland flow rates can range widely (from 5 % to 80 %) of precipitation, depending on soil preparation technique and antecedent wetness conditions (*Ferreira et al.*, 2000; *Leighton-Boyce et al.*, 2007; *Martins et al.*, 2013; *Boulet et al.*, 2015).
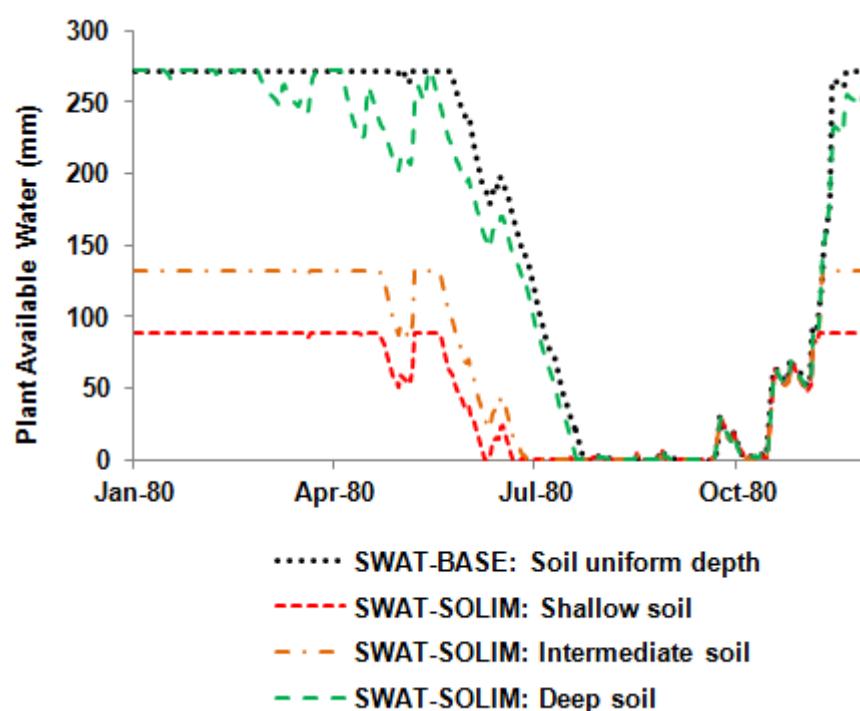
Fig. 3. 27: Simulated plant-available water for one HRU of SWAT-BASE and three HRUs of SWAT-SOLIM. All HRUs represent Humic Cambisols (with different depths) on granite, are located on slope class N 18°, have eucalypt land-use and are located in the same sub-basin. Example for the year 1980 within the validation period (May 1979–1981).

The dependence of the surface runoff generation process on effective soil depth and soil texture is highlighted in Figure 3.29. The figure shows the average annual surface runoff generation within one sub-basin (to ensure equal climatic conditions) of all HRUs aggregated by soil class. The average annual surface runoff is the highest for shallow soils over schist, as it would be expected given the low effective soil depth and fine texture. The second highest value of surface runoff generation is the one of shallow soils over granite. This suggests that

the impact of the effective soil depth on surface runoff generation prevails over the effect of texture.
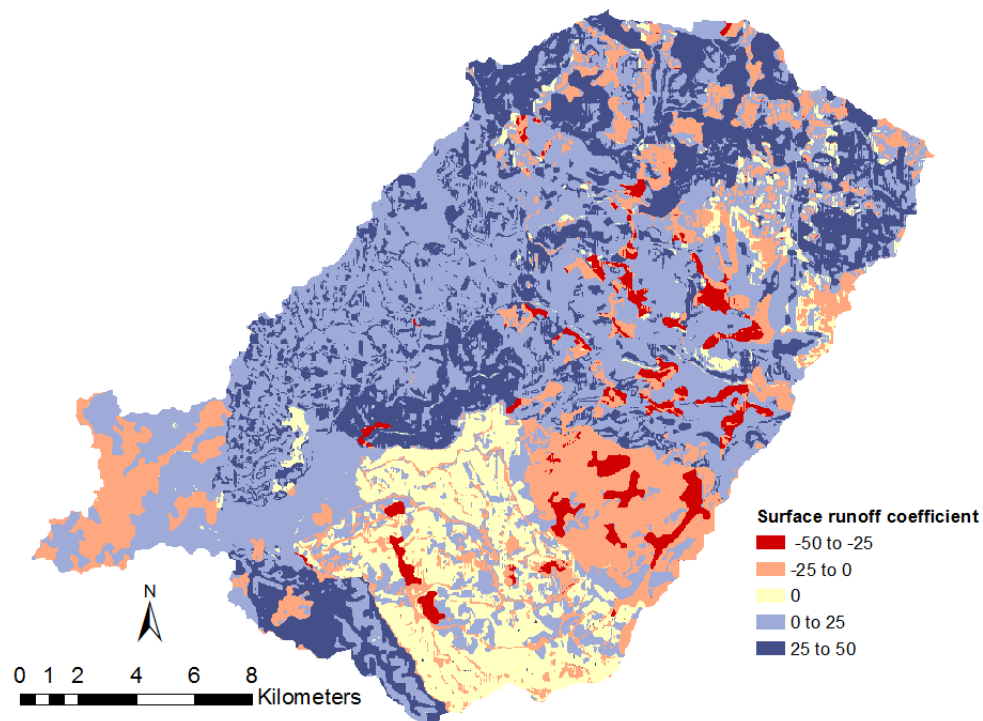
Fig. 3. 28: Average annual difference of percentage of precipitation that originates surface runoff (surface runoff coefficient), calculated as subtraction of contribution of precipitation to surface runoff from SWAT-SOLIM and contribution of precipitation to surface runoff from SWAT-BASE.
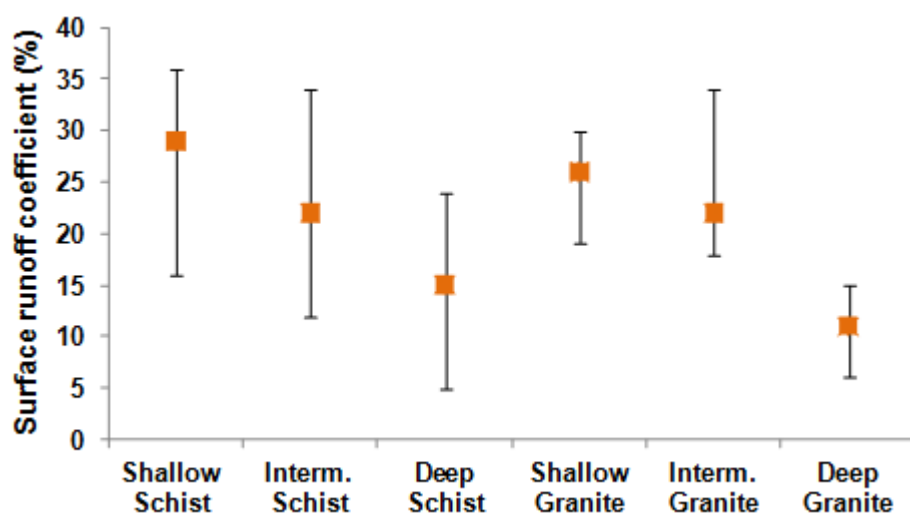
Fig. 3. 29: SWAT-SOLIM ensemble median (marker) and spread of average annual surface runoff generation within one sub-basin of all HRUs aggregated by soil class.

3.2.2.2   Sediment loads modelling

The most sensitive parameters for erosion simulations were the USLE land cover factor (USLE_C) for various land use, USLE support practice factor (USLE P), linear re-entrainment parameter for channel sediment routing (SPCON), exponent of re-entrainment parameter for channel sediment routing (SPEXP) and soil erodibility factor K (USLE_K).Sediment related parameters were used to compute the amount of erosion from the watershed. These parameters and their calibrated values are displayed in Table 3.12.

Table 3. 12: SWAT parameter sediment yield simulations and their calibrated values.

Parameter	Parameter Description[1]	Land cover	Fitted value
ADJ_PKR	Peak rate adjustment factor for sediment routing in the sub-basin (tributary channels).	All	0.63
PRF_BSN	Peak rate adjustment factor for sediment routing in the main channel.	All	0.0013
SPCON	Linear parameter for calculating the maximum amount of sediment that can be retained during channel sediment routing.	All	0.005
SPEXP	Exponent parameter for calculating sediment retained in channel sediment routing.	All	1.03
CH_COV1	Channel erodibility factor.	All	0,6
CH COV2	Channel cover factor.	All	1
USLE_K	USLE Soil erodibility factor	All	0.12
USLE_C	Minimum value of USLE C factor for water erosion (factor)	Pasture	0.10
		Corn	0.13
		Potato	0.2
		P. pinaster	0.002
		E. globulus	0.09
		Mediterranean shrub	0.004
USLE_P	Support practice factor	Pasture	0.86
		Corn	0.6
		Potato	0.86
		P. pinaster	0.9
		E. globulus	0.8
		Mediterranean shrub	0.86

The SWAT sediment predictions were calibrated against measured data at the Ponte de Águeda gauging station for the period 1992 to 1995 and validated for the period 1996 to 1998 as depicted in Figure 3.30.
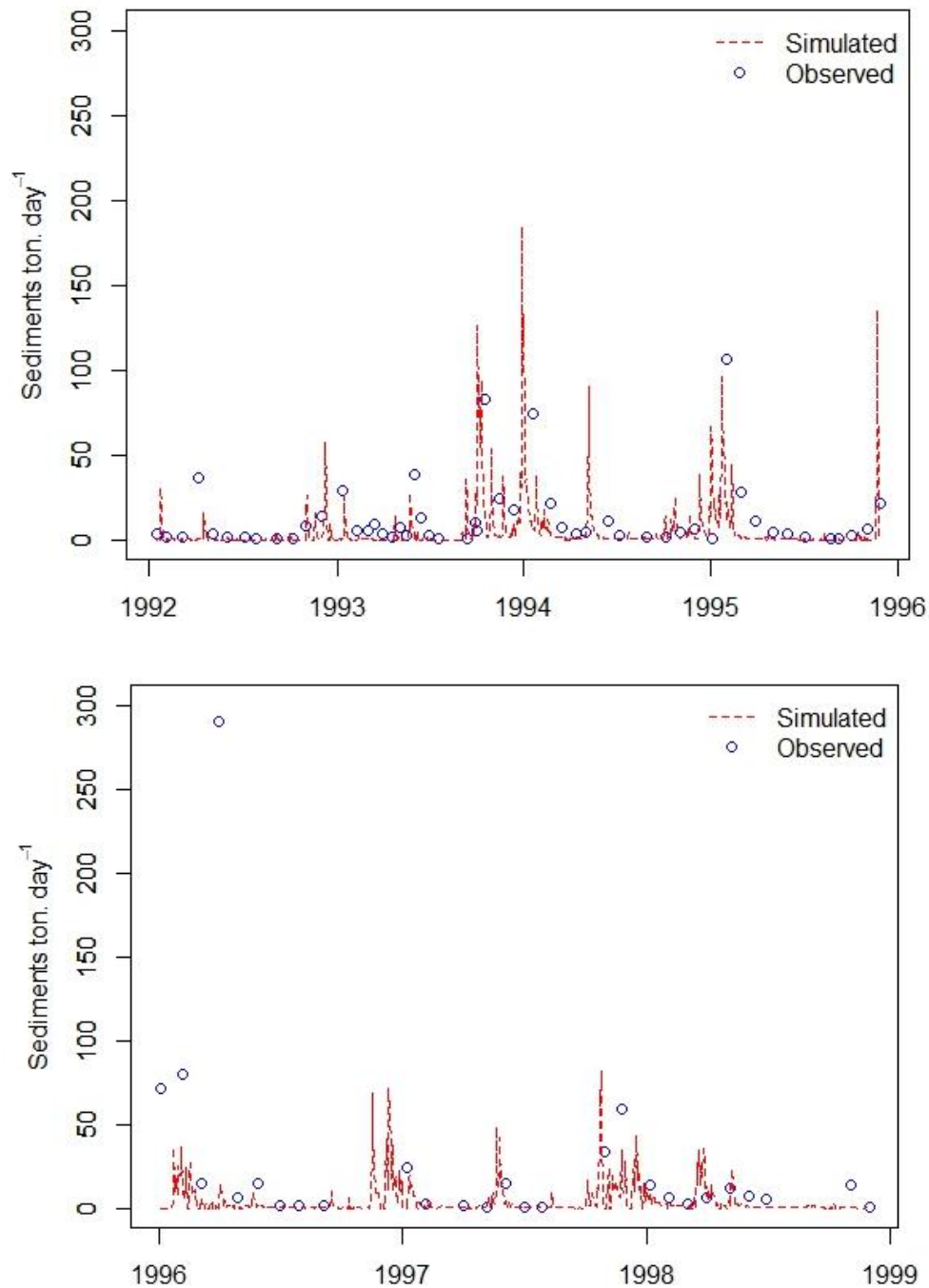
Fig. 3. 30: Measured and simulated daily sediment loads at the Águeda watershed gage Ponte Redonda, for the calibration period 1992-1995 (above) and validation period 1996 – 1999 (below).

The fit between sediment predictions and the observed concentrations demonstrates that the model is able to reproduce the overall sediment dynamics. Still, only R^2 is within a reportable range for the calibration period with R^2= 0.65 and 0.28 for the validation period.

The available data does not allow a detailed behavior assessment, nonetheless, most low flow periods were well simulated, while peaks (particularly during the year 1994) were over predicted and sediment recession curves were underestimated. At the beginning of the validation period (Fig. 3.31 b) the model fails to predict the high sediment loads, particularly for the event of 1st April 1996. These peak events may be related to the forest fires of late summer 1995, which, are not included in the model parameterization to simulate the watershed's recurring soil erosion rates. Given the limitation further assessments are conducted at the average annual base.

3.2.2.3 Spatial variability of sediment yields and intervention options

The predicted annual average sediment yield at the HRU level ranges from 0.2 to 15 ton.ha⁻¹.yr⁻¹ (Fig. 3.32 – upper corner left). Soil formation rates in Europe under current conditions are estimated to vary in between 0.3 and 1.2 ton.ha⁻¹.yr⁻¹ (*Verheijen et al.*, 2009). Losses exceeding 1 ton.ha⁻¹.yr⁻¹can be considered irreversible and unsustainable while losses between 5 to 20 ton.ha⁻¹.yr⁻¹ can have serious impacts, both at the site where the soil is lost and off-site in downstream flood zones (*Van-Camp et al.*, 2004; *Verheijen et al.*, 2009). Taking this into consideration the annual soil erosion rates predicted by the model could lead to environmental problems in the watershed as further downstream. In the study on soil losses in Europe, conducted by *Panagos et al.* (2015c), soil erosion rates ranging between 0.5 to 2 ton.ha⁻¹.yr⁻¹ have been reported for this region of Portugal. The model predicts around 93 % of the watersheds area fitting the assessment of *Panagos et al.* (2015c). Almost 4 % of the watershed was predicted with an erosion rate of 5 to 15 ton.ha⁻¹.yr⁻¹ and 3 % between 2 to 5 ton.ha⁻¹.yr⁻¹. Eucalypt plantation areas and non-terraced on steep slopes showed the highest

soil loss rates. Several authors (*Shakesby et al.*, 1996; *Prats et al.,* 2012; and *Malvar et al.*, 2016) have reported for the Águeda watershed region soil loss rates under eucalypt ranging from 4 to 6 ton.ha^{-1}.yr^{-1}. *P. pinaster* areas are generally in higher steep landscape positions when compared with eucalypt plantations. Higher surface runoff rates and soil loss should be therefore expected to be generated, this may be countered by the closed litter layer and the tree canopy, which may serve as shield and reduce the rainfall energy. *Shakesby et al.* (1996) and *Prats et al.* (2012) reported for this land use erosion values up to 1 ton.ha^{-1}.yr^{-1}similarly to the values predicted by the model. The model results for annual and daily sediment loads for the base simulation can be considered a sufficient basis for the simulation of management options scenarios. Nevertheless, it is important to consider the uncertainties in the model results, which can originate from the input data, the model parameters and the model structure (*Breuer et al*. 2006). Nevertheless, while conducting scenario analyses, all scenarios shall be exposed to the same uncertainties in data input and model structure, thus relative differences should be attributed to the scenario changes (*Bieger et al*., 2012).

At the spatial scale (Fig. 3.31) soil losses seem to be consistently distributed throughout the watershed, this could mean that the effect of geology on sediment export could be masked by other ruling processes as slope, land use and management. Still, the higher soil loss HRUs have a schist geology. The simulation of the RESTILL scenario resulted in an average annual watershed sediment reduction of 90 %, the TER scenario showed the least reduction of sediment loads from current conditions with 48 % and the combined bmp scenario (TER+RESTILL) resulted in the greatest reduction with 95 %. At the HRU level the RESTILL scenario shows a smaller area of impact (which is attributed to the location of the land use) at larger reduction rates when compared to the TER scenario. The TER scenario had mostly sediment export reductions on the range of 75 to 80 % particularly on strong sloping areas, while the RESTILL scenario exhibits a greater reductions of 90 to 100 % in areas with geology schist. The combination of the management options, since they do not create land completion to their implementation, provide the best spatially reduction opportunity.
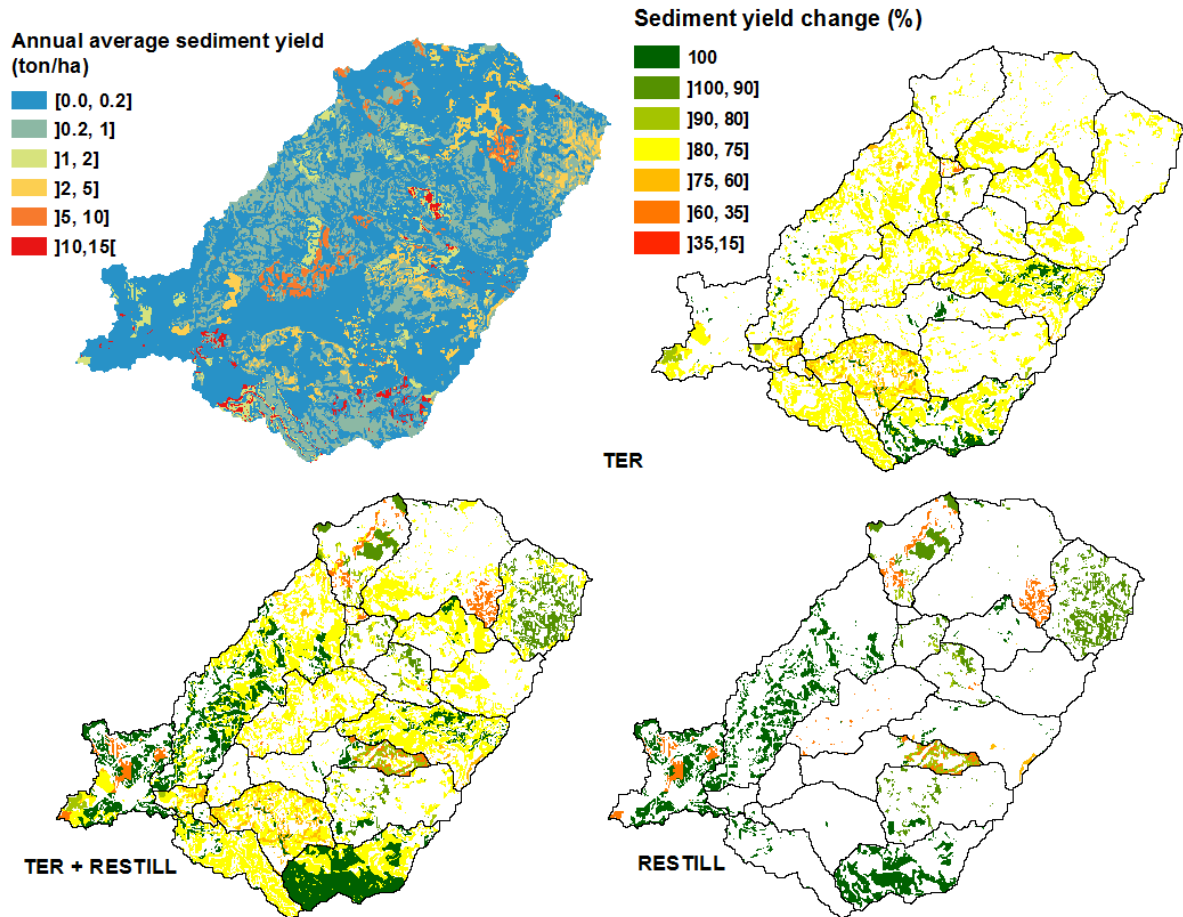
Fig. 3. 31: Spatial distribution of annual average sediment yield at HRU scale of Águeda watershed during the period 1992-1998 and relative reduction in annual average sediment yield for the intervention options scenarios TER, RESTILL and the combined scenario TER+RESTILL.

Although the differences in the magnitude of the reduction of average annual sediment yields of the simulated management scenarios are not extreme, still, the simulation bring to light that tillage operations on steep to moderate sloped agricultural fields are the main responsible for the annual recurring sediment exports (*i.e.* disregarding event based forest fires and terrace construction with large machineries).

Figure 3.32 gives the comparison between the RESTILL and BASE scenario for the different slope and soil depth classes under agriculture. On average, soil losses from agricultural lands calculated in this study ranged from 0.002 to 8.3 ton.ha^{-1}.yr^{-1} with only about 5 % of the watershed belonging to agricultural areas in the exhibiting values above the 2 ton.ha^{-1}.yr^{-1}.

These areas are within the class of moderate to strongly sloping, furthermore, the sediment exports follow a rational increase with increasing slope. This is expected because a higher overland flow concentration occurs as the steepness increases.
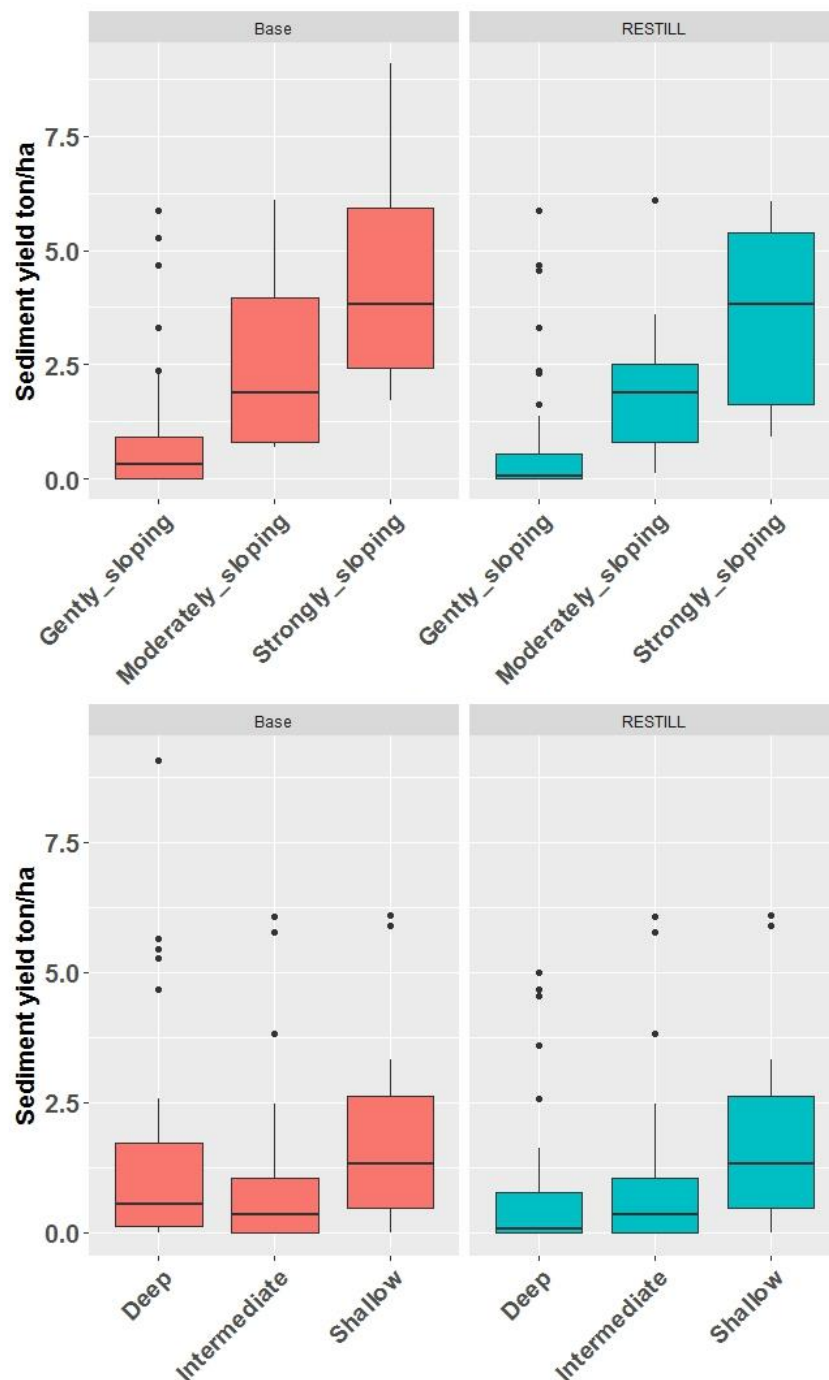
Fig. 3. 32: Annual average sediment yield of agriculturally used HRUs per slope class (above) and soil depth (bellow) for the period 1992 – 1998.

The applied RESTILL scenario achieved a sediment reduction in all slope classes. The overall HRU average sediment yield of the BASE simulation decreased from 1.2 to 0.5 ton.ha^{-1}.yr^{-1}.
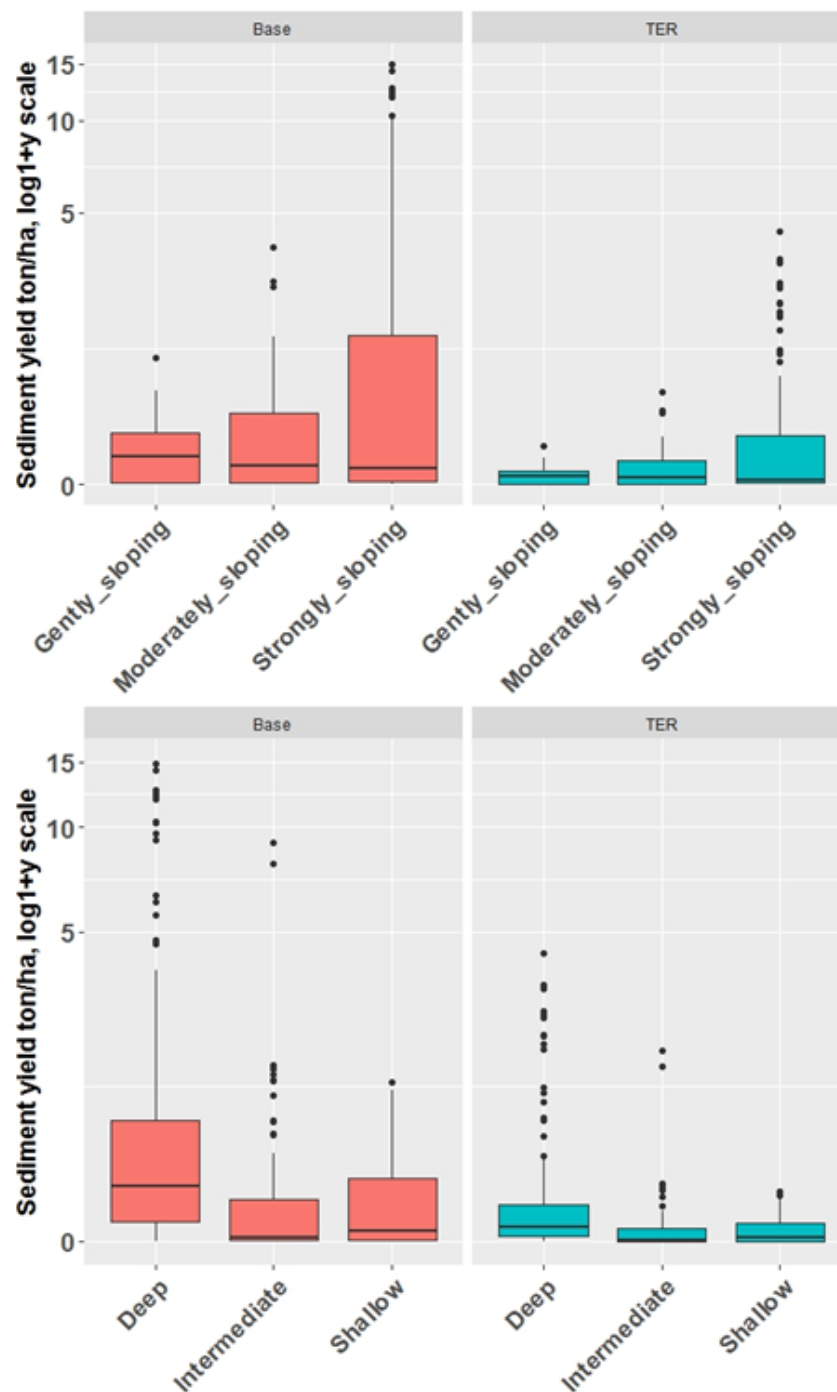
Fig. 3. 33: Annual average sediment yield of *E. globulus* stocked HRUs per slope class (above) and soil depth (bellow) for the period 1992 – 1998.

The dependence of sediment yield and soil depth do not follow logical sequence of sediment yield increase from deep to shallow soil profile since soil depth strongly affects the storage capacity, water infiltration and accordingly runoff generation. Still, the higher soil losses occur in shallow soils.

The model set up allowed corn with tillage operation to grow on HRUs with a deep soil profile, this may be the reason for the higher exports. Furthermore the sediment export results mainly from HRUs under schist geology since HRUs on granite were set up as terraced. Once the tillage operation is removed in the scenario RESTILL the logical increase of soil loss with decreasing soil depth can be observed.

Erosion rates for *E. globulus* stocked HRUs range from 0 to 14.9 ton.ha^{-1}.yr^{-1}(Fig 3.33) with an average HRU soil loss of 0.6 ton.ha^{-1}.yr^{-1}. Particularly at HRUs with strong slope and deep soil higher sediment yields are observed. This can indicate that the model effect of soil profile depth is overridden by slope in the model. HRUs with exports above 2 ton.ha^{-1}.yr^{-1}only account for 2 % of the watershed. The TER scenario reduced the erosion rates to a maximum of 4.3 ton.ha^{-1}.yr^{-1} and the average HRU soil loss to 0.2 ton.ha^{-1}.yr^{-1}.

The analysis of HRU annual average helps to identify critical source areas for sediment and therefore locate areas where intervention options should be prioritized. It is debatable if the simulated scenarios were to be applied to the entire watershed since adequate machinery for terrace management and policy incentives would be necessary. Yet, these scenarios can be considered as realistic since current policy both favors eucalypt exploitation (*Carvalho Santos et al.*, 2015) as great emphasis is being placed in fighting soil degradation in Mediterranean land-use systems (*Madeira and Araújo*, 2015; *Stolte et al.*, 2016).

From the modelling set up improved result could be achieved when incorporating different growth stages of *E. globulus*. A plantation of young eucalypts is often portrayed by small growing tree individuals on bare ground, thus providing low rainfall interception and soil protection. While the overall average annual soil loss values are relatively low, it should be

kept in mind that erosion at the watershed scale can be severe when it is disturbance driven as post-fire or terrace ploughing. Further improvements would be possible if the eucalypt management techniques (as terrace building and harvesting after the 3rd generation) could be included. For this dedicated field surveys are essential in order to reduce uncertainties in model parameterization, still, this study is able to give relative estimates of the erosion measures.

4. CENTRAL FINDINGS AND CONCLUSIONS

4.1 Synoptic answers to research questions

This work is based on two case studies in which the SWAT model was applied to meso-scale rural watershed in two contrasting regions of Europe. Each of the studies had a different focus but faced similar restrictions in the application brought by limited spatially differentiated soil information for model set-up and data for calibration, particularly, data related to water quality parameters. The main objective of this work was achieved, while groundwork for the application of SWAT in both regions was conducted. The research questions formulated in Chapter 1.5 can be answered as follows:

Research question 1 - Can Soil-landscape models close gaps in spatially distributed soil data for hydrological modelling?

In the Ukraine study case, soil data availability was addressed in Chapter 2.1.2.1. The built soil landscape model (presented in Chapter 2.3.2) enabled the construction of a detailed new soil map, which does not contain gaps as in the existing conventional soil map. The level of detail achieved is similar, which is a logical consequence of using the conventional map as the primary base for the derivation of the soil landscape model. At the field scale a better representation of the soil distribution was achieved with the new area wide soil map, as each soil class is best predicted using a different combination of predictors filtered at different scales, such as digital terrain analysis, land use distribution, and expert knowledge. The soil texture transformations, needed for the prediction of spatially distributed soil hydraulic properties, were suitable to represent cumulative particle size distribution curves. The estimated water content at field capacity was well reproduced by all PTFs. However, only the PTF of *Wösten et al.* (1999) provided available water capacity estimates with high accuracy.

Even though the initially available data was sparse, the combined application of fieldwork and modelling techniques was advantageous. The results achieved allowed the parameterization of the SWAT model in the Dobrotvir watershed.

In the study case in Portugal, the soil-landscape model presented in Chapter 2.3.3 proposes a simple approach for addressing limitations in spatially differentiated soil information, in the context of hydrological assessments. The SoLIM model was used to develop a map of effective soil depths for the Águeda watershed (north-central Portugal), based on the empirical relationships between effective soil depth and environmental conditions. The effective soil depth predictions were validated in the field and found to provide a satisfactory representation of the watershed profile depth variation. *Geza and McCray* (2008) state that more precise topographic or soil information does not necessarily increase model performance in a significant manner, in spite of the additional efforts and costs of collecting this additional information. However, the assessment of management options – for which SWAT was designed and often used (*e.g., Ulrich and Volk*, 2009) – may be negatively affected by a coarser model structure (such as SWAT-BASE), since an implicit misrepresentation hydrological process can occur. Such a misrepresentation may take place both in time (*e.g.*, in the intra-annual water balance with a late soil dry out) and space (*e.g.*, misrepresentation of areas prone to surface runoff generation). To evaluate the impact of the changed soil map on the hydrologic assessment two SWAT models applications were implemented only differing in the soil profile depth representation (as described in Chapter 2.4.3).

In areas where soil data is scarce, it is possible to estimate soil properties using associated environmental variables. The improved representation of soil variation in the SWAT hydrologic model provides a valuable tool for water resource planners and managers, which will produce a more plausible picture of the effectiveness of management practices and produce more reliable results.

Research question 2 - How adequately could SWAT be parameterized in order to simulate water balance and water quality under data scarcity conditions?

Complex distributed hydrological models are valuable tools for land use planning and decision making, in the context of dealing with emerging environmental stressors, such as climate change and water resource competition. However, the baseline level of data needed to support such models has frequently not kept pace with model complexity (*Hörmann et al.*, 2009). In addition, adequate parameter data is often unavailable or is of poor quality (*Bossa et al.*, 2012; *Heuvelmans et al.*, 2004), and hydrologic models must frequently rely on rough parameter estimates (*Hörmann et al.*, 2009). This is a major concern for hydrologic assessments. *Heuvelmans et al.* (2004) pointed to the problem of non-independent parameters, in which the effect of one parameter on model output will depend on the values of other (supposedly independent) parameters. In this context, *Beven* (1993) stressed the importance of a parameter set based analysis, where the parameter set is examined as a functional whole, rather than as individual values. Following the theory of parameter equifinality (*i.e.*, multiple different parameter sets producing indistinguishable model outputs), *Beven* (1993, 1996) suggested that the predictions of all acceptable parameter set combinations should be included into the assessment, which allows the nonlinear response of parameters to be taken into account in predictions (*Beven and Freer*, 2001). Following this approach, a common modelling practice involves merging individual model outputs from numerous acceptable parameter sets, rather than restricting the focus on only the "best" parameter set. To test this parameterization approach at the Águeda watershed parameter ensembles were evaluated (Chapter 3.2.2.1) while calibrating water balance. It was noticeable that a better model set-up, which a better representation of the soil spatial distribution, was reflected in narrower model output spreads and narrower parameter distances.

In the Dobrotvir study case the lack of representation of spatial rainfall variability was a great source of model error, which was reflected by the evaluation criteria results as described in

Chapter 3.2.11. Overall, both study cases were satisfactorily calibrated and validated for water balance whereas water quality criteria was more problematic due to lack of reliable input information (*e.g.* timing and quantities of applied fertilizers in the Ukraine study case, *E. globulus* growth stages and terraces preparation dates in the Portuguese study case) and calibration data. Generally, the SWAT simulations appeared to be suitable to achieve the objectives of this work and further evaluate land management scenarios.

Research question 3 -To which extent does a HRU-based assessment allow model verification under data scarcity conditions?

In data scarce regions it is common that the only observed data available for calibration is the one related to the watershed's outlet. In many occasions even the outlet observed data may be unreliable or not have the needed frequency to ensure an adequate calibration. This was the situation of both study cases especially, for the water quality parameters being in focus. In these cases, even when the main calibration is conducted for the watersheds outlet, it should be avoided to focus exclusively at the outlet. *Wi et al.* (2014) stated that a major source of model uncertainty originates from the lack of proper identification of parameter values across the watershed, particularly when model calibration is reliant on stream flow data from only a few available points within a watershed. *Bieger et al.* (2015) stressed the importance of having HRU-based assessments as complementary tools to conventional hydrological model evaluations. HRU assessments can provide the needed process verification, particularly since simulations start at the HRU level and the examined process occurs at the HRU level (*e.g.* leaching of nitrate, crop yield). This type of assessment was essential to verify the nitrate-N dynamics (Chapter 3.2.1.2) for the Dobrotvir watershed where the denitrification rates after fertilization were analysed. Furthermore, a direct HRU-based comparison allowed a more detailed comprehension of the implemented scenarios effect on both runoff components (*e.g.* surface runoff, lateral flow), as on nitrate-N exports and biomass production (Chapter 3.2.1.3).

At the Águeda watershed study site the HRU-based assessment (Chapter 3.2.2.1) made visible the differences on plant available water. When incorporating further detail in soil depth, critical source areas for surface runoff generation and critical areas for soil loss were better identified. Areas with shallow soils need to be carefully represented since these have a large impact in water balance calculations and sediment yield. The analysis of SWAT output at HRU level also allowed to identify further uncertainties as *e.g.* the high sediment yields obtained in HRUs with strong slope and deep soil profiles. Further plausibility checks relating HRU area to HRU-SWAT output could be further conducted in order to improve model set-up and parameterization.

Still, the utilized HRU-based assessment allowed model verification under data scarcity conditions when statistical evaluation criteria are not applicable while providing information on critical processes, areas and pinpointing subjects where further investigations are needed.

Research question 4 - *Do analysis of observed data and model outputs help to acquire information about ruling hydrological processes?*

The modeller's (user's) understanding of key hydrological processes in the watershed is vital when working with hydrological models, since direction and "endpoint" decisions are a responsibility of the user. When observed data is of good quality and enough quantity, such information is readily available. In situations of data scarcity, either there is the possibility to gain knowledge via specific field measurements or it can be gained through the analysis of model outputs. In the Dobrotvir watershed the importance of the interactions between surface and groundwater with a large storage component were illustrated by the auto-correlation analyses with a time lag of 30 and 550 days. Further, monthly observations assessment allowed to depict the effect of a slower snowmelt response in the system. In the Águeda watershed study case the water regulating role of the soils was assessed by means of field investigations described in Chapter 2.2.1.1. The results are evaluated in Chapter 3.1.2.1. The

role of soil shallowness and soil water repellency was further corroborated by the modelling results of the more detailed SWAT model application SWAT-SOLIM. As stressed by several authors (*e.g.*, *Bieger et al.*, 2015; *Bossa et al.*, 2012) the representation of a realistic simulation of key hydrological processes for the spatial distribution of runoff components in SWAT is fundamental.

Research question 5 -*Under data scarcity condition, to what extent can the model be used to simulate management scenarios on rural systems?*

Studies using SWAT to assess management practices typically focus on the land use within a watershed (*Easton et al.*, 2008). In SWAT, management practices such as planting, harvesting, and tillage can be simulated for each HRU, by explicitly defining the appropriate management parameters and dates. Both temporal and spatial scales play an important role when designing management practices. Despite the difficulties brought by the data scarcity, successful scenario implementations were possible as shown in Chapters 3.2.1.3 and 3.2.2.3.

The impacts of the different intervention options were evaluated on water balance, Nitrate-N export and sediment yield at the watershed, sub-watershed and, when feasible, HRU level. Given the uncertainties in model implementation and calibration, most of the results were evaluated as relative change to a base simulation. The model simulations showed the anticipated response to changes in management and reflected the rational spatial variation within the watershed reasonably well. A detailed assessment of model shortages in setup, parameterization and calibration should be a key part of modelling activities. Above all, in areas with data scarcity, it should be avoided focusing exclusively on discharge at the watershed's outlet. An assessment of runoff components that is based on a more reasonable spatial differentiation needs to go along with in-stream assessments. Such an assessment should particularly focus on areas where strategies and plans are developed to achieve the good ecological status required by the EU Water- Framework-Directive (EC, 2000).

4.2   Conclusions and Outlook

In this thesis, the SWAT model was utilized to simulate hydrological processes, nitrate-N export, and sediment yield in response to land intervention options in agricultural areas and forested areas stocked with *E. globulus*. In the Ukraine study case, as expected, greater reductions of fertilizer application lead to smaller rates of diffuse pollutions. This is a logical result, which arises no great surprise. A recommendation to whether test or not such a fertilization reduction must never be done without considering the effects such a management practice would have on agricultural yield and far more on farmer income. A perhaps better option would be the SRC scenario, which not only would allow a reduction in nitrate-N export but also provide a nowadays highly requested raw material: woody biomass. This scenario provided the higher spatially differentiated results per sub-basins which is due to the area suitability for SRC as identified in this work. Being the Dobrotvir watershed largely groundwater fed, pressure on the water resource should not pose a risk as SRC plantations are known for higher water consumptions. The feasibility of this scenario and, furthermore, necessity of this raw material is illustrated by the existence of the EU funded project SEEMLA ("Sustainable exploitation of biomass for bioenergy from marginal lands" H2020 Grant nr. 691874; *SEEMLA*, 2016b) where suitable innovative land-use strategies for a sustainable production of plant-based energy on marginal lands while improving general ecosystem services was tested, or the ongoing EU BBI-JU project Dendromass4Europe ("Securing Sustainable Dendromass Production with Poplar Plantations in European Rural Areas"; Grant nr 745874; *D4EU*, 2017).

The research conducted in the Águeda watershed in Portugal provides a base for future modelling investigations in the area. Possible modelling improvements of the hydrological simulation for the region were depicted such as the inclusion of soil water repellency, which greatly influences the infiltration patterns in the watershed. Improvements in the sediment yield simulation should notably be related with the representation of the *E. globulus* plantations growth patterns and management operations (*e.g.* terrace building) in the region. Furthermore,

the inclusion of post wildfire erosion in the model remains a challenging task for future investigations. The scenarios evaluated in this work pinpointed the importance of tillage operations in the active recurring soil loss in this rural watershed.

Further simulation improvements, particularly for N and sediments evaluations, would be possible if uncertainties related to model structure would be addressed. The SWAT version used in this work assumes an artificial connectivity which results from the aggregation of areas with the same land use/soil/slope characteristics which are spatially disconnected into one single HRU within a sub-watershed. Further, the routing between spatially discrete HRUs, prior to their contribution to the sub-watershed's water balance and matter transport would greatly improve the results of sediment yield (by *e.g.* taking into account deposition in adjacent fields or back slopes) as for N exports (*e.g.* denitrification in areas with lowland characteristics). An option would be the application of one of the SWAT routed modifications (*e.g.* SWAT Landscape by *Arnold et al.,* 2010; SWAT-GRID by *Rathjens and Oppelt*, 2012; grid-based version of SWAT landscape by *Rahtjens et al*., 2014) are being tested in different regions of the world. Still, the only way to improve model behaviour would be to conduct dedicated studies in the region of focus.

Although important research questions were evaluated when considering the impact of management practices changes on water quality, the meaning of this thesis rests on demonstrating how relevant it is to tackle shortages of spatially differentiated soil information. A representative prediction of the spatial extent of the soil water storage system is of great importance for the simulation of water, sediment and nutrient transport. In turn they are often the aim of the development of management scenarios and best management practices. Furthermore, the proposed ensemble-based assessment allows hydrological models not to rely upon the single true model set up, given by statistical criteria, while making possible an evaluation of parameter ranges and of model output uncertainties. Such approaches contribute toward more reliable model predictions and the tested methods are transferable to

other regions with differing landscape and climate conditions with similar problems of data scarcity, particularly soil spatially differentiated information.

5. REFERENCES

Abbaspour, K.C. (2007): User Manual for SWAT-CUP SWAT Calibration and Uncertainty Analysis
Programs Swiss Federal Institute of Aquatic Science and Technology, Eawag, Dübendorf,
Switzerland, available at:
http://www.eawag.ch/organisation/abteilungen/siam/software/swat/indexEN (last access:
January 2010).

Abbaspour, K.C., Yang, J., Maximov, I., Siber, R., Bogner, K., Mieleitner, J., Zobrist, J., Srinivasan, R.
(2007): Modelling hydrology and water quality in the prealpine/alpine Thur watershed using
SWAT. J. Hydrol. 333, 413–430.

Albert, E., Förster, F., Ernst, H., Kolbe, H., Dittrich, B., Laber, H., Handschack, M., Krieghoff, G.,
Heidenreich, T., Riehl, G., Heinrich, S., Zorn, W.(2007): Umsetzung der Düngeverordnung -
Hinweise und Richtwerte für die Praxis. Landesamt für Umwelt, Landwirtschaft und Geologie.
https://publikationen.sachsen.de/bdb/artikel/15242/documents/18421.

Arnold, J.G., Srinivasan, R., Muttiah, R.S., Williams, J.R. (1998): Large area hydrologic modeling and
assessment – Part 1. Model development. J. Am. Water Resour. As. 34, 73–89.

Arnold, J.G., Allen, P.M., Volk, M., Williams, J.R., Bosch, D.D. (2010): Assessment of Different
Representations of Spatial Variability on SWAT Model Performance. Trans. ASABE 53, 1433–
1443.

Arnold, J.G., Kiniry, J.R., Srinivasan, R., Williams, J.R., Haney, E.B., Neitsch, S.L. (2011); Soil and
Water Assessment Tool Input/ Output Documentation Version 2009. Texas Water Resources
Institute Technical Report No. 365.

Aronsson, P.G., Bergström, L.F., Elowson, S.N.E. (2000): Long-term influence of intensively cultured
short-rotation Willow Coppice on nitrogen concentrations in groundwater. J. Environ. Manage.
58, 135–145.

Aronsson, P.G., Bergström, L.F. (2001): Nitrate leaching from lysimeter-grown short-rotation willow coppice in relation to N-application, irrigation and soil type. Biomass Bioenerg. 21, 155–164.

Atlas Digital do Ambiente (1982): Carta litológica; - Start distribution, 1982; Agência Portuguesa do Ambiente I.P. http://sniamb.apambiente.pt/. (last access: September 2016).

Bagnold, R.A. (1977): Bed load transport by natural rivers. Water Resour. Res. 13, 303–12.

Baumann, M., Kuemmerle, T., Elbakidze, M., Ozdogan, M., Radeloff, V.C., Keuler, N.S., Prishchepov, A.V., Kruhlov, I., Hostert, P. (2011): Patterns and drivers of post-socialist farmland abandonment in Western Ukraine. Land Use Policy; 28, 552–562.

Becker, A., Braun, P. (1999): Disaggregation, aggregation and spatial scaling in hydrological modelling. J. Hydrol. 217, 239–252.

Behrens, T., Zhu, A.X., Schmidt, K., Scholten, T. (2010): Multi-scale digital terrain analysis and feature selection in digital soil mapping. Geoderma; 155, 3–4, 175–185.

Bekele, E.G., Nicklow, J.W. (2007): Multi-objective automatic calibration of SWAT using NSGA-II. J. Hydrol. 341, 165–176.

Beven, K.J., Kirkby, M.J. (1979): A physically-based variable contributing area model of basin hydrology. Hydrol. Sci. Bull. 24, 43–69.

Beven, K.J. (1993): Prophecy, reality and uncertainty in distributed hydrological modeling; Adv. Water Resourc. 16, 41–51.

Beven, K.J. (1996): Equifinality and Uncertainty in Geomorphological Modelling. In: Rhoads, B.L., Thorn, C.E. (Eds.) The Scientific Nature of Geomorphology. John Wily & Sons, Chichester, UK, pp. 289–313.

Beven, K., Freer, J. (2001): Equifinality, data assimilation, and uncertainty estimation in mechanistic modelling of complex environmental systems using the GLUE methodology. J. Hydrol. 249, 11–29.

Bieger, K., Hörmann, G., Fohrer, N. (2012): Simulation of streamflow and sediment with the SWAT model in a data scarce catchment in the Three Gorges Region, China. J. Environ. Qual. doi: 10.2134/jeq2011.0383.

Bieger, K., Hörmann, G., Fohrer, N. (2015): Detailed spatial analysis of SWAT-simulated surface runoff and sediment yield in a mountainous watershed in China. Hydrolog Sci J. 60, 784–800.

Blackwell, P.S. (2000): Management of water repellency in Australia, and risks associated with preferential flow, pesticide concentration and leaching. J. Hydrol. 231–232, 384–395.

Bloemen, J., Fichot, R., Horemans, J. A., Broeckx, L. S., Verlinden, M. S., Zenone, T., Ceulemans, R. (2017): Water use of a multigenotype poplar short-rotation coppice from tree to stand scale. GCB Bioenergy; 9, 370–384.

Blumensaat, F., Wolfram, M., Krebs, P. (2012): Sewer model development under minimum data requirements. Environ Earth Sci. 65, 1427–1437 doi/10.1007/s12665-011-1146-1 .

Boden AG (2005): Bodenkundliche Kartieranleitung. 5. Aufl. Bundesanstalt für Geowissenschaften und Rohstoffe. Hannover.

Bossa, A.Y., Diekkrüger, B., Igué, A.M., Gaiser, T. (2012): Analyzing the effects of different soil databases on modeling of hydrological processes and sediment yield in Benin (West Africa). Geoderma; 173–174, 61–74.

Boulet, A.K., Prats, S.A., Malvar, M.C., González-Pelayo, O., Coelho, C.O.A., Ferreira, A.J.D., Keizer, J.J. (2015): Surface and subsurface flow in eucalyptus plantations in north-central Portugal; J. Hydrol. Hydromech. 63, 3, 193–200 .

Bouma, J. (1989) Using Soil Survey Data for Quantitative Land Evaluation. In: Stewart B.A. (eds) Advances in Soil Science. Adv Soil Sci. 9, 177–213 Springer, New York, NY.

Breda, N., Granier A., Barataud, F., Moyne, C. (1995): Soil water dynamics in an oak stand. 1: soil-moisture, water potentials and water-uptake by roots. Plant Soil 172, 1, 17–27 .

Breuer, L., Huisman, J.A., Frede, H.G. (2006): Monte Carlo assessment of uncertainty in the simulated hydrological response to land use change. Environ. Model Assess. 11, 209 https://doi.org/10.1007/s10666-006-9051-9.

Brown, K.R., van den Driessche, R. (2002): Growth and nutrition of hybrid poplars over 3 years after fertilization at planting. Can. J. For. Res. Can. la Rech. For. 32, 226–232.

Cardoso, J.V. (1965): Os solos de Portugal, sua classificação, caracterização e génese: 1- a sul do rio Tejo (Portuguese soils, their classification, characterization and genesis: 1- south from the Tagus river). General- Directorate for Agricultural Services, Lisbon.

Cardoso, L.C., Bessa, M.T., Marado, M.B. (1973): Carta dos solos de Portugal na escala 1: 1,000,000. Agron. Lusitana. 33, 481-602.

Cardoso, J.C. (1974): A classificacao dos solos de Portugal-nova versão. Bol. Solos SROA; 17, 14– 46.

Carpenter, S.R., Correll, D.L., Howarth, R.W., Shar,, C.N.F. (1998): Nonpoint pollution of surface waters with phosphorus and nitrogen. Ecol. Appl. 8, 559–568.

Carvalho-Santos, C., Nunes, J.P., Monteiro, A., Hein, L., Honrado, J.P. (2016): Assessing the effects of land cover and future climate conditions on the provision of hydrological services in a medium-sized watershed of Portugal. Hydrol. Process. 30, 720-738.

Cerdà, A., Morera, A.G., Bodí, M.B. (2009): Soil and water losses from new citrus orchards growing on sloped soils in the western Mediterranean basin. Earth Surf. Process. Landforms; 34, 1822–1830.

CLC: Corine Land Cover (2006): Raster data, European Environment Agency (EEA) [online] Available from: http://www.eea.europa.eu/data-and-maps/data/ds_resolveuid/a645109f7a11d43f5d7e275d81f35c61,2010.

Coelho, C.O.A., Shakesby, R.A.,Walsh, R.P.D. (1995a): Effects of forest fires and post-fire land management practice on soil erosion and stream dynamics. Águeda Basin, Portugal —Soil and Groundwater Research Report V. European Commission (ISBN 92-826-9687-1).

Coelho, C.O.A., Shakesby, R.A., González, M., Ternan, L., Walsh, R.P.D., Williams, A.G., (1995b): IBERLIM: land management and erosion limitation in the Iberian Peninsula. Final Report to the EC in Fulfilment of Project EV5V-0041 Land Management Practice and Erosion Limitation in Contrasting Wildfire and Gullied Locations in the Iberian Peninsula ((unpublished), 246 pp.).

Coelho, C.O.A., Ferreira, A.J.D., Prats, S.A., Tomé, M., Soares, P., Cortiçada, A., Tomé, J.A., Salas, G.R., Páscoa, F., Amaral, A. (2008): Assessment of climatic change impact on water resources and CO2 fixation in fast growing stand in Portugal. Final Report Silvaqua Project POCTI/MGS/49210/2002. University of Aveiro.

Colin Cameron, A., Windmeijer, F.A.G. (1997): An R-squared measure of goodness of fit for some common nonlinear regression models. J. Econom. 77, 329–342.

D4EU: Dendromass 4 Europe (2017): Securing Sustainable Dendromass Production with Poplar Plantations in European Rural Areas. Bio Based Industries Joint Undertaking under the European Union's Horizon 2020. Project Grant Agreement No 745874. www.dendromass4europe.eu.

Dane, J., Hopmans, J. (2002): Hanging water column, in methods of soil analysis Part 4: Physical methods, Soil Science Society, Am. Book ser.

Daniel, E.B., Camp, J.V., LeBoeuf, E.J., Penrod, J.R., Dobbins, J.P., Abkowitz, M.D. (2011): Watershed Modeling and its Applications: A State-of-the-Art Review. Open Hydrol. J. 5, 26–50.

DEFRA (2004): Best Practice Guidelines for Applicants to Defra's Energy Crops Scheme - Growing Short Rotation Coppice. Department for Environment, Food and Rural Affairs, Defra Publications, London. URL: http://www.naturalengland.org.uk/Images/short-rotation-coppice_tcm6-4262.pdf (last accessed November 2014).

Diek, S., Temme, A.J.A.M., Teuling, A.J. (2014): The effect of spatial soil variation on the hydrology of a semi-arid Rocky Mountains catchment. Geoderma; 235–236, 113–126.

Dimitriou, I., Aronsson, P. (2011): Wastewater and sewage sludge application to willows and poplars grown in lysimeters–Plant response and treatment efficiency. Biomass Bioenerg. 35, 161–170.

Dimitriou, I., Rosenqvist, H. (2011): Sewage sludge and wastewater fertilisation of Short Rotation Coppice (SRC) for increased bioenergy production—Biological and economic potential. Biomass Bioenerg. 35, 835–842.

Directive 2009/28/EC of the European Parliament and of the Council of 23 April 2009 on the promotion of the use of energy from renewable sources and amending and subsequently repealing Directives 2001/77/EC and 2003/30/EC.

Doerr, S.H., Shakesby, R.A.,Walsh, R.P.D. (1996): Soil hydrophobicity variations with depth and particle size fraction in burned and unburned Eucalyptus globulus and Pinus pinaster forest terrain in the Agueda Basin, Portugal. Catena; 27, 25–47.

Doerr, S.H., Thomas, A.D. (2000): The role of soil moisture in controlling water repellency: New evidence from forest soils in Portugal. J. Hydrol. 231-232, 134-47.

Doerr, S.H., Shakesby, R.A., Walsh, R.P.D. (2000): Soil water repellency: its causes, characteristics and hydrogeomorphological significance. Earth-Sci. Rev. 51, 33–65.

Easton, Z.M., Fuka, D.R., Walter, M.T., Cowan, D.M., Schneiderman, E.M., Steenhuis, T.S. (2008): Re-conceptualizing the soil and water assessment tool (SWAT) model to predict runoff from variable source areas. J. Hydrol. 348, 279–291.

EC (2000): Directive 2000/60/EC of the European Parliament and of the Council, published in the Official Journal of the European Union, L 288/27, 22 December 2000.

ECA&D (2010): European Climate Assessment & Dataset – Daily data. http://eca.knmi.nl/, last access: November 2010.

Eckhardt, K., Haverkamp, S., Fohrer, N., Frede, H.-G. (2002): SWATG, a version of SWAT99.2 modified for application to low mountain range catchments. Phys. Chem. Earth; 27, 641–644.

Elsenbeer, H., Coelho, R.M., Newton, B. (2002): Spatial variability of soil hydraulic conductivity along a tropical rainforest catena. Geoderma; 108, 1–2, 79–90.

Ertel, A.-M., Lupo, A., Scheifhacken, N., Bodnarchuk, T., Manturova, O., Berendonk, T. U., Petzoldt, T, (2012): Heavy load and high potential: anthropogenic pressures and their impacts on the

water quality along a lowland river (Western Bug, Ukraine). Environ. Earth Sci. 65, 1459–1473 doi:10.1007/s12665-011-1289-0.

ESDBv2 (2006): European Soil Database v2 Raster Library 1kmx1km. European Commission – DG JRC. https://esdac.jrc.ec.europa.eu/content/european-soil-database-v2-raster-library-1kmx1km. (last access October 2015).

European Commission Environment (2011): Water scarcity and droughts in the European Union. http://ec.europa.eu/environment/water/quantity/scarcity_en.htm (last access July 2013).

FAO (1996): Control of water pollution from agriculture. Irrigation and Drainage Papers 55. http://www.fao.org/docrep/W2598E/W2598E00.htm (last access July 2013).

FAO (2005): Fertilizer use by crop in Ukraine. Land and Plant Nutrition Management Service.http://www.fao.org/tempref/agl/agll/docs/fertuseukraine.pdf (last access July 2013).

Faramarzi, M., Abbaspour, K. C., Schulin, R., Yang, H. (2009): Modelling blue and green water resources availability in Iran. Hydrol. Process. 23, 486–501.

Feger, K.H., Petzold, R., Schmidt, P.A., Glaser, T., Schroiff, A., Döring, N., Feldwisch, N., Friedrich, C., Peters, W., Schmelter, H. (2010): Standortpotenziale, Standards und Gebietskulissen für eine natur- und bodenschutzgerechte Nutzung von Biomasse zur Energiegewinnung in Sachsen unter besonderer Berücksichtigung von Kurzumtriebsplantagen und ähnlichen Dauerkulturen. Schriftenreihe des Sächsischen Landesamtes für Umwelt, Landwirtschaft und Geologie, Dresden.

Fernández-Raga, M., Fraile, R., Keizer, J.J., Varela Teijeiro, M.E., Castro, A., Palencia, C., Calvo, A. I., Koenders, J., Da Costa Marques, R.L. (2010): The kinetic energy of rain measured with an optical disdrometer: An application to splash erosion. Atmos. Res. 96, 225–240.

Ferreira, A.J.D., Coelho, C.O.A., Walsh, R.P.D., Shakesby, R.A., Ceballos, A., Doerr, S.H. (2000): Hydrological implications of soil water-repellency in Eucalyptus globulus forests, north-central Portugal. J. Hydrol. 231–232, 165–177.

Fiorillo, F., Doglioni, A. (2010): The relation between karst spring discharge and rainfall by cross-correlation analysis (Campania, southern Italy). Hydrogeol. J. 18, 1881–1895.

Fischer, M., Trnka, M., Kučera, J., Deckmyn, G., Orság, M., Sedlák, P., Žalud, Z., Ceulemans, R. (2013): Evapotranspiration of a high-density poplar stand in comparison with a reference grass cover in the Czech–Moravian Highlands. Agric. For. Meteorol. 181, 43–60.

Flury, M., Flühler, H. (1994): Brilliant Blue FCF as a dye tracer for solute transport studies − a toxicological overview. J. Environ. Qual. 23, 1108-1112.

Flury, M., Flühler, H. (1995): Tracer Characteristics of Brilliant Blue FCF. Soil Sci. Soc. Am. J. 59, 22–27.

Gassman, P.W., Reyes, M.R., Green, C.H., Arnold, J.G. (2007): The soil and water assessment tool: historical development, applications, and future research directions. Trans. ASABE; 50, 1211–1250.

Georgiadis, P., Taeroe, A., Stupak, I., Kepfer-Rojas, S., Zhang, W., Pinheiro Bastos, R., Raulund-Rasmussen, K. (2017): Fertilization effects on biomass production, nutrient leaching and budgets in four stand development stages of short rotation forest poplar. For. Ecol. Manage. 397, 18–26.

Geroy, I.J., Gribb, M.M., Marshall, H.P., Chandler, D.G., Benner, S.G., McNamara, J.P. (2011): Aspect influences on soil water retention and storage. Hydrol. Process. 25, 25, 3836–3842.

Gessler, P.E., Moore, I.D., Mckenzie, N.J., Ryan, P.J. (1995): Soil–landscape modelling and spatial prediction of soil attributes. Int. J. Geogr. Inf. Syst. 9 (4), 421–432.

Geza, M., McCray, J.E. (2008): Effects of soil data resolution on SWAT model stream flow and water quality predictions. J. Environ. Manage. 88, 393–406.

González-Pelayo, O., Andreu, V., Gimeno-García, E., Campo, J., Pascual-Aguilar, J.A., Rubio, J.L. (2010): The use of Mini Disk Infiltrometer (MDI) for testing infiltration, sorptivity and water repellence on slopes affected by fire. Seminario de Evaluación de Procesos de Degradación de Suelos: Problemas Metodólogicos. http://hdl.handle.net/10261/95305.

Gosch, L. (2012): Einfluss unterschiedlicher Forstmanagementstrategien auf bodenhydraulische Parameter zur Standortswassermodellierung im Águeda Einzugsgebiet Zentralportugal; Unpublished M.Sc. Thesis, Technische Universität Dresden.

Gregory, J. H., Dukes, M. D., Miller, G. L., Jones, P. H. (2005): Analysis of Double-Ring Infiltration Techniques and Development of a Simple Automatic Water Delivery System. Appl. Turfgrass Sci. doi:10.1094/ATS-2005-0531-01-MG.

Guswa, A. J. (2010): Effect of plant uptake strategy on the water−optimal root depth. Water Resour. Res. 46, W09601, doi:10.1029/2010WR009122.

Hall, R. L. (2003): Short Rotation Coppice for Energy Production Hydrological Guidelines B/CR/00783/GUIDELINES/SRC URN 03/883. Centre for Ecology and Hydroloy, Department of Trade and Industry, Bristol, United Kingdom.

Haycock, N. E., Pinay, G. (1993): Groundwater nitrate dynamics in grass and poplar vegetated riparian buffer strips during the winter. J. Environ. Qual. 22, 273.

Helm, B., Terekhanova, T., Tränckner, J., Venohr, M., Krebs, P. (2013): Attributiveness of a mass flow analysis model for integrated water resources assessment under data-scarce conditions. Water Sci. Technol. 67, 261–270.

Hendrayanto, Kosugi K., Uchida T., Matsuda S., Mizuyama T. (1999): Spatial variability of soil hydraulic properties in a forested hillslope. J. For. Res. 4, 2, 107–114.

Heuvelmans, G., Muys, B., Feyen, J. (2004): Analysis of the spatial variation in the parameters of the SWAT model with application in Flanders, Northern Belgium. Hydrol. Earth Syst. Sci. 8, 5, 931–939.

Hollis, J.M., Jones, R.J.A., Marshall, C.J., Holden, A., VandeVeen, J.R., Montanarella, L. (2006): SPADE-2: the soil profile analytical database for Europe, version 1.0. European Soil Bureau Research Report No. 19, EUR 22127 EN. Office for Official Publications of the European Communities, Luxembourg (38 pp.).

Holvoet, K., van Griensven, A., Seuntjens, P., Vanrolleghem, P. A. (2005): Sensitivity analysis for hydrology and pesticide supply towards the river in SWAT. Phys. Chem. Earth. 30, 518–526 .

Hörmann, G., Köplin, N., Cai, Q., Fohrer, N. (2009): Using a simple model as a tool to parameterise the SWATmodel of the Xiangxi River in China. Quatern. Int. 208, 116–120.

ICNF (2015): Defesa da Floresta Contra Incêndios, Instituto de Conservaçao da Natureza e das Florestas, available at: http://www2.icnf.pt/portal/florestas/dfci (last access 7 April 2017).

Inamdar, S., Naumov, A. (2006): Assessment of sediment yields for a mixed-landuse great lakes watershed: lessons from field measurements and modeling. J. Great Lakes Res. 32, 471–488.

Jajarmizadeh, M., Harum, S., Salapour, M. (2012): A Review on Theoretical Consideration and Types of Models in Hydrology. Journal of Environmental Science and Technology. J. Environ. Sci. Technol. 5, 249–261.

Johnson, N., Revenga, C., Echeverria, J. (2001): Ecology–managing water for people and nature. Science; 292, 1071–1072.

Julich, S. (2009): Unsicherheiten in der Modellierung des Wasser- und Stickstoffhaushaltes von Flusseinzugsgebieten der Mikro- und Mesoskala. Dissertation. Justus-Liebig-Universität Gießen. Germany. (Ph.D. thesis).

Kalbacher, T., Delfs, J.-O., Shao, H., Wang, W., Walther, M., Samaniego, L., Schneider, C., Musolff, M., Centler, F., Sun, F., Hildebrandt, A., Liedl, L., Borchardt, D., Krebs, P., Kolditz, O. (2012) The IWAS-ToolBox: Software coupling for an Integrated Water Resources Management. Environ. Earth Sci. 65, 1367–1380 doi:10.1007/s12665-011-1270-y.

Katschinski, N.A. (1956): Die mechanische Bodenanalyse und die Klassifikation der Böden nach ihrer mechanischen Zusammensetzung. Rapports aux Sixième Congrès International de la Science du Sol, Paris 321–327 .

Keizer, J.J., Coelho, C.O.A., Matias, M.J.S., Domingues, C.S.P., Ferreira, A.J.D. (2005): Soil water repellency under dry and wet antecedent weather conditions for selected land-cover types in the coastal zone of central Portugal. Soil Research; 43, 297-308.

Keizer, J.J., Doerr, S.H., Malvar, M.C., Prats, S.A., Ferreira, R.S.V., Oñate, M.G., Coelho, C.O.A., Ferreira, J.D. (2008): Temporal variation in topsoil water repellency in two recently burnt Eucalypt stands in north-central Portugal. Catena; 74, 192–204.

Ketelsen, H., Meyer-Windel, S. (1999): Adsorption of brilliant blue FCF by soils. Geoderma; 90, 131–145.

Kiesel, J., Fohrer, N., Schmalz, B., White, M.J. (2010): Incorporating landscape depressions and tile drainages of lowland catchments into spatially distributed hydrologic modelling. Hydrol. Process. 24, 1472–1486.

King, P.M. (1981): Comparison of methods for measuring severity of water repellence of sandy soils and assessment of some factors that affect its measurement. Australian Journal of Soil Research; 19, 275–285.

Kirsch, K., Kirsch, A., Arnold, J.G. (2002): Predicting Sediment and Phosphorus Loads in the Rock River Basin Using SWAT. T. ASAE. 45, 1757–1769.

Krasilnikov, P., Ibanez Marti, J.J., Arnold, R., Shoba, S. (2009): A handbook of soil terminology, correlation and classification. Earthscan, Uk and USA; pp 189–207.

Krause, P., Boyle, D.P., Bäse, F. (2005): Comparison of different efficiency criteria for hydrological model assessment. Adv. Geosci. 5, 89–97.

Krysanova, V., Arnold, J.G. (2008): Advances in ecohydrological modelling with SWAT—a review. Hydrolog. Sci. J., 53, 5, 939–947 doi:10.1623/hysj.53.5.939.

KTBL: Kuratorium für Technik und Bauwesen in der Landwirtschaft e.V (2009): Faustzahlen für die Landwirtschaft. 14. Auflage. Darmstadt. ISBN: 978-3-939371-91-5.

Lal, R. (2015): The nexus approach to managing water, soil and waste und changing climate and growing demands on natural resources. In: Kurian, M., Ardakanian, R. (Eds.), Governing the Nexus: Water, Soil and Waste Resources Considering Global Change. Springer, Cham, Heidelberg, New York, Dordrecht, London, pp. 39e60. http://dx.doi.org/10.1007/978-3-319-05747-7.

Lam, Q.D., Schmalz, B., Fohrer, N. (2010): Modelling point and diffuse source pollution of nitrate in a rural lowland catchment using the SWAT model. Agric. Water Manage. 97, 317–325.

Legates, D.R., McCabe Jr., G.J. (1999): Evaluating the use of "goodness-of-fit" measures in hydrologic and hydroclimatic model validation. Water Resour. Res. 35, 1, 233–241.

Leidel, M., Niemann, S., Hagemann, N. (2012): Capacity development as a key factor for integrated water resources management (IWRM): Improving water management in the Western Bug River Basin, Ukraine. Environ. Earth Sci. 65, 1415–1426.

Leighton-Boyce, G., Doerr, S.H., Shakesby, R.A., Rory, P.D., Walsh, A., António, J.D., Ferreira, B.C., Boullet, A.K., Coelho, C.O.A. (2005): Temporal dynamics of water repellency and soil moisture in Eucalypt plantations, Portugal. Aust. J. Soil Res. 43, 269–280.

Leighton-Boyce, G., Doerr, S.H., Shakesby, R.A., Walsh, R.P.D. (2007): Quantifying the impact of soil water repellency on overland flow generation and erosion: a new approach using rainfall simulation and wetting agent on in situ soil. Hydrol. Process. 21, 2337–2345.

Lenhart, T., Eckhardt, K., Fohrer, N., Frede, H.-G. (2002): Comparison of two different approaches of sensitivity analysis. Phys. Chem. Earth. 27, 645–654.

Liu, J., Mooney, H., Hull, V., Davis, S.J., Gaskell, J., Hertel, T., Lubchenco, J., Seto, K.C., Gleick, P., Kremen, C., Li, S. (2015): Systems integration for global sustainability. Science; 347, 1258832.

Madeira, M., Araújo, C. (2015): Soil degradation risks and prevention measures in planted forests. The case of eucalyptus plantations in Portugal. pp. 107–117.

Malagó, A., Bouraoui, F., Vigiak, O., Grizzetti, B., Pastori, M. (2017): Modelling water and nutrient fluxes in the Danube River Basin with SWAT. Sci. Total Environ. 603–604, 196–218.

Mallants D., Mohanty B.P., Jacques D., Feyen J. (1996): Spatial variability of hydraulic properties in a multi-layered soil profile. Soil Sci. 161, 167–181.

Malvar, M., Prats, S., Nunes, J., Keizer, J.J. (2011): Post-fire overland flow generation and inter-rill erosion under simulated rainfall in two eucalypt stands in north-central Portugal. Environ. Res. 111, 2, 226-236.

Malvar, M.C., Prats, S.A., Keizer, J.J. (2016): Runoff and inter-rill erosion affected by wildfire and pre-fire ploughing in eucalyptus plantations of north-central Portugal. Land Degrad. Develop. 27, 1366–1378.

Mander, U., Kull, A., Kuusemets, V., Tamm, T. (2000): Nutrient runoff dynamics in a rural catchment: influence of land-use changes, climatic fluctuations and ecotechnological measures. Ecol. Eng. 14, 405–417.

Martins, J., Chamine, H.I., Afonso, M.J., Espinha, J., Medeiros, A., Garcia, S., Gomes, A., Teixeira, J., Fonseca, P. E. (2005): Productivity and water cost in fissured-aquifers from the iberian crystaline basement (Portugal): hydrogeological constrains. Libro homenaje al Prof. D. Rafael Fernandez Rubio, 193-207.

Martins, M.A.S., Machado, A.I., Serpa, D., Prats, S.A., Faria, S.R., Varela, M.E.T., González-Pelayo, Ó., Keizer, J.J. (2013): Runoff and inter-rill erosion in a Maritime Pine and a Eucalypt plantation following wildfire and terracing in north-central Portugal. J. Hydrol. Hydromechanics; 61, 261–268.

McBratney, A.B., Mendonca Santos, M.L., Minasny, B. (2003): On digital soil mapping. Geoderma; 117, 3–52.

McKeague, J.A., Eilers, R.G., Thomasson, A.J., Reeve, M.J., Bouma, J., Grossman, R.B., Favrot, J.C., Renger, M., Strebel, O. (1984): Tentative assessment of soil survey approaches to the characterization and interpretation of air-water properties of soils. Geoderma; 34, 69–100.

Meissner, R., Seeger, J., Rupp, H. (1998): Lysimeter studies in East Germany concerning the influence of set aside of intensively farmed land on the seepage water quality. Agr. Ecosyst. Environ. 67, 161–173.

Mendonça, J.L., Almeida, C.C., Marques da Silva, M. (1999): Produtividade de captaçoes e caracteristics hydrogeologicas dos sistemas aquiferos descontinuos do Maciço Hesperico na Bacia Hidrografica do rio Mondego. Resumo Serminário sobre Águas Subterrâneas, APRH, 11pp.

Merz, J., Mosley, M.P. (1998): Hydrological behaviour of pastoral hill country modified by extensive landsliding, northern Hawke's Bay, New Zealand. J. Hydrol. N. Z. 37, 2, 113–139.

METI and NASA (2009): ASTER Global DEM — Start Distribution 2009.

Milly, P.C.D., Eagleson, P.S. (1987): Effects of spatial variability on annual average water balance. Water Resour. Res. 23, 2135–2143.

Milly, P.C.D. (1994): Climate, interseasonal storage of soil water, and the annual water balance. Adv. Water Resour. 17, 19–24.

Milne, G. (1935): Some suggested units of classification and mapping particularly for East African soils. Soils Research 4, 183-198.

Moody, D.R., Schlossberg, M.J. (2010): Soil water repellency index prediction using the molarity of ethanol droplet test. Vadose Zo. J. 9, 1046–1051.

Moore, I.D., Gessler, P.E., Nielsen, G.A., Peterson, G.A. (1993): Soil attribute prediction using terrain analysis. Soil Sci. Soc. Am. J. 57, 3, 443–452.

Moriasi, D.N., Arnold, J.G., Van Liew, M.W., Bingner, R.L., Harmel, R.D., Veith, T.L. (2007): Model evaluation guidelines for systematic quantification of accuracy in watershed simulations. Trans. ASABE; 50, 885–900.

Mueller E.N., Wainwright J., Parsons A.J. (2008): Spatial variability of soil and nutrient characteristics of semi-arid grasslands and shrublands, Jornada Basin, New Mexico. Ecohydrol. 1, 3–12.

Mwangi, H.M., Julich, S., Patil, S.D., McDonald, M.A., Feger, K.H. (2016): Modelling the impact of agroforestry on hydrology of Mara River Basin in East Africa. Hydrol. Process. 30, 3139-3155 DOI: 10.1002/hyp.10852.

Nash, J.E., Sutcliffe, J.V. (1970): River flow forecasting through conceptual models. Part I: a discussion on principles. J. Hydrol. 10, 282–290.

Neitsch, S.L., Arnold, J. G., Kiniry, J R., Srinivasan, R., Williams, J.R. (2002): Soil and Water Assessment Tool. User's Manual, Version 2005, GSWRL Report 02-02, BRC Report 2-06, Temple, Texas, USA.

Neitsch, S.L., Arnold, J.G., Kiniry, J.R., Williams, J.R., King, K.W. (2005): Soil and water assessment tool. in: Theoretical Documentation: Version 2005, TWRI TR-191 .

Neitsch, S.L., Arnold, J.G., Kiniry, J.R.,Williams, J.R. (2009): Soil andWater Assessment Tool Theoretical Documentation, Version 2009; USDA-ARS Grassland, Soil And Water Research Laboratory, Temple, Tex (available at: www.brc.tamus.edu/swat/doc. html, last access: 19 February 2015).

Neitsch, S.L., Arnold, J.G., Kiniry, J.R., Williams, J.R. (2011): Soil and Water Assessment Tool Theoretical Documentation Version 2009, Texas Water Resources Institute Technical Report No. 406. Texas A&M University System, College Station, TX.

Nemes, A., Rawls, W.J. (2006): Evaluation of different representations of the particle-size distribution to predict soil water retention. Geoderma; 132, 1–2, 47–58.

Nijnik, M. (2017): To sustainability in forestry: The Ukraine's case. Dissertation, Wageningen Universiteit, Netherlands. (Ph.D. thesis).

NOAA (2011): Climate data online: Daily observational data, available at: http://gis.ncdc.noaa.gov/map/cdo/, last access: November 2011. .

Nunes, M.C.S., Vasconcelos, M.J., Pereira, J.M.C., Dasgupta, N. Alldredge, R.J., Rego, F.C. (2005): Land cover type and fire in Portugal: do fires burn land cover selectively? Landsc. Ecol. 20, 6, 661-673.

Nunes, J.P. (2007): Vulnerability of Mediterranean Watersheds to Climate Change: The Desertification Context; Universidade Nova de Lisboa, Portugal. (Ph.D. thesis).

Osypov, V., Osadcha, N., Osadchyi, V. (2017): SWAT Model Application for Simulating Nutrients Emission from an Agricultural Catchment in Ukraine XV, 30–38.

Panagos, P. (2006): The European soil database. GEO: Connexion; 5, 7, 32–33.

Panagos, P., Van Liedekerke, M., Jones, A., Montanarella, L. (2012): European Soil Data Centre: response to European policy support and public data requirements. Land Use Policy; 29, 329–338. http://dx.doi.org/10.1016/j.landusepol.2011. 07.00.

Panagos, P., Meusburger, K., Ballabio, C., Borrelli, P., Alewell, C. (2014): Soil erodibility in Europe: A high-resolution dataset based on LUCAS. Sci. Total Environ. 479-480, 189-200.

Panagos, P., Borrelli, P., Meusburger, K., Alewell, C., Lugato, E., Montanarella, L. (2015a): Estimating the soil erosion cover-management factor at the European scale. Land use policy; 48, 38-50.

Panagos, P., Borrelli, P., Meusburger, K., van der Zanden, E. H., Poesen, J., Alewell, C. (2015b): Modelling the effect of support practices (P-factor) on the reduction of soil erosion by water at European scale. Environ. Sci. Policy. 51, 23-34.

Panagos, P., Borrelli, P., Poesen, J., Ballabio, C., Lugato, E., Meusburger, K., Montanarella, L., Alewell, C. (2015c): The new assessment of soil loss by water erosion in Europe. Environ. Sci. Policy; 54, 438-447.

Pavlik, D., Söhl, D., Pluntke, T., Mykhnovych, A., Bernhofer, C. (2012): Dynamic downscaling of global climate projections for Eastern Europe with a horizontal resolution of 7 km. Environ. Earth. Sci. 65, 1475 doi/10.1007/s12665-011-1081-1.

PBH (2011): Plano de Gestão das Bacias Hidrográficas dos rios Vouga, Mondego e Lis (Rev. Final). Administracão da Região Hidrográfica do Centro I.P.,Ministério da Agricultura, Mar, Ambiente e Ordenamento do Território. Portugal.

Pekarova, P., Pekar, J. (1996): The impact of land use on stream water quality in Slovakia. J. Hydrol. 180, 333–350.

Pereira, V., FitzPatrick, E.A. (1995): Cambisols and related soils in north-central Portugal: their genesis and classification. Geoderma; 66, 185–212.

Petzold, R., Schwärzel, K., Feger, K.H. (2011): Transpiration of a hybrid poplar plantation in Saxony (NE Germany) in response to climate and soil conditions. Eur. J. Forest Res. 130, 695-706.

Pluntke, T., Pavlik, D., Bernhofer, C. (2014): Reducing uncertainty in hydrological modelling in a data sparse region. Environ. Earth Sci. 72, 4801–4816.

Pohlert, T., Huisman, J. A., Breuer, L., Frede, H.-G. (2005): Modelling of point and non-point source pollution of nitrate with SWAT in the river Dill, Germany. Adv. Geosci. 5, 7–12.

Pospelova, G. (1997): Anbau und Züchtung von Weizen in der Ukraine Giessener Abhandlungen zur Agrar- und Wirtschaftsforschung des europäischen Ostens, Band 218, Osteuropastudien der Hochschulen des Landes Hessen, Reihe I, Duncker & Humblot, Berlin .

Pospelova, G. Schinke, E. (1997): Anbau und Verarbeitung von Zuckerrüben in der Ukraine Giessener Abhandlungen zur Agrarund Wirtschaftsforschung des europäischen Ostens Band 221, Osteuropatsuiden der Hochschule des Landes Hessen, Reihe I, Duncker & Humboldt, Berlin .

Pott, C.A., Fohrer, N. (2017): Hydrological modeling in a rural catchment in Germany. Rev. Bras. Tecnol. Apl. nas Ciências Agrárias 10.

Prats, S.A., Macdonald, L.H., Monteiro, M., Ferreira, A.J., Coelho, C.O., Keizer, J.J. (2012): Effectiveness of forest residue mulching in reducing post-fire runoff and erosion in a pine and a eucalypt plantation in north-central Portugal. Geoderma; 191, 115-124.

Publishing House of Ukrainian Academy of Agrological Sciences (1998): Terminological dictionary of soil science questions, agrochemistry and soil amelioration. Kharkiv, Ukraine, 80p.

Quinn, T., Zhu, A.X., Burt, J.E. (2005): Effects of detailed soil spatial information on watershed modeling across different model scales. Int. J. Appl. Earth Obs. and Geoinformation; 7, 324–338.

Rathjens, H., Oppelt, N. (2012): SWATgrid: An interface for setting up SWAT in a grid-based discretization scheme. Comput. Geosci. 45, 161–167.

Rathjens, H., Oppelt, N., Bosch, D.D., Arnold, J.G., Volk, M. (2014): Development of a grid-based version of the SWAT landscape model. Hydrol. Process. 29, 900– 914, doi: 10.1002/hyp.10197.

Rawson, H.M, Gómez Macpherson, H. (2000): Irrigated Wheat. Food and Agriculture Organization of the United Nations, Rome. ISBN 92-5-104488-0.

Renger, M., Strebel, O. (1980): Beregnungsbedarf landwirtschaftlicher Kulturen in Abhängigkeit vom Boden. Boden und Wasser; 32, 572–575.

Romanowicz, A.A., Vancloostera, M., Rounsevellb, M., La Junesseb, I. (2005): Sensitivity of the SWAT model to the soil and land use data parametrisation: a case study in the Thyle catchment, Belgium. Ecol. Model. 187, 27–39.

Rousseva, S. (1997): Data transformations between soil texture schemes. Eur. J. Soil Sci. 48, 4, 749–758.

Santos, J.M., Verheijen, F.G.A., Tavares Wahren, F., Wahren, A., Feger, K.-H., Bernard- Jannin, L., Rial-Rivas,M.E., Keizer, J.J., Nunes, J.P. (2013): Soil water repellency dynamics in pine and eucalypt plantations in Portugal — a high-resolution time series. Land Degrad. Dev. 27, 5, 1334-1343 http://dx.doi.org/10.1002/ldr.2251.

Schanze, J., Trümper, J., Burmeister, C., Pavlik, D., Kruglov, I. (2012): A methodology for dealing with regional change in integrated water resource management. Environ. Earth Sci. 65, 1405–1414 doi:10.1007/s12665-011-1311-6.

Scheifhacken, N., Haase, U., Gram-Radu, L., Kozovyi, R., Berendonk, T.U. (2012): How to assess hydromorphology? A comparison of Ukrainian and German approaches. Environ. Earth Sci. 65, 1483–1499 doi:10.1007/s12665-011-1218-2.

Schmalz, B. Fohrer, N. (2009): Comparing model sensitivities of different landscapes using the ecohydrological SWAT model. Adv. Geosci. 21, 91–98 doi:10.5194/adgeo-21-91-2009.

Schuol, J., Abbaspour, K.C., Srinivasan, R., Yang, H. (2008): Estimation of freshwater availability in the West African sub-continent using the SWAT hydrologic model. J. Hydrol. 352, 30–49.

Schwarze, H., Röhricht, C. (2006): Untersuchungen zum Pappel- Und Weidenanbau im Kurzumtrieb auf landwirtschaftlichen Flächen. In Vortrag auf der Fachtagung „Anbau und Nutzung von Bäumen auf landwirtschaftlichen Flächen". Tharandt: TU Dresenden. Retrieved from

http://www.agrowood.de/download/19_Roehricht_Untersuchungen_zu_KUP.pdf (last access January 2018).

Schwärzel, K., Menzer, A., Spank, U., Clausnitzer, F., Häntzschel, J., Grünwald, T., Köstner, B., Bernhofer, C., Feger, K.H. (2009a): Soil water content measurements deliver reliable estimates of water fluxes. A comparative study in a beech and a spruce stand in the Tharandt Forest (Saxony, Germany). Agric. For. Meteorol. 149, 1994–2006.

Schwärzel K., Feger K.H., Häntzschel J., Menzer A., Spank U., Clausnitzer F., Köstner B., Bernhofer C. (2009b): A novel approach in model-based mapping of soil water conditions at forest sites. Forest Ecol. Manag. 258, 2163–2174.

SCS: Soil Conservation Service (1972): Section 4: hydrology. National Engineering Handbook; Soil Conservation Service US Department of Agriculture, Washington, DC.

SEEMLA: Sustainable exploitation of biomass for bioenergy from marginal lands (2016a): Catalogue for bioenergy crops and their suitability in the categories of MagLs. European Union's Horizon 2020, SEEMLA Project Grant Agreement no. 691874.

SEEMLA: Sustainable exploitation of biomass for bioenergy from marginal lands (2016b): European Union's Horizon 2020, Project Grant Agreement no. 691874. http://seemla.eu/en/home/.

Shakesby, R.A., Coelho, C.O.A., Ferreira, A.J.D., Terry, J.P., Walsh, R.P.D. (1994): Fire, post-burn land management practice and soil erosion response curves in eucalypt and pine forests, north-central Portugal. In: Sala, M., Rubio, J.L. (Eds.): Soil erosion and degradation as a consequence of forest fires, 111–132. Geoforma Ediciones, Logroñes.

Shakesby, R.A., Boakes, D.J., Coelho, C.D., Goncalves, A.J., Walsh, R.P. (1996): Limiting the soil degradational impacts of wildfire in pine and eucalyptus forests in Portugal. Pergamon; 16, 337-355.

Shanti, C., Arnold, J., Williams, J., Hauck, L., Dugas, W. (2001): Application of a watershed model to evaluate management effects on point and non-point source pollution. T. ASAE; 44, 1559–1570 .

Shen, Z.Y., Chen, L., Chen, T. (2012): Analysis of parameter uncertainty in hydrological and sediment modeling using GLUE method: a case study of SWAT model applied to Three Gorges Reservoir Region, China. Hydrol. Earth Syst. Sci. 16, 121–132.

Singh, J., Knapp, H.V., Demissie, M. (2004): Hydrologic modeling of the Iroquois River watershed using HSPF and SWAT; ISWS CR 2004–08. Illinois State Water Survey, Champaign, Ill.

SNIRH (2014): Sistema Nacional de Informação de Recursos Hídricos, Agência Portuguesa do Ambiente, Lisbon available at:, http://snirh.pt (last access: 10 November 2014).

Some'e, B.S., Hassanpour, F., Ezani, A., Miremadi, S.R., Tabari, H. (2011): Investigation of spatial variability and pattern analysis of soil properties in the northwest of Iran. Environ. Earth Sci. 64, 7, 1849-1864 doi:10.1007/s12665-011-0993-0.

Spruill, C.A., Workman, S.R., Taraba, J.L. (2000): Simulation of daily and monthly stream discharge from small watersheds using the SWAT model. T. ASAE. 43, 1431–1439.

Stalnacke, P., Grimvall, A., Libiseller, C., Laznik, M., Kokorite, I. (2003): Trends in nutrient concentrations in Latvian rivers and the response to the dramatic change in agriculture. J. Hydrol. 283, 184–205.

Stolte, J., Tesfai, M., Øygarden, L., Kværnø, S., Keizer, J., Verheijen, F., Panagos, P., Ballabio, C., Hessel, R. (2016): Soil threats in Europe. EUR 27607 EN; doi:10.2788/488054 (print); doi:10.2788/828742 (online).

Stone, M. Krishnappan, B. G. (2002): The effect of irrigation on tile sediment transport in a headwater stream. Water Res. 36, 3439–3448.

Strauch, M., Bernhofer, C., Koide, S., Volk, M., Lorz, C., Makeschin, F. (2012): Using precipitation data ensemble for uncertainty analysis in SWAT streamflow simulation. J. Hydrol. 414–415, 413–424.

Szolgayov´a, E., Blöschl, G., Bucher, C. (2012): Factors influencing long range dependence in stream flow of European rivers. Geophys. Res. Abstr., EGU2012-10776, EGU General Assembly, Vienna, Austria.

TACIS (2001): Transboundary Water Quality Monitoring and Assessment: Bug and Latorica/Uzh Kyiv
TACIS.

Takagi, K., Lin, H.S. (2012): Changing controls of soil moisture spatial organization in the Shale Hills
Catchment. Geoderma; 173–174, 289–302.

Terekhanova, T. (2009): Quantification of water and nutrient flows on a river catchment under scarce
data conditions – A case study of Western Bug river basin, Ukraine. MSc Thesis, Intitute of
Urban Water Management, TU Dresden, Germany.

Terry, J.P. (1992): Rainsplash detachment and soil erosion in the Agueda Basin, Portugal: the effects
of forest fire and land management changes; Unpublished Ph.D. thesis, University of Wales.

Thomas, A.D., Walsh, R.P.D., Shakesby, R.A. (1999): Nutrient losses in eroded sediment after fire in
eucalyptus and pine forest in the wet Mediterranean environment of northern Portugal. Catena;
36, 283–302.

Thompson, J.A., Bell, J.C., Butler, C.A. (2001): Digital elevation model resolution effects on terrain
attribute calculation and quantitative soil-landscape Modeling. Geoderma; 100, 67–89.

Tubby, I., Armstrong, A. (2002): Establishment and Management of Short Rotation Coppice - Practice
Note. Forest Research, Forestry Comission Edinburgh.
https://www.forestresearch.gov.uk/documents/6958/FCPN007.pdf.

UA: University of Aveiro (2006): HIDRIA (PTDC/CTE-GEX/71651/2006) — A Multi-stage Approach for
Addressing Input Data Uncertainties in Process-based Rainfall–Runoff Modelling for Small
Forested Catchments Upstream of the Ria de Aveiro. Universidade de Aveiro, Portugal
www.cesam.ua.pt/index.php?menu=198&language=eng&tabela=projectosdetail&projectid=26.

UA: University of Aveiro (2008): ERLAND (PTDC/AAC-AMB/100520/2008) — Direct and Indirect
Impacts of Climate Change on Soil Erosion and Land Degradation in Mediterranean
Watersheds. Universidade de Aveiro, Portugal
www.cesam.ua.pt/index.php?menu=82&language=eng&tabela=projectosdetail&projectid=246.

Ulrich, A., Volk, M. (2009): Application of the Soil and Water Assessment Tool (SWAT) to predict the impact of alternative management practices on water quality and quantity. Agric. Water Manage. 96, 1207–1217.

UNECE: United Nations Economic Commission for Europe (2017): REN21 UNECE Status Report. Ministerial Conference and the Eighth International Forum on Energy for Sustainable Development in Astana/Kazakhstan http://www.ren21.net/status-of-renewables/regional-status-reports/.

United Nations (2015): Framework Convention on Climate Change - Adoption of the Paris Agreement, 21st Conference of the Parties, Paris: United Nations.

Vachaud, G., Passerat De Silans, A., Balabanis, P., Vauclin, M. (1985): Temporal stability of spatially measured soil water probability density function. Soil Sci. Soc. Am. J. 49, 4, 822–828.

Van Herwaarden, A., Gómez Macpherson, H., Rawson, H M., Kirkegaard, J.A., Bligh, K.J., Anderson, W.K. (2003): Explore On-Farm - On-Farm Trials for Adapting and Adopting Good Agricultural Practices. Food and Agriculture Organization of the United Nations, Rome. ISBN 92-5-105078-3.

Van-Camp, L., Bujarrabal, B., Gentile, A.R., Jones, R.J.A., Montanarella, L., Olazabal, C., Selvaradjou, S.K. (2004): Reports of the technical working groups established under the thematic strategy for soil protection. EUR 21319 EN/2. Luxembourg: Office for Official Publications of the European Communities.

Venables, W.N., Ripley, B.D. (2002): Modern Applied Statistics with S. Fourth Edition, Springer-Verlag.

Verheijen, F.G.A., Jones, R.J.A., Rickson, R.J., Smith, C.J. (2009): Tolerable versus actual soil erosion rates in Europe. Earth-Science Rev. 94, 23–38.

Vieira, D.C.S., Prats, S.A., Nunes, J.P., Shakesby, R.A., Coelho, C.O.A., Keizer, J.J. (2014): Modelling runoff and erosion, and their mitigation, in burned Portuguese forest using the revised Morgan–Morgan–Finney model. For. Ecol. Manag. 314, 150–165.

Wagener, T., Kollat, J. (2007): Visual and numerical evaluation of hydrologic and environmental models using the Monte Carlo Analysis Toolbox (MCAT). Environ. Model Softw. 22, 1021–1033.

Wagener, T., McIntyre, N., Lees, M.J., Wheater, H.S., Gupta, H.V. (2003): Towards reduced uncertainty in conceptual rainfall-runoff modeling: dynamic identifiability analysis. Hydrol. Process. 17, 455–476.

Wahren, A., Feger, K.H., Schwärzel, K., Münch, A. (2009): Land-use effects on flood generation - Considering soil hydraulic measurements in modelling. Adv. Geosci. 21, 99–107.

Wahren, A., Richter, F., Julich, S., Jansen, M., Feger, K.H. (2015): The Influence of More Widespread Cultivation of Short Rotation Coppice on theWater Balance: From the Site to Regional Scale. – In: Butler-Manning, D. Bemmann, A., Bredemeier, M. Lamersdorf, N., Ammer, C. (Eds.): Bioenergy from Dendromass for the Sustainable Development of Rural Areas, Wiley-VCH, pp. 45-63.

Walczak, R.T., Witowska-Walczak, B., Slawinski, C. (2004): Pedotransfer studies in Poland. In: Pachepsky Ya, Rawls WJ (Eds) Development of pedotransfer functions in soil hydrology. Elsevir Boston, Heidelberg, London, 449–462.

Walczak, R.T., Moreno, F., Slawinski, C., Fernandez, E., Arrue, J. L. (2006): Modeling of soil water retention curve using soil solid phase parameters. J. Hydrol. 329, 3–4, 527–533 .

WDC: World Data Center (2008): Ukraine: Agricultural Overview. Available at: http://wdc.org.ua/en/node/29 (last accessed: August 2011).

Wi, S., Yang, Y.C.E., Steinschneider, S., Khalil, A., Brown, C.M. (2014): Calibration approaches for distributed hydrologic models using high performance computing: implication for streamflow projections under climate change. Hydrol. Earth Syst. Sci. Discuss. 11, 10273–10317.

Williams, J.R. (1975): Sediment routing for agricultural watersheds. Water Resour. Bull. 11,5, 965–974.

Williams, J., Ross, P., Bristow, K. (1992): Prediction of the Campbell water retention function from texture, structure, and organic matter. In. van Genuchten MTh, Leij FJ, Lund LJ (Eds.): Proc. Int. Workshop on Indirect Methods for Estimating the Hydraulic Properties of Unsaturated Soils. University of California, Riverside, CA, 427–442.

Wischmeier, W.H., Smith, D.D. (1978): Predicting rainfall erosion losses: a guide to conservation planning. Agriculture Handbook 282, USDA-ARS.

World Health Organization (2011): Global water scarcity. http://www.who.int/features/factfiles/water/en/ (last access September 2011).

Wösten, J.H.M., Lilly, A., Nemes, A., Le Bas, C. (1999): Development and use of a database of hydraulic properties of European soils. Geoderma; 90, 3–4, 169–185 .

Wösten, J.H.M., Pachepsky, Y.A., Rawls, W.J. (2001): Pedotransfer functions bridging the gap between available basic soil data and missing soil hydraulic characteristics. J. Hydrol. 251, 123–150.

WU: Wageningen University (2013): RECARE - Preventing and Remediating degradation of soils in Europe through Land Care. European Commission FP7 Programme, ENV.2013.6.2-4 'Sustainable land care in Europe'. EU grant agreement: 603498. http://www.recare-project.eu/.

Young, P., Parkinson, S., Lees, M. (1996): Simplicity out of complexity in environmental modelling: Occam's razor revisited. J. Appl. Stat. 23, 2-3, 165-210.

Zacharias, S., Wessolek, G. (2007): Excluding organic matter content from pedotransfer predictors of soil water retention. Soil Sci. Soc. Am. J. 71, 1, 43–50 .

Zhang, R. (1997): Determination of Soil Sorptivity and Hydraulic Conductivity from the Disk Infiltrometer. Soil Sci. Soc. Am. J. 61, 1024-1030.

Zhu, A. X. (1997): A similarity model for representing soil spatial information. Geoderma; 77, 217–242.

Zhu, A. X. (1999): A personal construct-based knowledge acquisition process for natural resource mapping. Int. J. Geogr. Informat. Sci. 13, 119–141.

Zhu, A.X., Mackay, D.S. (2001): Effects of spatial detail of soil information on watershed modeling. J. Hydrol. 248, 54–77.

Zhu, A.-X., Burt, J.E., Moore, A.C., Smith, M.P., Liu, J., Qi, F. (2007): SoLIM: A New Technology For Soil Mapping Using GIS, Expert Knowledge & Fuzzy Logic Overview. University of Wisconsin-Madison, U.S. Department of Agriculture.

Zingstra, H., Simeonova, V., Kitnaes, K. (2009): Protection and management of the Bug River as an ecological corridor in the Pan European Ecological Network. Final report of the BBI-MATRA project 2006/015, Wageningen International.